

EPA-650/2-73-022

September 1973

ENVIRONMENTAL PROTECTION TECHNOLOGY SERIES

**STATE OF THE ART:
1971 INSTRUMENTATION
FOR MEASUREMENT
OF PARTICULATE EMISSIONS
FROM COMBUSTION SOURCES**

VOLUME IV

**EXPERIMENTS AND
FINAL REPORT**



Office of Research and Development
U.S. Environmental Protection Agency
Washington, D.C. 20460

STATE OF THE ART: 1971
INSTRUMENTATION FOR
MEASUREMENT OF PARTICULATE EMISSIONS
FROM COMBUSTION SOURCES
VOLUME IV: EXPERIMENTS & FINAL REPORT

by

Gilmore J. Sem and John A. Borgos

Thermo-Systems, Inc.
1500 N. Cleveland Avenue
St. Paul, Minnesota 55113

Contract Number CPA 70-23
Program Element No. 1AA010

EPA Project Officer: John O. Burckle

Control Systems Laboratory
National Environmental Research Center
Research Triangle Park, N.C. 27711

Prepared for

OFFICE OF RESEARCH AND DEVELOPMENT
U.S. ENVIRONMENTAL PROTECTION AGENCY
WASHINGTON, D.C. 20460

September 1973

THERMO-SYSTEMS INC.

(Printed in U.S.A.)

When U. S. Government drawings, specifications, or other data are used for any purpose other than a definitely related Government procurement operation, the Government thereby incurs no responsibility nor any obligations whatsoever, and the fact that the Government may have formulated, furnished, or in any way supplied the said drawings, specifications, or other data is not to be regarded by implication or otherwise, or in any manner licensing the holder or any other person or corporation, or conveying any rights or permission to manufacture, use, or sell any patented invention that may in any way be related thereto.

References to names commercial products in this report are not to be considered in any sense as an endorsement of the product by the Government.

This report has been reviewed by the Environmental Protection Agency and approved for publication. Approval does not signify that the contents necessarily reflect the views and policies of the Agency, nor does mention of trade names or commercial products constitute endorsement or recommendation for use.

TABLE OF CONTENTS

VOLUME IV

	<u>Page</u>
FOREWORD	vi
ABSTRACT	viii
SECTION 1. EXECUTIVE SUMMARY: AUTOMATIC MONITORS OF PARTICULATE MASS EMISSIONS FROM STATIONARY FOSSIL-FUEL COMBUSTION SOURCES	1
1.1 INTRODUCTION	1
1.2 DEFINITION OF STACK PROPERTIES	2
1.3 NON-APPLICABLE SENSING METHODS	4
1.4 BETA RADIATION ATTENUATION	6
1.5 PIEZOELECTRIC MICROBALANCE	10
1.6 ELECTROSTATIC METHODS	14
1.6.a. ION CAPTURE	14
1.6.b. CONTACT CHARGING	18
1.7 LIGHT TRANSMISSION	20
1.8 REVIEW OF EXPERIMENTAL WORK	24
1.8.a. LABORATORY EXPERIMENTS	24
1.8.b. FIELD EXPERIMENT STATION	25
1.8.c. FIELD EVALUATION OF TWO PROTOTYPE BETA INSTRUMENTS	26
1.9 CONCLUSIONS AND RECOMMENDATIONS	26
1.10 ACKNOWLEDGMENTS	27
1.11 BIBLIOGRAPHY	28
DETAILED REPORT:	
SECTION 2. PRELIMINARY LABORATORY EXPERIMENTS	31
2.1 INTRODUCTION	31
2.2 CALIBRATION REPEATABILITY	31
2.3 EXPERIMENTS WITH PROMETHIUM-147	39

TABLE OF CONTENTS (continued)

	<u>Page</u>
2.4 RADIATION SOURCE CHARACTERISTICS	39
2.5 EXPERIMENTS WITH FLY ASH	47
2.6 SUMMARY	51
SECTION 3. DESIGN OF FIELD EXPERIMENT STATION	52
3.1 INTRODUCTION	52
3.2 NSP POWER PLANT	52
3.3 GENERAL LAYOUT	54
3.4 INSTRUMENTATION	54
3.5 SUMMARY	60
SECTION 4. CALIBRATION OF STACK FACILITY AT THE FIELD EXPERIMENT STATION	61
4.1 PROCEDURE	61
4.2 RESULTS OF FILTER TESTS	62
4.2.a. INTRODUCTION	62
4.2.b. GAS FLOW MEASUREMENT	68
4.2.c. EFFECT OF SAMPLING TIME	71
4.2.d. PARTICLE LINE LOSSES	74
4.2.e. PARALLEL FILTER TESTS IN MAY	76
SECTION 5. FIELD EVALUATION OF TWO PROTOTYPE BETA INSTRUMENTS	78
5.1 PROCEDURE	78
5.2 RESULTS AND DISCUSSION	78
SECTION 6. EVALUATION OF TRANSMISSOMETER TECHNOLOGY	83
6.1 INTRODUCTION	83
6.2 RECOMMENDED DESIGN FEATURES	83
6.3 MINIMUM RECOMMENDATIONS GOVERNING INSTRUMENT INSTALLATION AND OPERATION	84

TABLE OF CONTENTS (continued)

	<u>Page</u>
6.4 PRESENT COMMERCIAL INSTRUMENTS	85
6.5 MEANING OF THE MEASUREMENT	87
6.6 CORRELATION OF THE MEASUREMENT WITH MASS	88
6.7 CONCLUSIONS	89
6.8 ACKNOWLEDGMENT	90
6.9 REFERENCES	90
SECTION 7. APPENDICES	91
APPENDIX A. COMPLETE DATA FOR THE AUGUST TESTS OF THE SAMPLING SYSTEM	92
APPENDIX B. COMPLETE DATA FOR THE MAY TESTS OF TWO BETA INSTRUMENTS	99

FOREWORD

Airborne particulate matter is a major air pollutant having significant effects on health, economics, ecology, visibility, and aesthetics. Effective techniques and hardware systems for source emissions measurement are needed for application to the various sources to achieve control of particulate emissions and thus protect the environment.

This contract work, begun before the institution of the EPA, has been sponsored to completion by the National Environmental Research Center at Research Triangle Park, North Carolina for the purpose of the field evaluation of two research prototype instrument systems based upon beta radiation attenuation as applied to the measurement of emissions from a coal-fired power plant.

This report constitutes the last of a four volume series which, taken together, comprise the final report for the contract effort. These volumes have been issued separately as each phase of work was completed to make them available to the public as soon as possible. These volumes contain the following:

Volume I of this report was written for the engineer or planner who needs to know a few basic facts about a particulate mass measurement technique and wishes to minimize the time required to obtain this information. Volume I is intended for use as a quick reference guide. This volume is available from the National Technical Information Service (NTIS), order number PB 202-665.

Volume II of this report is designed as a detailed in-depth report on operating principles, techniques, historical data, and discussion of the more viable techniques for particulate mass monitoring. Volume II is designed for the plant engineer, abatement and control officials, and others who may not be familiar with the detailed technology of these areas. Included are sections on power plant emissions properties and extraction sampling probes. This volume is available from the NTIS, order number PB 202-666.

Volume III of this report is a comprehensive survey and critique of particle sizing techniques which could possibly form the basis for automatic particle size measurement. This volume is available from the NTIS.

Volume IV of the report (this volume) provides a recapitulation of the various sensing techniques and their applicability to mass monitoring instrumentation and describes an experimental field evaluation of two research prototype instruments based on beta radiation attenuation as applied to a coal-fired power plant effluent. Problem areas requiring further research and development efforts are identified for those persons concerned with instrument development.

This report is included in the Environmental Protection Technology series - the series, devoted to new and improved technology required for control and treatment of pollution sources to meet environmental quality goals, includes reports of work dealing with research, development, and demonstration of instrumentation, equipment, and methodology to repair or prevent environmental degradation from point and non-point sources of pollution.

John O. Burckle
Project Officer
U.S. Environmental Protection Agency
Office of Research and Development

ABSTRACT

As this program began, no automatic particle mass concentration monitor had been suitably developed for use in monitoring effluents from large coal-fired combustion sources. It was not clear which of several measurement techniques offered the greatest chance of success as a result of further development programs. It was also not clear what operational problems would be encountered in the use of such a monitor on an actual effluent stream.

The first phase of this program was a literature study and evaluation of potential measurement techniques and a more precise definition of the stack environment. Volumes I and II of this report series and Section 1 of this report contain the results of this study. The second phase was an experimental evaluation of the most promising technique: beta radiation attenuation. Sections 2-5 of this report discuss both laboratory and field experiments performed with several beta radiation instruments.

Section 1 discusses various approaches for automatic, continuous measurement of the rate of particulate mass emissions from smoke stacks on large coal and oil combustion facilities. Reasons are given for rejecting a number of particle sensing techniques. Inherent and practical strengths and weaknesses of the following methods are included: beta radiation attenuation, piezoelectric microbalance, electrostatic, and light transmission. Comparative evaluation shows that the beta radiation attenuation and piezoelectric microbalance techniques offer the best possibilities for accurate monitoring at the present time. Although the electrostatic and light transmission techniques offer several desirable operational features, their inability to sense the mass of particles severely limits their usefulness for monitoring particulate mass emissions. Section 1 includes a summary of Volumes I and II of this report series.

Section 2 describes early laboratory tests performed with the sensing head of a Gelman beta radiation instrument. The tests resulted in a set of calibration curves, each curve representing a different initial clean filter thickness. The importance of knowing the initial clean filter thickness accurately is illustrated. This section discusses the reasons for the different calibration curves for different initial clean filter thicknesses. Tests were performed with C-14 and Pm-147 as beta sources. Pm-147 is affected significantly less than C-14 by variations in initial clean filter thickness. For C-14, a commonly-encountered filter thickness variation of about 10% results in a deposit measurement uncertainty of about 10%, even with the standard before-and-after radiation counting technique.

Section 3 describes a sampling facility, designed specifically for the evaluation of the instruments which measure particle mass concentration of stack effluents, which was designed, constructed, evaluated, and operated on a section of breeching of a coal-fired power plant. Identical parallel sampling systems supply nearly identical particulate samples to a high-efficiency

filter and to the instrument under test. The sampling facility includes heated sampling lines and boundary-layer diluters to reduce condensation and the resulting particle wall losses. The sampling line leading into the test instrument can be adapted to a variety of lengths and configurations; and the sampling flow rate, dilution ratio, and heater power can be adjusted. Each of the two parallel sample lines contains a high-accuracy flowmeter and a valving system which allows the operator to measure both dilution clean air flow rate and total diluted aerosol flow rate with the single flowmeter. Thus, most flowmeter errors are eliminated resulting in more accurate measurement of sampling rates and dilution ratios. The facility was not designed nor intended to obtain an optimum measurement of effluent particle concentration, but rather to deliver representative and identical effluent samples to the test instrument and its parallel filter.

Section 4 describes results of the calibration of the sampling facilities in the field experiment station under several normal operating conditions with identical high-efficiency filters in both parallel sampling lines. The ratio, R_F , (instrument (beta) filter collected weight)/(parallel filter collected weight) was near or somewhat less than 1.0 for nearly all runs.

Section 5 describes tests of two prototype instruments with beta radiation particle mass sensors and with filter collectors which were tested for a short time in the stack facility. Both were developed for auto exhaust particle measurements under separate and parallel contracts funded by EPA. One was developed by GCA Corporation (GCA)* and one by Industrial Nucleonics Corporation (IN)**. The GCA instrument yielded highly consistent results and R_F was nearly 1.0. The IN instrument yielded considerably less consistent results with R_F usually varying between 0.33 and 0.65. The sampling systems up to the two instruments were plumbed and operated nearly identically, evidence that the error of the IN instrument was instrument error and not sampling technique error. The highly encouraging measurements with the GCA instrument indicate that beta radiation sensing with filter collection of particles is a strong candidate for the measurement of particle mass concentration in smoke stacks.

Section 6 presents candid comments regarding the state-of-the-art of commercial transmissometers in January 1971. Recommendations regarding the design, installation, and operation are included. The section briefly discusses what a transmissometer measurement means and how well the measurement correlates with particle mass concentration.

*GCA Technology Division, Bedford, Massachusetts 01730

**Industrial Nucleonics Corporation, Columbus, Ohio 43202

SECTION 1. EXECUTIVE SUMMARY: AUTOMATIC MONITORS OF PARTICULATE MASS EMISSIONS FROM STATIONARY FOSSIL-FUEL COMBUSTION SOURCES

1.1 INTRODUCTION

Measurement of the total mass flow of particulate emissions from smoke stacks on large combustion facilities is a major problem facing stack owners, pollution control officials, and emissions control equipment manufacturers. Stack owners need such measurements to more carefully control the combustion efficiency and emissions of the facility. Pollution control officials need permanent records of stack mass emissions to aid in law enforcement. Emission control equipment manufacturers need more efficient ways to evaluate the performance of their equipment. As a result, instruments that automatically and continuously record particulate mass emissions are now necessary.

Presently, particulate emissions measurements are made by sampling a known volume of effluent gas through a filter, and weighing the filter before and after sampling to find the particle mass concentration. By traversing the effluent gas stream cross-section to measure gas velocity as well as to obtain the filter samples, an estimate of the total mass of particles emitted per hour is made. Such measurements require considerable equipment, labor, and time. One series of measurements typically takes about four hours with perhaps three man-days of labor for planning, equipment transport, setup, sampling, and data reduction. Therefore, this method cannot economically be used for measuring combustion efficiency, for monitoring pollutant emissions, or for extensively evaluating pollution control equipment on a continuous basis.

There are several reasons for choosing mass as the measured particulate emission parameter. Mass is a basic parameter of the particles which does not depend on the instrument used to measure it. A familiar laboratory balance can be used to check or calibrate mass sensing instruments. Since manual stack sampling techniques measure the mass of particles, much of the existing data, and most new regulations, are expressed in terms of particulate mass. As will be seen below, mass is one of the easiest particle parameters to sense accurately because most mass sensing techniques are not very sensitive to secondary particle parameters.

The primary aim of this discussion is not to defend the case for measuring particulate mass, however. It is rather to explain the relative merits of several particle sensing techniques with regard to the measurement of particulate mass or mass concentration.

Particle sensing techniques have many monitoring applications ranging from clean rooms to pneumatic conveying systems. Only a few of the techniques are applicable to the sensing of particles in effluent gas streams from coal combustion sources. Fewer yet are applicable to the sensing of particulate mass

in such streams. The measurement of primary interest from a pollution standpoint is the particulate mass flow rate, i.e., the total mass of particles leaving the stack per hour. Most particulate mass sensors, on the other hand, measure particle concentration in terms of the mass of particles per unit of gas volume. This discussion assumes that the measurement of particulate mass concentration is sufficient to define particulate mass flow rate. The volumetric gas flow rate must be measured separately or estimated from the operating conditions of the process.

There is a question about the relative merits of integrated versus point measurements of particle concentration. The most commonly used particle monitors, light transmissometers, are integrating instruments. They measure the average particle concentration along the measuring path. Most other potential and existing particle monitoring instruments measure the particle concentration at a point within the duct. If the gas velocity and particle concentration profiles were relatively homogeneous across the duct, either integrated or point sampling could yield good results with little trouble. However, such conditions seldom exist. Not only is the gas velocity profile usually skewed, but the particle concentration profile may be skewed in a different way. Thus, it is not clear which sampling method has the advantage. One conclusion is certain, however: the placement of any instrument within an effluent duct must be done carefully so that a representative measurement is made.

1.2 DEFINITION OF STACK PROPERTIES

The operating environment strongly affects the design of any instrument for measuring particulate emissions. Table 1 is a brief summary of typical effluent gas stream conditions for large, modern coal combustion facilities with electrostatic precipitator control equipment¹. The data was obtained through an extensive survey of the open literature and private reports. Table 2 is a brief summary of typical effluent gas stream conditions for large, modern oil combustion facilities with no control equipment. Since the effluent from oil combustion facilities is relatively free of particles and since only a small portion of the electric power in the U.S. is generated by such plants, the remainder of the discussion is directed primarily toward coal combustion facilities.

Particulate emissions from coal combustion facilities are usually measured in the breeching, a section of rectangular duct between the collector equipment and the vertical stack. Because the breeching is usually quite short and is seldom straight, ideal sampling conditions seldom occur. The choice of the sampling location is very important. Most manual sampling procedures specify that the duct being sampled must be traversed in a specified manner. This makes the choice of a sampling location even more critical. This problem should be considered carefully whenever emissions measurements are made. In most cases, the accuracy of the measurement depends as much on the representativeness of the sample as on the accuracy of the sensor.

TABLE 1. TYPICAL COAL COMBUSTION EMISSIONS DATA

Particulate mass loading, after precipitator	0.03 - 3.0 gm/cu meter*
before precipitator	0.2 - 12 gm/cu meter
Mass loading spatial variation at duct cross-section	$\pm 50\%$
Particle size, after precipitator	Mass median diameter $\approx 5\mu\text{m}$ 95% $< 25\mu\text{m}$ (by mass)
before precipitator	Mass median diameter $\approx 3-70\mu\text{m}$ 95% $< 100\mu\text{m}$, 5% $< 1\mu\text{m}$ (by mass)
Extreme particle size range	0.01 - 300 μm
Flue gas velocity	Average: 15 - 20 m/sec. Range: 10 - 40 m/sec.
Flue gas temperature	Typical: 140 - 165°C Range: 130 - 205°C
Dew point	Acid: 105 - 130°C Water: $< 60^\circ\text{C}$
Moisture content of gas	5 - 10% by volume
Static pressure at sample ports	Range: 15 cm positive to 35 cm negative water pressure
Turbulent flow fluctuations	30 - 120 cycles per minute
Existing sampling port size	As small as 3 in. ID hole
Traversing distance across duct from port	Typical: 2 - 5 meters Range: 1.5 - 10 meters
*2.29 gm/cu meter = 1 grain/cu foot	

TABLE 2. TYPICAL OIL COMBUSTION EMISSIONS DATA

Particulate mass loading, uncontrolled	Typical: 0.06 - 0.2 gm/cu meter Range: 0.015 - 1.0 gm/cu meter
Mass loading variation with time	As much as a 10-fold in- crease over typical
Mass loading variation during soot blowing	About 4-fold increase over typical
Particle size	Typical: 0.01 - 1.0 μm Range: < 0.01 - 40 μm
Flue gas temperature range	120 - 165°C
Flow conditions	Similar to those for coal combustion (see Table 1)

1.3 NON-APPLICABLE SENSING METHODS

The following discussion briefly describes many of the particle sensing techniques which are not presently applicable to particulate mass monitoring from coal combustion sources and lists reasons for rejecting each one. Later, the applicable techniques will be covered in more detail, including the positive and negative features of each.

Acoustic attenuation is the decrease in amplitude of a sound wave when particles are added to an acoustic field. Use of this technique has been strictly limited to research². Acoustic attenuation appears useful only after considerably more research and then only for concentrations several orders-of-magnitude greater than the 0.1 gm/cu meter found in effluent gas streams.

The pressure drop across a nozzle increases if particles are added to the carrier gas. This technique has been successfully used only for measuring particle flow in pneumatic conveying systems with particle concentrations three orders-of-magnitude greater than the typical values found in effluent gas streams³. A cyclone has been used to enrich the particle concentration of industrial dust emissions before it enters the sensing nozzle, but large fluctuations in the enriched particle concentration leaving the cyclone severely limited the instrument's usefulness⁴.

The pressure drop across a filter increases as the filter becomes loaded. However, the rate of increase of pressure drop depends not only on particle concentration but also on particle size, shape, and stickiness, on particle penetration into the filter, and on filter characteristics. Because of the many variables the relationship between the particulate mass loading and pressure drop is too erratic to make accurate measurements.

The unbalance of a centrifuge measured by a displacement sensor as particles are deposited at one spot on the circumference is a direct measure of particle mass⁵. Another closely related method is the change in inertia of a rotating mass caused by the addition of particles, which can be sensed by measuring changes in acceleration or deceleration of the rotating mass under the influence of a constant torque. Both methods offer some promise for monitoring effluent gas streams primarily because they sense mass directly. However, neither method has been developed. A possible problem is lack of sensitivity.

An acoustic particle counter detects the audible click as individual particles greater than 5 - 10 μm pass through a laminar capillary⁶. This method, about which little is known, requires low, clean-room concentrations, making it unusable in effluent gas streams.

A hot-wire anemometer detects the number and size of liquid droplets which impact on the surface of a hot cylindrical film⁷. The response of the instrument to solid particles is not understood, so the method is unsuitable for stack monitoring.

A vibrating band or wire stretched across a portion of an effluent gas stream vibrates at a decreasing natural frequency as it becomes contaminated with particles⁸. The frequency change is directly proportional to the mass of particles added to the band. However, the mechanism by which particles reach the band depends on particle size, particle stickiness, and aerodynamic factors. Correlation with particulate mass flow is questionable. Other methods of particle deposition, such as impaction or electrostatic precipitation, could make this method similar to the piezoelectric microbalance method discussed below. Considerably more development is needed on this method.

An automatic weighing instrument uses an automated gravimetric balance to sense the mass of particles deposited by electrostatic precipitation, impaction, or other collection methods⁹. The deposit surface must be cleaned or replaced periodically, requiring complicated mechanisms. The cost of potential commercial models appears high. Considerable development is needed to make this method useful. Since it gravimetrically measures true particulate mass, further development appears justified.

The tape spot photometer measures the blockage or attenuation of a light beam shining through an indexing tape filter as the filter becomes loaded with particles¹⁰. The measurement is often called the soiling index. Correlation of this measurement with particulate mass concentration is poor because the attenuation of light does not depend on particle mass, but on particle size, shape, refractive index, and surface characteristics, on filter variations, and on light-beam wavelength, intensity, and geometry.

Light-scattering photometers, or nephelometers, measure the light scattered by a cloud of suspended particles within a measuring chamber^{11,12}. The measurement correlates poorly with particulate mass concentration because light scattering depends on particle size, shape, refractive index, and surface characteristics and on light-beam wavelength, intensity, and geometry.

Lidar uses a laser light source and measures the light scattered from the particles back toward the source¹³. Lidar measures particle concentrations remotely (>5m) from the instrument, making installation in an effluent gas stream difficult, but offering the possibility of monitoring emissions from several stacks with one instrument located in some central location outside the stacks. Lidar suffers all the problems of light-scattering photometers in correlating its measurement with particulate mass. The method is presently expensive and requires more development for use in the remote monitoring of stack emissions.

Single-particle light-scattering detects light scattered by individual particles as they pass single file through a light beam^{14,15}. This method requires relatively low concentrations (<5,000 particles/cm³ all of which are >0.3 μ m diameter) in addition to the problems suffered by the light-scattering photometer.

Holography, a three-dimensional laser photographic technique, can be used to remotely measure the total volume of a sample of suspended particles¹⁶. It requires further development and is much too expensive for practical monitoring purposes at this time. The primary expense is in reducing the data.

A particle bounce technique has been tested which consists of an electrical condenser with a strong electric field between the plates of the condenser¹⁷. When a particle enters the air gap between the plates, the electric field accelerates it toward one side or the other, depending on its initial charge. When it strikes a plate, it exchanges its charge and is repelled toward the other plate. This process continues until the particle is carried out from the condenser by the air flow. Unfortunately, such instruments appear to sense only large ($>10\mu\text{m}$), non-adhesive particles, making correlations with mass highly questionable.

The probe-in-nozzle technique consists of a cone-shaped, electrically-insulated probe that is placed in the throat of a venturi nozzle¹⁸. Particles strike the probe and exchange electrical charge with it. The charge exchange is sensed by an electrometer. This technique is sensitive only to dry, abrasive particles and is dependent upon particle composition. The measurement does not correlate well with particulate mass.

1.4 BETA RADIATION ATTENUATION

If beta particles (electrons) pass through a medium, some will be absorbed and some reflected, resulting in a net reduction in the beam intensity. Such a reduction is known as beta radiation attenuation and is a measure of the mass of material through which the beam passes. The attenuation of beta particles depends statistically on the number of electrons with which they interact. Correlation of attenuation with particulate mass depends on the relationship between the number of electrons per molecule (atomic number) and the mass of the molecule (atomic number) and the mass of the molecular nucleus (atomic weight) of the particulate material. This ratio is between 0.4 and 0.5 for all elements except hydrogen, and is between 0.45 and 0.5 for nearly all elements normally found in coal combustion particles. Figure 1¹⁹ verifies that beta attenuation is not significantly different for a wide variety of particulate materials. The close correlation with particulate mass appears to be better than any other known technique except automatic weighing and piezoelectric microbalance measurements.

Instruments using this technique, shown schematically in Figure 2, have recently measured the concentration of airborne particles in ambient air and effluent gas streams^{19,20,21,22}. Carbon-14, with a half-life of 5568 years, is a typical beta radiation source; thallium-204, cesium-137, and promethium-147 could also be used. Geiger-Muller (GM) counters are the most common detectors, but proportional and scintillation counters have also been used. The particles

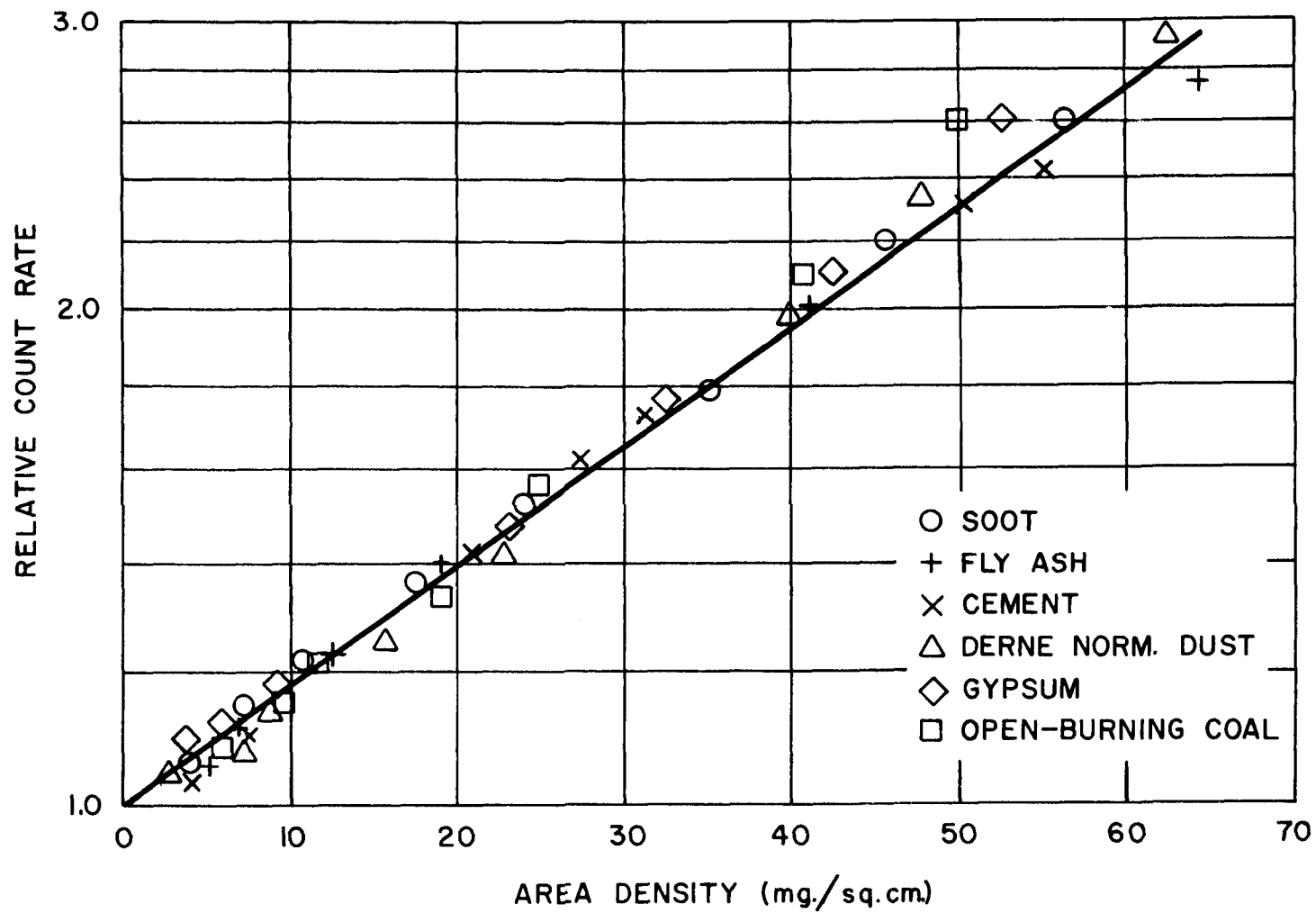


Figure 1. Calibration of a beta radiation attenuation instrument for several dusts.

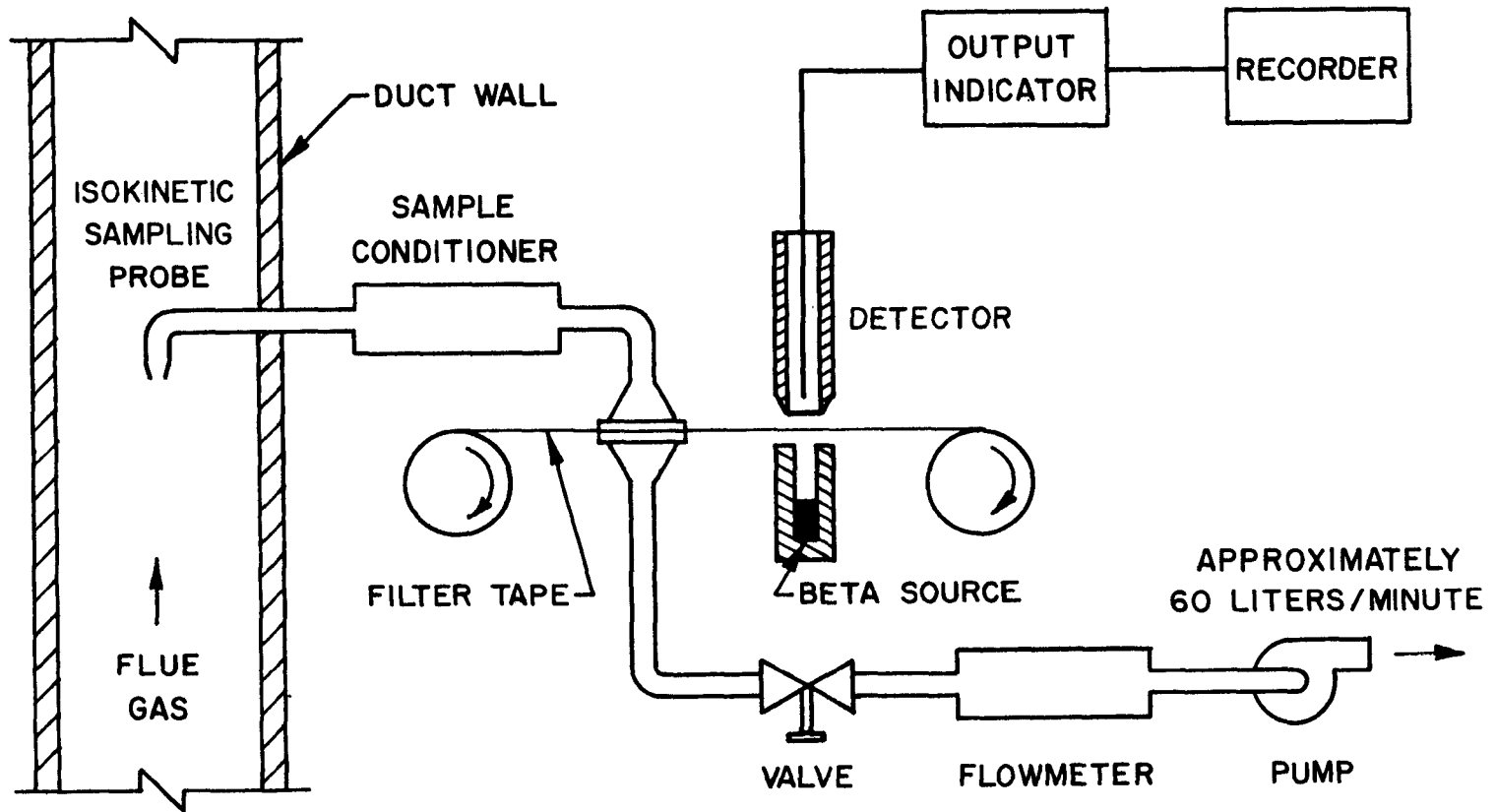


Figure 2. Beta radiation attenuation instrument.

from a known volume of effluent gas are usually first collected on a filter, which is then placed between the beta source and GM detector. The difference in count rate of the GM detector before and after the particles are collected is a measure of the mass of particles on the filter. This method has been automated by using an indexing tape filter as the collector and a recorder to collect data. Strictly speaking, practical beta instruments are only quasi-continuous. Sensitivity is high enough so that an average measurement, when the sampling flow rate is 60 liters per minute (2 cu ft/min) through a glass-fiber filter, can be made in a 1-to 15- minute period. This is sufficient for most monitoring purposes.

Some measurement errors are associated with source, specimen, and detector geometry. These errors can usually be minimized with good design, and the system can be calibrated to reduce measurement uncertainty to an acceptable value. The source and detector must be shaped and spaced such that beta radiation scattered by the particle sample is not detected. The gas molecules within the beam of beta particles must not become a significant portion of the total mass through which the beam passes. Finally, the particles must be distributed uniformly on the filter so that the measured filter mass loading is not dependent on the position of the radiation beam.

The sampling system which brings the particle sample to the sensing head can be the greatest source of error with this method. This error can also be minimized by careful design, including simple heating of the probe and filter holder to prevent condensation of vapors, or dilution of the effluent sample to prevent condensation as the sample cools. Since the particle sensor is normally separated from the particle collector, the radiation source and detector are not exposed to the high temperature gas stream.

Several particle collection techniques other than filters can be used with beta radiation attenuation. A cyclone can collect particles with typically higher gas flow rates providing better time resolution²⁰. However, Table 1 shows that a significant portion of the mass of particles in coal combustion emissions is below the particle size cutoff of practical cyclones ($\approx 1\mu\text{m}$), introducing some uncertainty to measurements made with such instruments. An impactor can collect particles larger than about $0.5\mu\text{m}$, giving a highly concentrated sample on a small deposit area²¹. However, large particles may tend to become reentrained in the air stream because of the high jet velocities needed to collect small particles. Electrostatic precipitation has also been used to collect particles for beta attenuation sensing²³. Cyclones, impactors, and electrostatic precipitators all offer advantages for application to certain particle concentration measurements. Further investigation is necessary to fully evaluate each collection method for coal combustion emissions.

The beta radiation attenuation particulate mass sensing technique, with one of the several possible particle collection devices, is a promising contender for monitoring the particulate mass concentration in stack emissions.

1.5 PIEZOELECTRIC MICROBALANCE

Piezoelectricity is the property of certain crystals, including quartz, which results in an electrical charge on certain surfaces of the crystal when the crystal becomes mechanically stressed. Conversely, a piezoelectric material becomes mechanically strained if an electrical charge is placed on certain of its crystal faces. A piezoelectric crystal, when placed in an appropriate electronic oscillating circuit, will cause the circuit to oscillate at the natural vibrational frequency of the crystal. Some piezoelectric materials, such as quartz, vibrate at very precise natural frequencies, so that frequency changes of one part in 10 million are significant and easily detectable.

When foreign material adheres to the surface of a vibrating piezoelectric crystal, the natural frequency of vibration of the crystal decreases. The magnitude of the frequency change is directly proportional to the mass of foreign material. This principle has been used recently to measure the mass of ambient atmospheric and automobile exhaust particles deposited onto the sensing surface by an electrostatic precipitator or an impactor^{24,25,26}.

The vibrational mode normally used in piezoelectric microbalances is one in which the two parallel faces of a plate-like crystal move parallel to each other. With this type of vibration, using type AT crystals as shown in Figure 3, particles will be weighed if they adhere to any point on the two electrodes. A particle must be deposited on one of the two metal-film electrodes to be sensed because only the portion of the crystal between the electrodes vibrates. The relationship between added mass and the shift in natural vibrational frequency for AT crystals is²⁴:

$$\Delta m = - \frac{A}{K f_o^2} \Delta f \quad (1)$$

where:

K = constant which depends only on crystal type (= $2.27 \frac{\text{cm}^2 \text{ Hz}}{\mu\text{gm MHz}}$ for type AT crystals),

Δf = change in natural vibrational frequency, Hz,

f_o = natural vibrational frequency of the crystal MHz,

A = electrode (active) area of the crystal, cm^2 , and

Δm = mass added to electrode area, μgm .

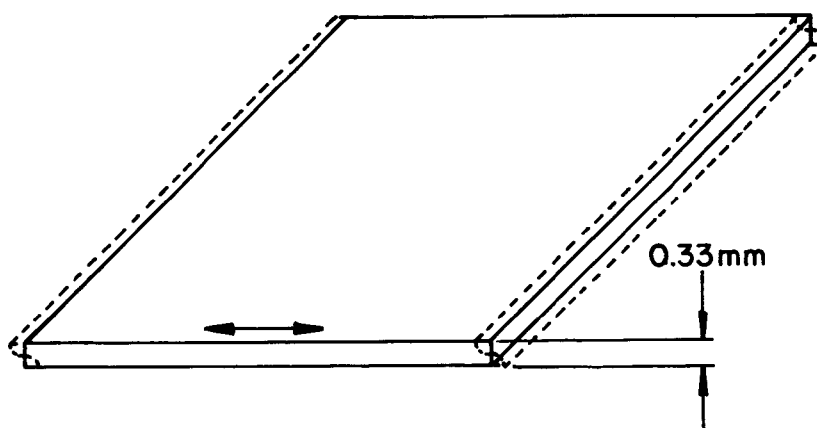
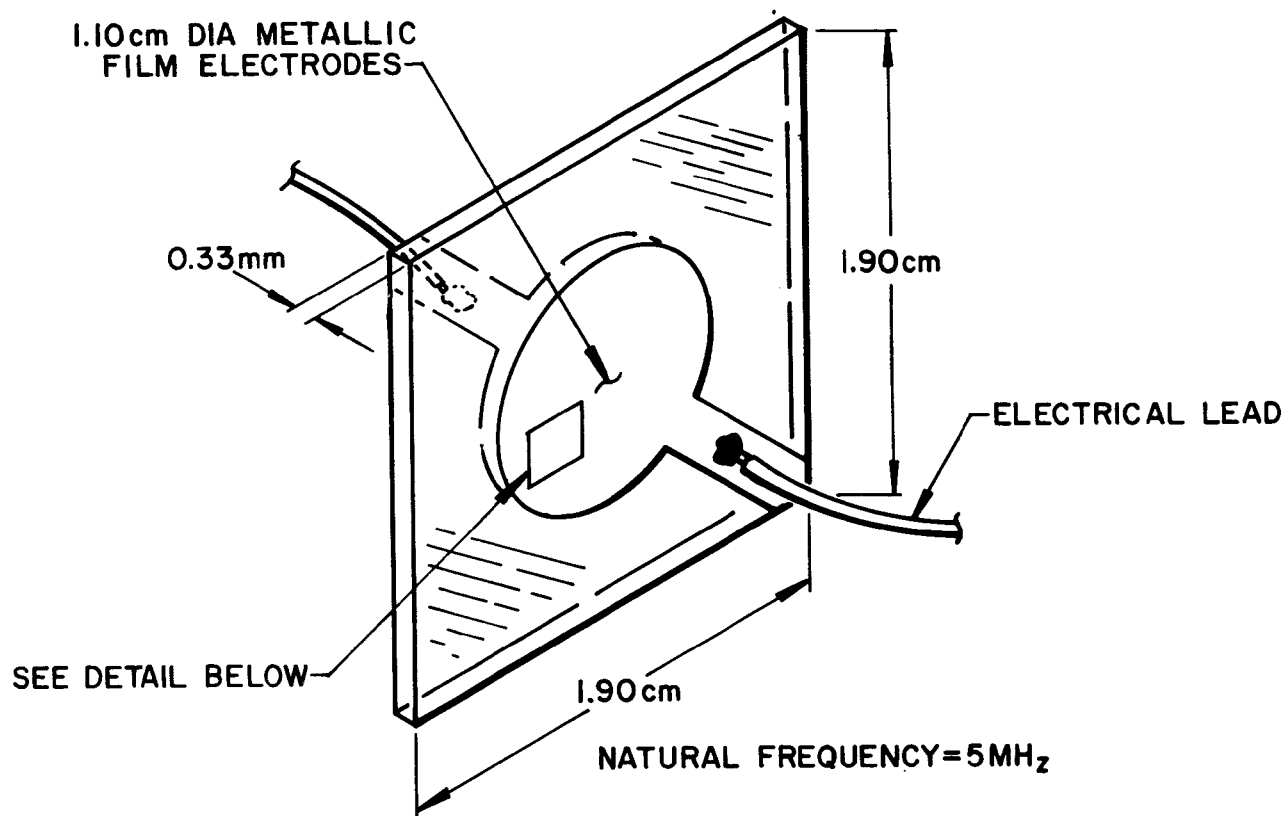


Figure 3. Typical type ΔT quartz crystal for particulate mass measurement showing the characteristic thickness shear mode of vibration.

If a collection device, such as an electrostatic precipitator or impactor, deposits particles onto the crystal electrode from a constant volume flow rate Q during the sampling period Δt , then the average particle mass concentration C_{ave} over the time interval Δt is:

$$C_{ave} = \frac{\Delta m}{Q \Delta t E} \quad (2)$$

where E is the particle mass collection efficiency of the collector. Combining Equations 1 and 2, the particle mass concentration becomes:

$$C_{ave} = - \frac{A}{2.27 Q E f_o^2} \frac{\Delta f}{\Delta t} \quad (3)$$

Thus, for a given electrode and a given collection device, particle mass concentration C_{ave} is directly and nearly linearly proportional to the rate of change of crystal frequency with time $\frac{\Delta f}{\Delta t}$. Strictly speaking, Equation 3 is somewhat non-linear since f_o^2 appears in the denominator. However, since Δf is normally measured in tens or hundreds of Hz and f_o is normally 3 - 10 MHz, any non-linearity is completely negligible.

Particles must adhere to the crystal electrode, i.e., the active, sensitive portion of the crystal, if they are to be weighed. Thus the forces causing particles to stick to the surface must be high enough with respect to the inertial forces acting on the vibrating particles so that particles do not roll or slide on the electrode surface. It appears that most particles smaller than about 10 μm diameter in ambient air adhere well enough to be weighed. Three modifications which may result in the weighing of larger effluent particles are: choosing crystals with lower vibrating frequency, reducing vibrational amplitude, and using various coating techniques to enhance the adherence of particles to the crystal electrode.

A piezoelectric microbalance system for use in monitoring effluent particles would consist of the components shown in Figure 4. Since the sensor samples only a few liters per minute, an auxiliary vacuum system is necessary to remove a representative sample from the effluent stream and deliver it to the sensor. A method of cleaning or replacing loaded crystals is necessary because crystals stop oscillating when over-loaded with particles. The output signal can be conditioned so that it becomes directly proportional to particulate mass concentration. It then can be recorded by either digital or analog recorders.

The high temperature of effluent gas streams and the vapor condensation which occurs while cooling the system are possible problems for piezoelectric microbalances. Two possible solutions exist. The first is to find a type of crystal which has a low temperature dependence and which operates at the gas

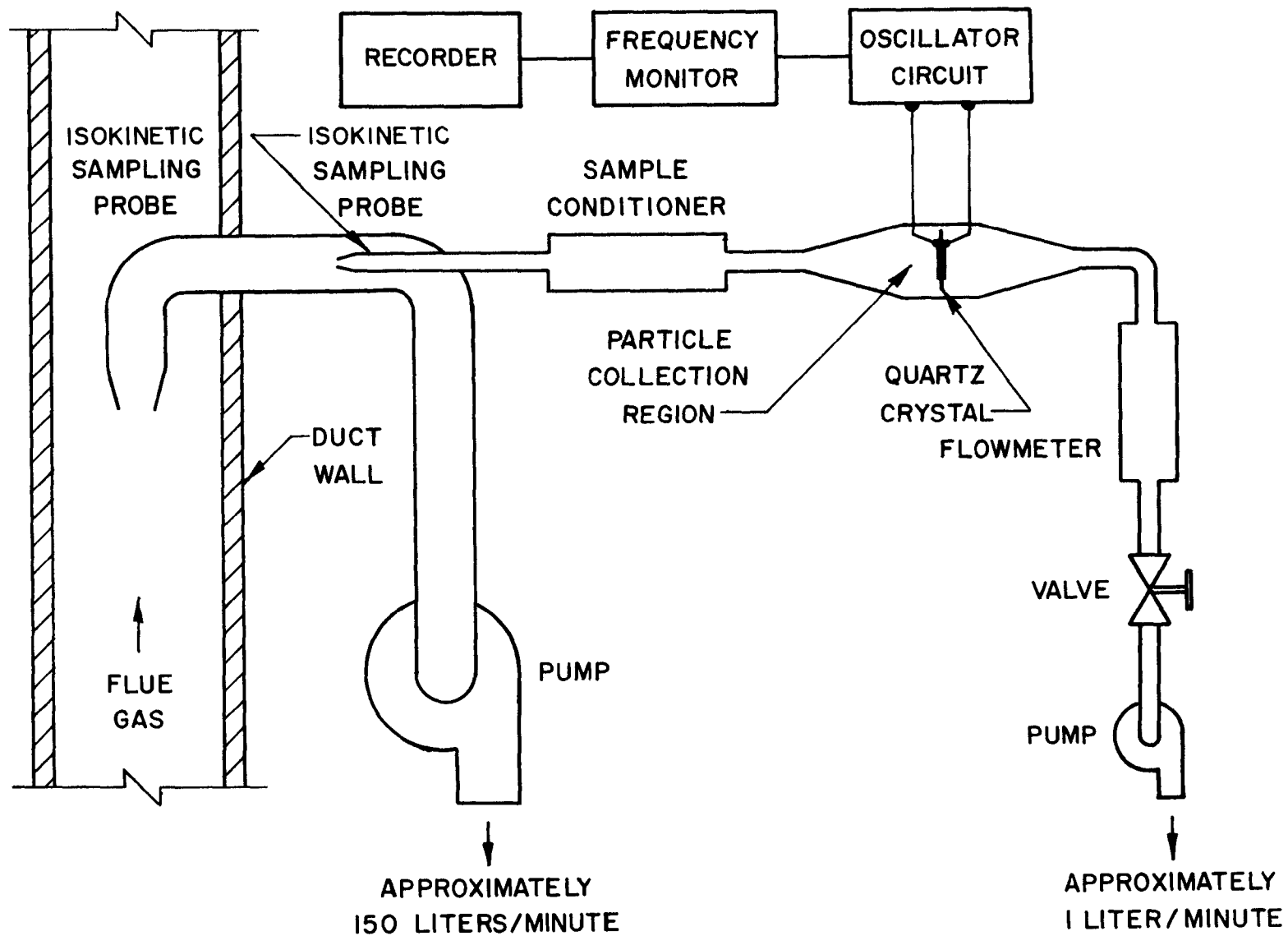


Figure 4. Piezoelectric microbalance instrument.

stream temperature. The entire sampling probe and sensor could then be heated to that temperature to prevent vapor condensation. The second solution is to dilute the extracted sample with cool air. This would prevent condensation of vapors and provide a more suitable environment for the crystals. Since this closely simulates what actually happens when effluents reach the ambient air, this method may be desirable to anyone wanting to measure the pollution hazard of the stack gas. The piezoelectric microbalance has enough sensitivity to measure typical effluent samples diluted by factors of 2 - 100 within a few seconds.

Other than its ability to sense the true mass of particles, the most important feature of this technique is its high sensitivity. Like the beta technique, the piezoelectric technique is quasi-continuous. However, a piezoelectric microbalance can detect mass changes of less than 0.005 μgm . Assuming an effluent particle concentration of 0.1 grams/cu meter (approx. 0.05 grains/cu ft), a piezoelectric microbalance sampling 1 liter/min can collect enough material for a measurement accurate to within $\pm 5\%$ in well under 1 second. A beta radiation attenuation instrument using a filter collector and sampling at 60 liters/min (2 cu ft/min) requires about 1 - 15 minutes.

Although the piezoelectric microbalance is relatively new and untried in effluent gas streams, its desirable features, particularly its high sensitivity to the direct sensing of particulate mass, make it a promising candidate for automatic particulate mass monitoring. A more complete evaluation awaits further development and testing.

1.6 ELECTROSTATIC METHODS

Electrostatic particle sensing methods include a number of instrument designs using several distinctly different principles. The following discussion includes the three principles most applicable to particle monitoring in effluent gas streams. The first two methods, variations of ion capture, are quite similar and are discussed together. The third method, contact charging, is a completely different technique.

1.6.a. Ion Capture

Imagine a constant supply of unipolar ions flowing perpendicularly across a stream of airborne particles toward the grid of an electrometer. Some of the ions will strike the particles and be carried away, thus reducing the ion current as measured by the electrometer. The reduction in ion current, known as the ion-current attenuation, is a measure of the particle flow rate.

Figure 5 shows a typical instrument design²⁷. A radioactive source, e.g., 8 microcuries of cobalt-60, distributed evenly around the inner wall of the outer tube, forms a convenient, constant ion supply. Ions of one polarity are drawn across the aerosol stream and ions of the opposite polarity are repelled

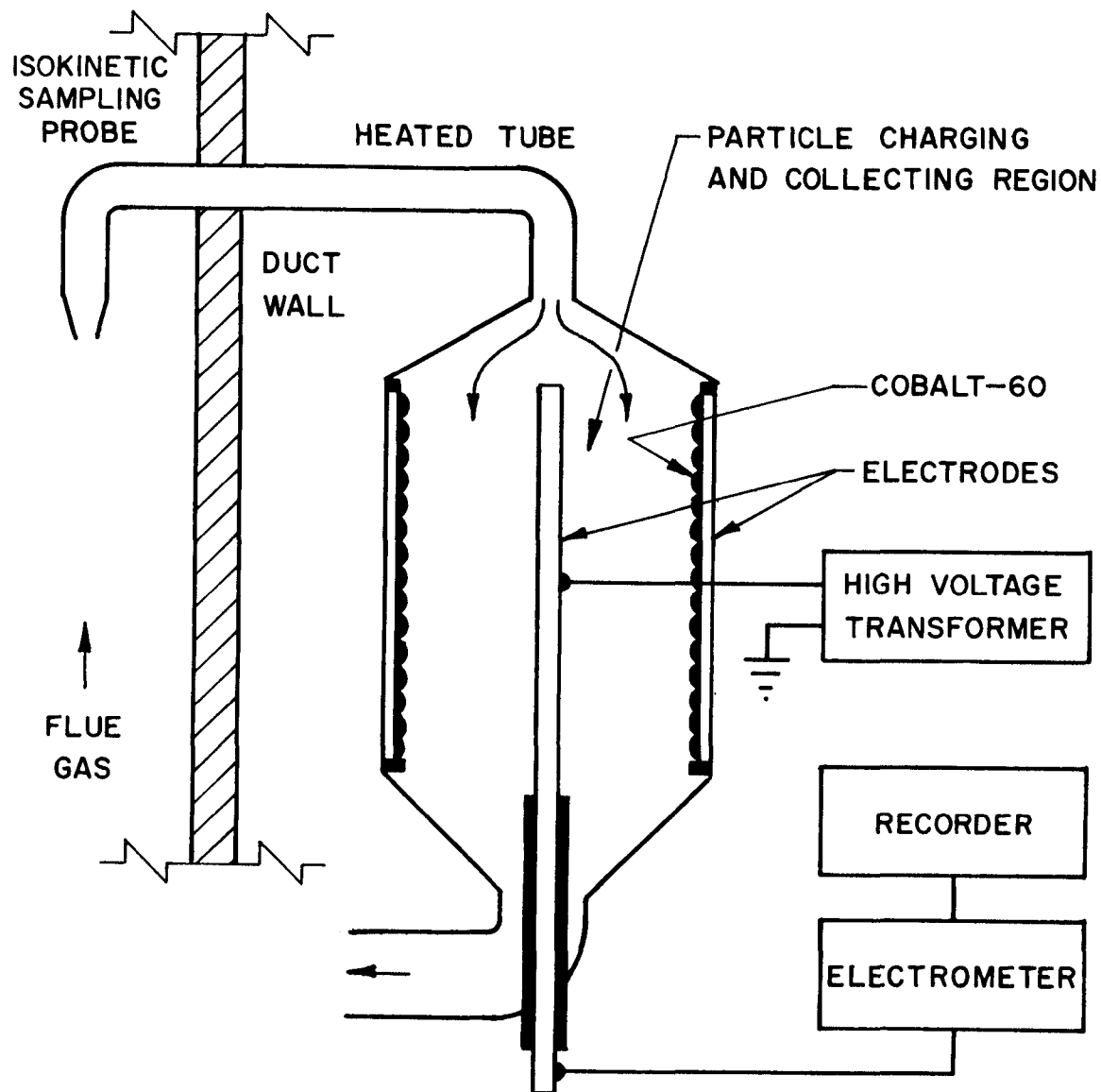


Figure 5. Ion-current attenuation instrument.

by a low-intensity, radial electric field. An electrometer measures the ion current reaching the central electrode. The difference between measured current with particles passing through and the current with clean gas passing through is a measure of particle concentration. A later design²⁸ uses two identical chambers, one with particles passing through and one with a high efficiency filter on the inlet allowing only gas to pass through. The difference between the two measured current levels is a measure of particle concentration. This technique has been used successfully with low concentration dusts such as atmospheric aerosol.

Rather than measuring the portion of the total ion current which does not attach itself to particles, as does the ion current attenuation method, the second ion capture method measures the other portion of the total ion current - the portion carried away by particles. Figure 6 shows one possible design using electrostatic precipitation to collect the charged particles²⁹. This design uses a periodic blast of clean scavenging air to clean the device. The effluent gas stream aspirates the sample through the instrument. It therefore responds directly to changes in gas velocity as well as particle concentration, yielding a measurement of particle flow rate. The design shown in Figure 6 has been operated in coal-fired effluent ducts. However, correlation of the measurement with mass is questionable.

It appears that three major problems limit the usefulness of the two ion capture techniques for measuring particulate mass in effluent gas streams.

First, the instruments do not sense particle mass or even volume, making their correlation with mass poor in effluent gas streams where large fluctuations in particle size probably occur. The ion current carried away by particles depends primarily on particle size and number concentration. Thus, if particle size and the charging mechanism remains constant, a calibrated instrument can measure particle number concentration. Particle chargers can be designed, within limits to place a constant, or saturation, charge on particles of a given size. However, particle size does not remain constant within a given effluent gas stream. Indeed, accurate measurements are most needed when something changes in the process, and most such process changes cause particle size to fluctuate. A look at the theory of particle charging³⁰ shows that the saturation charge level on a particle above $0.1 \mu\text{m}$ is proportional to D_p for diffusion charging and D_p^2 for field charging. Most instruments of this type reported in the literature appear to use field charging, causing the instrument to respond most closely to changes in the product of D_p^2 and particle number concentration, in other words, to changes in total particle surface area. This makes ion capture instruments extremely sensitive to fluctuations in the concentration of submicron particles³¹.

Second, as with any electrostatic method, the measurement of low current levels (10^{-6} - 10^{-12} amperes) within effluent streams requires careful design.

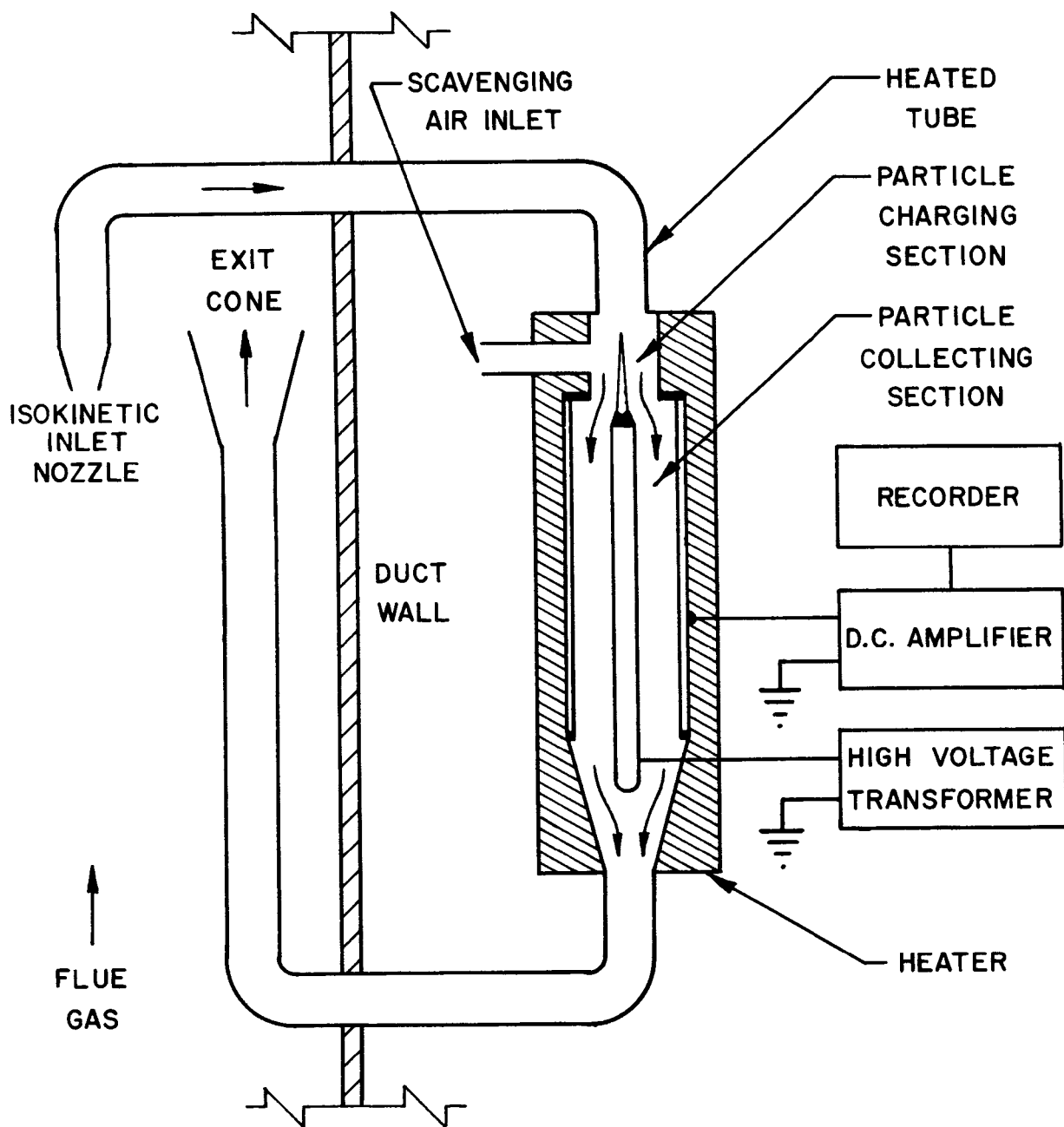


Figure 6. Ion capture instrument.

Third, instruments become contaminated within a short time because the electric field in the charging section causes particles to deposit on the walls of that section. Not only does the charging efficiency change if contamination becomes excessive but particles which collect in the charging region rather than pass through the instrument represent a measurement error. When monitoring dry, non-sticky particles, a periodic blast of air may be sufficient to clean the contaminated surfaces.

The first problem is inherent with particle charging methods. No particle charging technique exists in which the charge placed on a particle is proportional to its mass. The other two problems are basically design problems which may be eliminated by further development.

Ion capture instruments do pose several advantages which make these difficulties less serious. As was mentioned above, the design shown in Figure 6 has been used for monitoring particulate effluents from coal-fired sources. Therefore, many basic operational problems have been solved. If the particle size distribution and composition is known, the output of an ion capture instrument can be correlated with mass concentration. Furthermore, such an instrument does afford a truly continuous and automatic recording of the dust concentration; beta radiation attenuation and piezoelectric microbalance, on the other hand, are only quasi-continuous.

Although ion capture does not measure particulate mass, useful particle monitoring instruments may develop from this technique. Particulate mass measurements, however, will require other sensing techniques.

1.6.b. Contact Charging

When particles hit or slide along a surface, there is usually an electrical charge transfer between the surface and the particles. This principle, a form of contact charging, has been used in the design of the Konitest³² shown in Figure 7. This instrument consists of an electrically-floating tube through which airborne particles pass in a swirling, helical path. The entrance is a tangential slot which gives the air and particles the helical motion. The particles slide along the tube wall, causing an electrical charge transfer. An electrometer measures current draining from the tube wall.

At first glance, the Konitest appears to share the same problems as the previously discussed probe-in-nozzle technique, which is highly dependent on the charge transfer characteristics of the particles. Indeed, data shows a strong dependence on particle composition, and several reports indicate that submicron particles adhere to the tube wall and change the calibration of the instrument. However, several extensive experimental instrument evaluations within coal-fired effluent gas streams report surprisingly good correlation with gravimetric particulate mass concentration measurements^{4,22}. In fact, they also report few operational problems with the instrument, in contrast to several other reports.

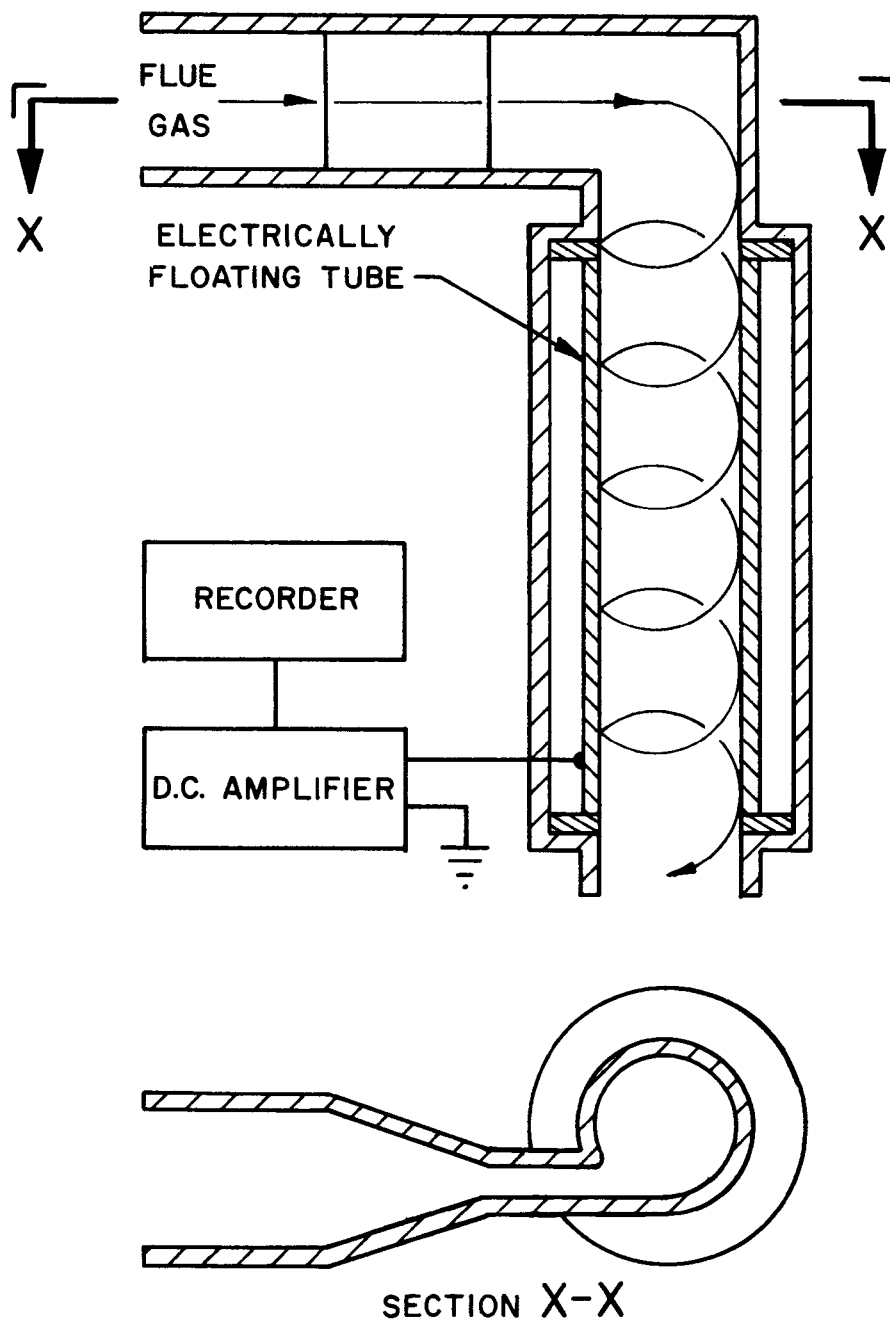


Figure 7. Principle of the Konitest instrument.

The Konitest cannot be thoroughly evaluated theoretically because the theory of contact charging is not well understood. A partial explanation for the apparently good correlation with particulate mass concentration may be that the force causing particles to hit the tube wall, namely centrifugal force, depends strongly on particle mass.

The Konitest offers nearly instantaneous response with direct analog output. Unless the particles are sticky, it is self-cleaning. This is a major practical advantage. The instrument has reportedly been used in several coal combustion effluent streams with no particle adhesion problem. The Konitest has simple construction and operation, and, therefore, low installation and operational cost. If it truly does measure a parameter which correlates well with particulate mass, a question which has yet to be fully answered, it will be a very useful instrument for mass emissions measurement.

1.7 LIGHT TRANSMISSION

When a beam of light is directed through a particle-laden gas stream, its intensity is reduced. This attenuation is a function of many variables, including: particle concentration, size, shape, refractive index, and surface characteristics; light wavelength and orientation; and sensor geometry, orientation, and sensitivity. Because there are so many variables, the physical laws governing light attenuation are extremely complex.

Past development has been concerned primarily with optimizing instrument design parameters, such as the light source and sensor, so that particle concentrations could be measured with a minimum of interference from the other variables. However, development for the true measurement of particulate mass concentration has either not been tried or has been unsuccessful.

Light transmission is presently the most popular method of monitoring particle loadings in effluent gas streams. Figure 8 shows the basic configuration of the simplest type of light-transmission instrument. A light source, mounted on one side of the duct, beams light across the duct to the light sensor. The sensor, or photocell, collects only the light that is not obscured by the particles. Its output signal is calibrated to read Ringelmann number or equivalent opacity. The portion of the beam through which particles are allowed to pass is usually 1 - 3 meters long. The remainder of the beam is usually enclosed by a pipe into the stack to protect the light source and detector from contamination.

The list of advantages of such an instrument is impressive. The measurement is made entirely within the gas stream; no sample extraction with its accompanying problems is necessary. The measurement is instantaneous and continuous in real time. The apparatus is simple and easy to understand, and little maintenance is necessary. The electrical readout is easy to record continuously. Practical problems such as contamination of the source and sensor windows can be easily solved.

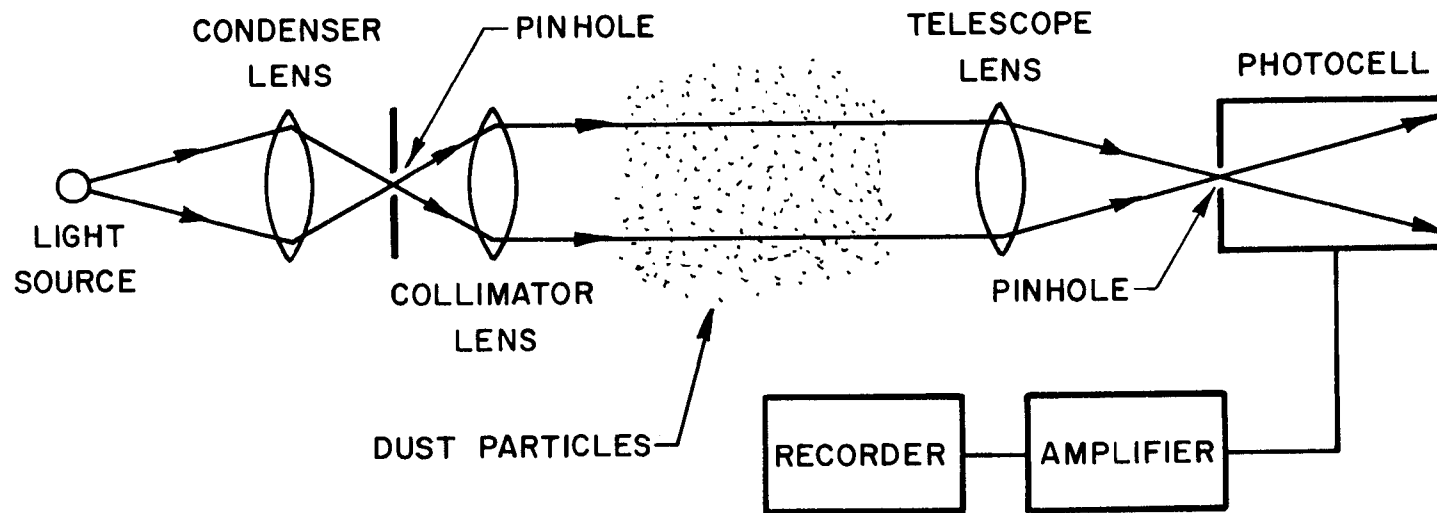


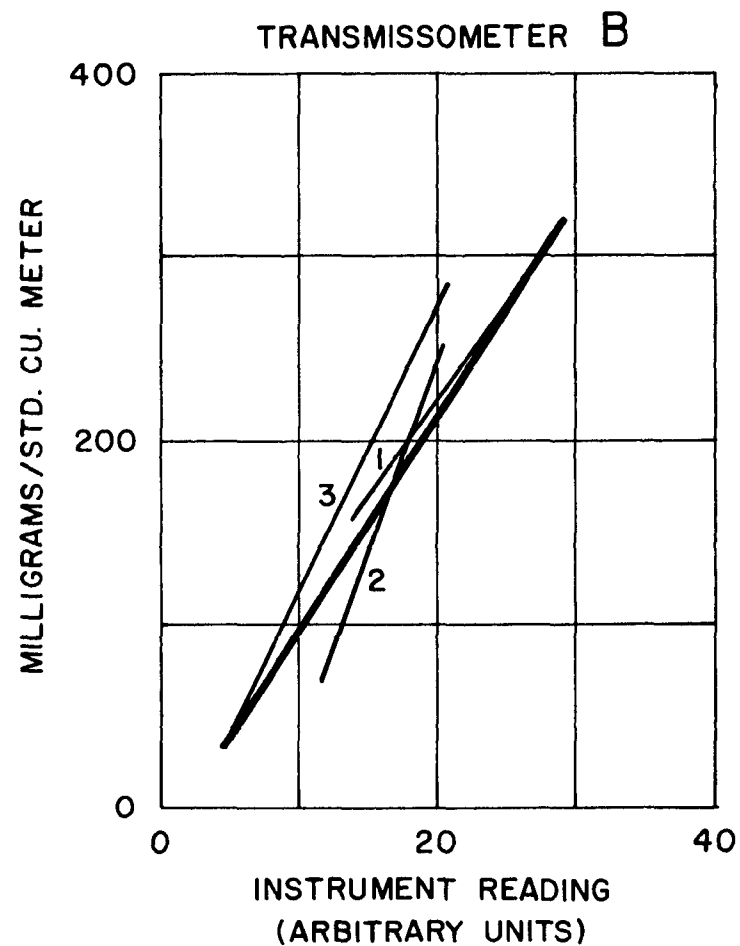
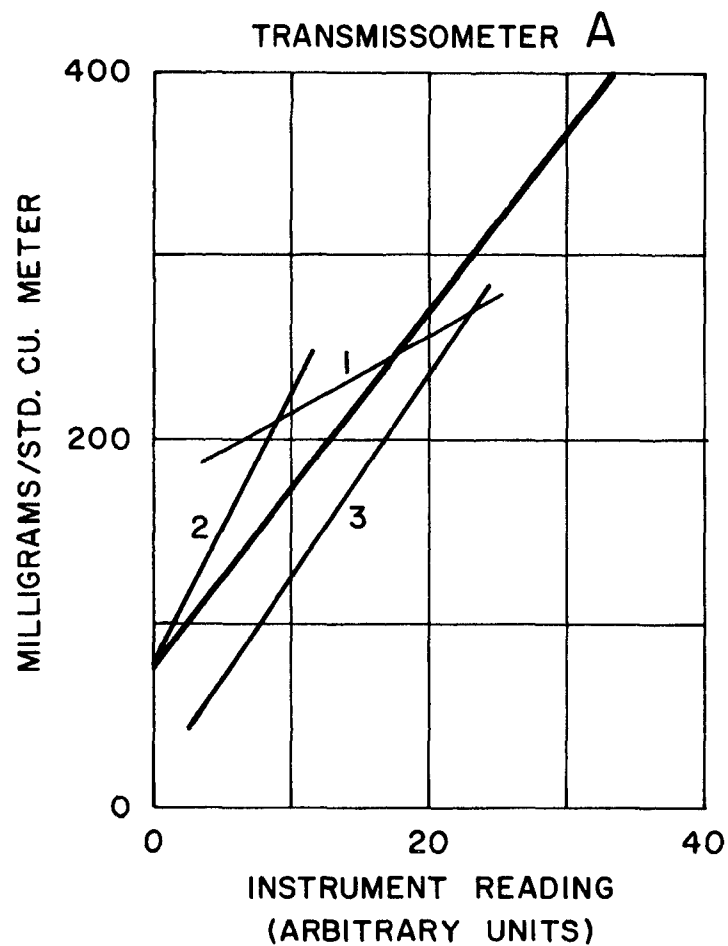
Figure 8. Principle of light-transmission measurements.

Unfortunately, this measurement technique does not measure particle mass. Rather, it measures the light opacity of the particle cloud. The instrument can be calibrated to give particle mass for a given set of conditions of particle size, shape, refractive index, surface characteristics, and density, but if any of these characteristics changes, as often happens in any effluent gas stream, the calibration is no longer valid. The time when accurate particulate measurements are most needed is precisely when such changes occur.

Figure 9²² shows particulate mass concentration calibration curves for two of the best light-transmission instruments for which such data exists. The two instruments were mounted on a modern power generating plant with a pulverized coal boiler and electrostatic precipitation particle collectors. Gravimetric filter samples were used as the calibration standard. About 300 calibration measurements were made with each instrument. Each measurement consisted of a comparison of a five-minute average of the instrument reading with a filter sample obtained during the corresponding five-minute period. Measurements were made with three plant operating conditions: 1) with soot blowing, 2) without soot blowing, and 3) with the plant operating at minimum load (about 50% of capacity). Soot blowing is a common procedure in which blasts of steam or air are used to clean soot off the heat exchanger, resulting in a substantial change in effluent particulate properties. The heavy lines in the curves represent the best fit calibration from data points. The numbered lines represent the best fit calibration for each of the three plant operating conditions.

Figure 9 shows significantly different mass loading calibrations for the three plant operating conditions. All methods which do not directly sense particle mass share this problem. Each instrument installation requires a separate calibration for each different operating condition. The calibration also must often be checked (every few months or so) to be sure no change has occurred. The cost of these calibrations raises the total instrument cost above the potential cost of direct mass sensing instruments such as beta radiation attenuation and piezoelectric microbalance instruments. In addition, the instrument operator must find which plant operating conditions are in use in order to know which calibration is correct.

With light-transmission instruments, the only alternative to such high maintenance and operations costs is to disregard the effects of the changing plant operating conditions and accept the poor correlation of the instrument with particulate mass concentration. The errors involved with typical mass loadings (less than 200 milligrams per cubic meter) are shown to be quite substantial even for the best instruments. Figure 9 represents the best particulate mass correlation found by the authors in the literature. The errors would no doubt be worse with instruments of lesser quality. Therefore, light-transmission instruments do not measure particulate mass concentration with acceptable accuracy in their present state of development.



LEGEND: 1-WITH SOOT BLOWING; 2-WITHOUT SOOT BLOWING; 3-MINIMUM LOAD

Figure 9. Results of an experimental calibration of two light-transmission instruments in a modern coal-fired power plant.

Several possible variations to light-transmission techniques exist which may improve the correlation with particulate mass concentration. One such variation involves the use of several monochromatic light beams with differing wavelengths. By proper data reduction, some particle size distribution information could be obtained. The particle concentration measurement could then be partially corrected for any size changes. Such changes, although easily automated, would significantly increase the cost of the instrument. The improvement in particulate mass correlation with such an instrument cannot be estimated at this time. However, correlation would still be poor in many cases since only the error due to variations in particle size is reduced. Errors due to variations in particle shape, refractive index, surface characteristics, and density are not reduced.

1.8 REVIEW OF EXPERIMENTAL WORK

Since one of the significant conclusions reached during the state-of-the-art study early in this program was that beta radiation attenuation was the most promising technique for measuring particulate mass concentration in stacks, experiments to uncover problem areas and to evaluate two prototype beta instruments were conducted. The emphasis was on evaluation of the beta technique itself, not on the features of a particular instrument design.

1.8.a. Laboratory Experiments

In preliminary laboratory experiments using a Geiger-Muller detector, two radiation sources, promethium 147 and carbon 14, were compared with each other and with theory. Several important results emerged.

First, it has been generally assumed in the past that the relationship between beta attenuation and particle loading can be expressed accurately by:

$$I/I_0 = \exp [-\mu_m X] \quad (1)$$

where:

I_0 = intensity of beta radiation passing through a clean filter,

I = intensity of beta radiation passing through a loaded filter,

X = weight of particles on the filter, mg/cm^2 , and

μ_m = calibration constant, usually assumed to be independent of everything except radiation source.

Our experimental results, explained in Section 2 of this report, show that I/I_0 is not a simple linear exponential and significant errors (greater than $\pm 10\%$) can result from assuming Equation 4 to be correct.

Secondly, we found experimentally that μ_m in Equation 4 depends on I_o . Stated differently, the calibration of a beta instrument depends on the initial filter thickness. Details are shown later in Section 2 of this report. Uncertainties in excess of $\pm 5\%$ can result (in addition to the errors caused by the non-linear exponential relationship) using ordinary filter tapes with $\pm 5\%$ variation in clean filter thickness, using C-14 as a beta source, and making the initial beta count (I_o) on the exact same spot of filter paper as the final beta count (I).

Third, although Pm-147 is somewhat less sensitive than C-14, uncertainties caused by variations in the initial filter thickness, using Pm-147 are about half as great as for C-14. Thus, it appears that Pm-147 may be slightly superior to C-14 as a beta radiation source from a technical standpoint. However, C-14 has less restrictive licensing laws making it easier to use and transport.

All three of the above-mentioned anomalies can be corrected on-line by using data from our extensive calibration of the instrument in a small computer program. Further work of this type is needed to identify other possible errors such as changes in particulate composition. Such work could further illuminate the magnitude of such errors in practical sampling applications.

1.8.b. Field Experiment Station

Because of the lack of a controlled facility to accurately simulate the stack environment, we designed, constructed, and tested a particle sampling facility on a 550-megawatt, coal-fired power plant owned by Northern State Power Company and located at Bayport, Minnesota. Not enough information is known at the present time about the stack environment to construct a simulation test facility to obtain information about the practical ability of instruments to obtain accurate particle mass concentration data. Although the samples reaching the test instruments in our facility are not truly representative of the conditions in the stack, the test samples are quite representative of samples obtained by a typical sampling system.

The sampling system removes a heated stream of effluent from the stack, splits the sample into 2 identical parts, and passes the 2 samples through identical boundary-layer dilution coolers to the 2 test instruments. The stream is heated to a temperature above the acid dew point to prevent condensation on the particles and on the sampling tubes. Since the instruments were not capable of high temperature operation, boundary-layer dilution cooling caused the effluent stream to cool while condensation particle losses were prevented by keeping the particles from the walls of the system until sufficient dilution had occurred. The 2 test instruments received identical samples so that any differences in measurement could be attributed primarily to instrument differences.

Tests of the sampling facility using a pair of identical 47-mm Nuclepore filters in identical filter holders identified acceptable operating conditions and showed a ratio R_F of nearly 1.0 where R_F is the ratio of (test instrument filter collected weight)/(reference parallel filter collected weight). The consistency of the results is good with the standard deviation of R_F for all acceptable operating conditions being less than 0.05.

1.8.c. Field Evaluation of Two Prototype Beta Instruments

Two prototype beta instruments, developed by GCA Corporation and Industrial Nucleonics, Inc., under EPA contracts, were evaluated in the field sampling facility. Each was compared with a reference parallel 47-mm Nuclepore filter in a modified Gelman filter holder. The particle mass concentration measured by the GCA instrument agreed very well with the reference parallel filter with $R_{GCA} = 0.98$ with a standard deviation of 0.04. The particle mass concentration measured by the Industrial Nucleonics instrument did not agree well with the reference parallel filter with R_{IN} generally between 0.33 and 0.65. Consistency was also poor.

1.9 CONCLUSIONS AND RECOMMENDATIONS

1. The highly consistent accuracy of the GCA instrument in our limited tests verifies the primary finding of the state-of-the-art study conducted earlier under this contract. Beta radiation attenuation is presently the best technique for automatically measuring effluent particulate mass concentration with the present state of development. Beta radiation attenuation actually senses a particle parameter very closely related to mass. One measurement takes only 1 - 15 minutes. Some of the other experimental results indicate that more experimental evaluation and development remains if an accurate, reliable particle mass concentration monitor is to result. Engineering design improvement of present commercial models appears to be needed, especially in the sample extraction probe, sensor geometry, and particle collection technique. Beta radiation attenuation will probably remain one of the most favorable particulate mass monitoring methods for some time in all three potential use areas: continuous monitoring by stack owners, by pollution abatement personnel, and by control equipment evaluators.
2. The piezoelectric microbalance technique detects particle mass directly. It could soon replace beta radiation attenuation as the most favorable and most accurate automatic particulate mass monitor for effluents, especially for measurement of low concentrations such as downstream of efficient control equipment and such as for measurement of particle mass size distributions

in the smaller size ranges. It remains to be proven whether the instrument can be made to operate with coal combustion effluent particles. The adherence of larger particles to the crystals appears to be the major potential problem. This technique is similar in many ways to the beta attenuation technique, but has the additional feature of higher sensitivity, which should allow significantly faster measurements (probably one measurement every few seconds).

3. The Konitest electrostatic contact charge technique reportedly shows surprisingly good correlation with gravimetric particulate mass concentration in several extensive experimental tests performed on coal combustion sources. It is known that particle composition and instrument contamination strongly affect the measurements. It is not clear whether these factors are problems in coal combustion effluents. Since the theoretical basis for the measurement is largely undefined, further testing is necessary to evaluate the Konitest for particulate mass monitoring in any coal combustion source. The instrument's primary features are its nearly instantaneous response, continuous readout, and simple construction.
4. Light-transmission and light-scattering techniques do not measure particulate mass concentration. Although light-transmission instruments are the most commonly used particulate emissions monitors today, they only measure something related to the visual appearance of the stack plume. However, since they are simple, inexpensive, and easy to operate and maintain, they will probably remain popular as emissions monitors even though they do not measure particle mass. Although a number of particle parameters, such as size and shape, affect the particle concentration measurement, light-transmission and light-scattering instruments can be calibrated to give rough measurements of particulate mass emissions under a given constant set of conditions, but the calibration is no longer valid when conditions change. Therefore, these instruments have serious limitations in their use as monitors of particulate mass concentration in effluent gas streams. Several interesting variations of light-transmission instruments have been suggested. Although they may improve the correlation with particle mass, no way can be seen to fully overcome the invalidation of mass calibration when particle properties change.

1.10 ACKNOWLEDGEMENTS

The authors thank Dr. John G. Olin for his many helpful suggestions and for critically reviewing an early manuscript of this section. The authors also thank Professors K. T. Whitby and B.Y.H. Liu, J. P. Pilney, N. Barsic, and F. D. Dorman for many helpful suggestions and much useful advice. Special thanks go to the Project Officer, J. O. Burckle for his continued interest in the work and for his critical review of the manuscript of this report.

1.11 BIBLIOGRAPHY

1. Sem, G. J., Borgos, J. A., Olin, J. G., Pilney, J. P., Liu, B.Y.H., Barsic, N., Whitby, K. T., and Dorman, F. D., "State of the Art: 1971 Instrumentation for Measurement of Particulate Emissions from Combustion Sources, Volume I: Particulate Mass - Summary Report, Volume II: Particulate Mass - Detail Report", Thermo-Systems Inc., St. Paul, Minn., report to EPA under Contract CPA 70-23 (1971).
2. Dobbins, R. A., and S. Tempkin, Journal of Colloid and Interface Science, 25, 329 (1967).
3. Beck, M. S., and N. Wainwright, Powder Technology, 2, 189 (1968).
4. Duwel, L., Staub-Reinhalt. der Luft (English Translation), 28, 42 (March, 1968).
5. Whitby, K. T., private communication to the authors (1970).
6. Langer, G., Powder Technology, 2, 307 (1968-69).
7. Goldschmidt, V. W., and M. K. Householder, Atmospheric Environment, 3, 643 (1969).
8. Gast, T., Staub-Reinhalt. der Luft, 30, 235 (1970).
9. Gast, T., Staub-Reinhlat. der Luft, 21, 136 (1961).
10. Gruber, C. W., and C. E. Schumann, Journal of the Air Pollution Control Association, 16, 272 (1966).
11. Sinclair, D., Journal of the Air Pollution Control Association, 17, 105 (1967).
12. Charlson, R. J., Environmental Science and Technology, 3, 913 (1969).
13. Barrett, E. W., and O. Ben-Dov, Journal of Applied Meteorology, 6, 499 (1967).
14. Ogle, H. M., Journal of the Air Pollution Control Association, 18, 657 (1968).
15. Martens, A. E., and J. D. Keller, Journal of the American Industrial Hygiene Association, 29, 257 (1968).
16. Belz, R. A., Clearinghouse No. AD 674 741 (1968).
17. Coenen, W., Staub-Reinhalt. der Luft (English Translation), 27, 32 (Dec., 1967).
18. Schutz, A., Staub-Reinhalt, der Luft (English Translation), 26, 18 (May, 1966).

19. Dresia, H., P. Fischotter, and G. Felden, VDI-Z, 106, 1191 (1964).
20. Jackson, M. R., A. Lieberman, L. B. Townsend, and W. Romanek, Proceedings of the National Incinerator Conference, 182 (1970).
21. Lilienfeld, P., Conference of the American Industrial Hygiene Association, Detroit (May, 1970).
22. Schnitzler, H., O. Maier, and K. Jander, SchrReihe Ver. Wass.-Boden-Lufthyg. Berlin-Dahlem, 33, 77 (1970).
23. Horn, W., Staub-Reinhalt. der Luft (English Translation), 28, 20 (Sept., 1968).
24. Olin, J. G., and G. J. Sem, Atmospheric Environment, Pergamon Press, 5, (1971).
25. Olin, J. G., and G. J. Sem, and D. L. Christenson, American Industrial Hygiene Association Journal, 32 (April, 1971).
26. Chuan, R. L., Journal of Aerosol Science, 1, 111 (1970).
27. Coenen, W., Staub-Reinhalt. der Luft, 24, 350 (1964).
28. Mohnen, V. A., and P. Holtz, Journal of the Air Pollution Control Association, 18, 667 (1968).
29. Grindell, D. H., AEI Engineering, 2, 229 (1962).
30. Whitby, K. T., and B.Y.H. Liu, Aerosol Science, ed. by C.N. Davies, p. 59, Academic Press, New York (1966).
31. Schutz, A., Staub-Reinhalt. der Luft (English Translation), 26, 1 (Oct., 1966).
32. Prochazka, R., Staub-Reinhalt. der Luft (English Translation), 26, 22 (May, 1966).

DETAILED REPORT

	<u>Page</u>
SECTION 2. PRELIMINARY LABORATORY EXPERIMENTS	31
SECTION 3. DESIGN OF FIELD EXPERIMENT STATION	52
SECTION 4. CALIBRATION OF STACK FACILITY AT THE FIELD EXPERIMENT STATION	61
SECTION 5. FIELD EVALUATION OF TWO PROTOTYPE BETA INSTRUMENTS .	78
SECTION 6. EVALUATION OF TRANSMISSOMETER TECHNOLOGY	83
SECTION 7. APPENDICES	91

SECTION 2. PRELIMINARY LABORATORY EXPERIMENTS

2.1 INTRODUCTION

Since one of the significant conclusions reached from the state-of-the-art study early in this program was that beta radiation attenuation was a promising technique, an instrument was purchased for experimentation. A Gelman* Model 25000 was selected on the basis of cost and delivery schedule. Most of the work with the Gelman instrument was performed in Thermo-Systems' laboratory. Limited testing was also done with this instrument at the stack facility described elsewhere in this report, but the instrument did not function well enough to produce any reliable data there.

This section discusses the results of various laboratory experiments performed with portions of the Gelman instrument. We were not so much interested in testing the Gelman design as the beta radiation attenuation technique itself. We experimented with two radiation sources: promethium 147 and carbon 14. Our data is compared with theory and to a limited extent with the data of other investigators. A treatment of the theoretical aspects of the use of this technique is given in the section of Volume II of this report entitled "Beta Radiation Attenuation."

2.2 CALIBRATION REPEATABILITY

It is frequently assumed, on the basis of several approximations, that the calibration curve of an instrument using the beta technique is of the form**

$$I/I_o = \exp [-\mu_m X] \quad (4)$$

where:

I_o is the intensity of the beta radiation passing through a clean filter,

I is the intensity of the beta radiation passing through a dirty filter,

X is the weight (mg/cm^2) of particles on the filter, and

μ_m is the calibration constant, usually assumed to be independent of everything but the radiation source.

*Manufactured by Gelman Instrument Co., Ann Arbor, Michigan

**See Volume II, pp. 70-85.

Such a calibration curve, shown in Figure 10, was provided with the Gelman instrument. The radioactive source is 50 microcuries of C-14. The radiation sensor is a Geiger-Muller tube, Amperex Type 18515.

We initially decided to verify whether the above calibration curve was accurate. The electronics, which basically consisted of a timing circuit, a counting circuit, and a digital printer, were found to be repeatable only to within about $\pm 5\%$ in the range of interest. To determine this, we substituted an extra filter to simulate particle loading. This allowed nearly exact reproduction of filter loadings, and the output varied $\pm 5\%$ from the average for several runs with the same loading. This occurred over nearly the entire portion of the calibration curve supplied with the instrument. A longer counting time or a larger radiation source might have decreased the variability, but we did not modify the instrument to check this. This variability affects the accuracy of all our results with the Gelman instrument.

As a first check, we used Whatman #4* filter paper and AN-5000** membrane filter to simulate particle loadings. The Gelman instrument uses Whatman #4 in the form of a filter tape as its standard for collecting particles. These tests revealed a significant error in the calibration curve as shown by the data points in Figure 11. The value of μ_m (see Equation 4) assumed by Gelman is $0.272 \text{ cm}^2/\text{mg}$. It would require a large adjustment of this coefficient to fit the data to the Gelman-supplied curve.***

We found that the consistency of the thickness of filter material (particularly Whatman #4 filter paper) is not very good. The paper contained variations ranging from about 8 to about 9 mg/cm^2 . Extensive testing was done in our home laboratory to determine the practical effect of filter thickness variations on the calibration of a beta instrument.

The results of the first series of these tests was summarized in Figure 12. Again, the procedure used was to add filter thicknesses of known density to simulate increased filter loadings. Each curve in Figure 12 has a different value of X_0 , which is the initial unloaded filter weight used to measure the I_0 radiation intensity. The value of X_0 in these tests varied from zero to 11.3 mg/cm^2 . This covers the thicknesses of most practical filter materials.

*Sold by H. Reeve Angel & Co., Inc., Clifton, New Jersey.

**Sold by Gelman Instrument Co., Ann Arbor, Michigan.

***See Volume II, p. 76 for typical values of μ_m .

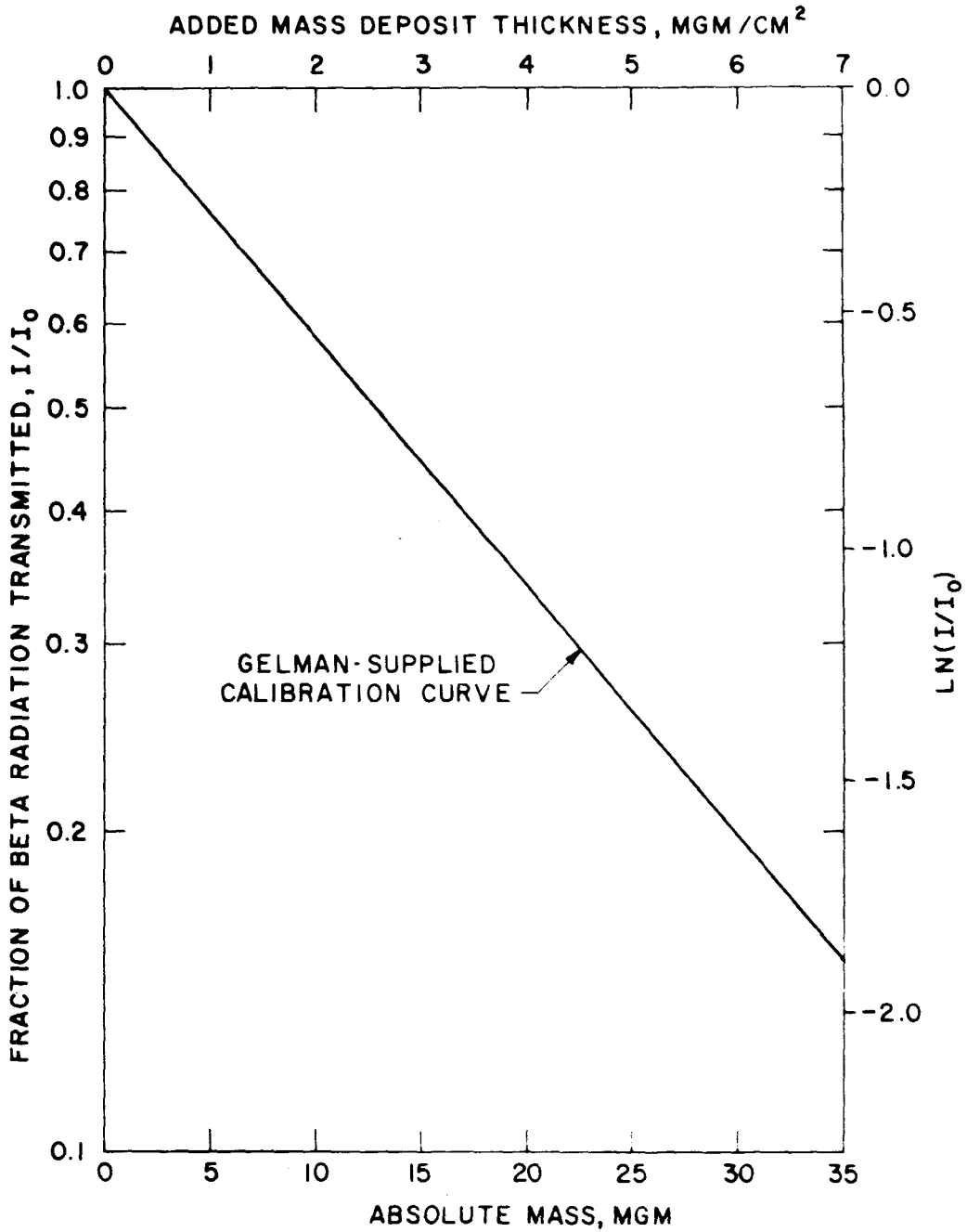


Figure 10. Calibration curve supplied with the Gelman Model 25000 beta radiation instrument for relating the beta transmission to either deposit thickness or absolute mass.

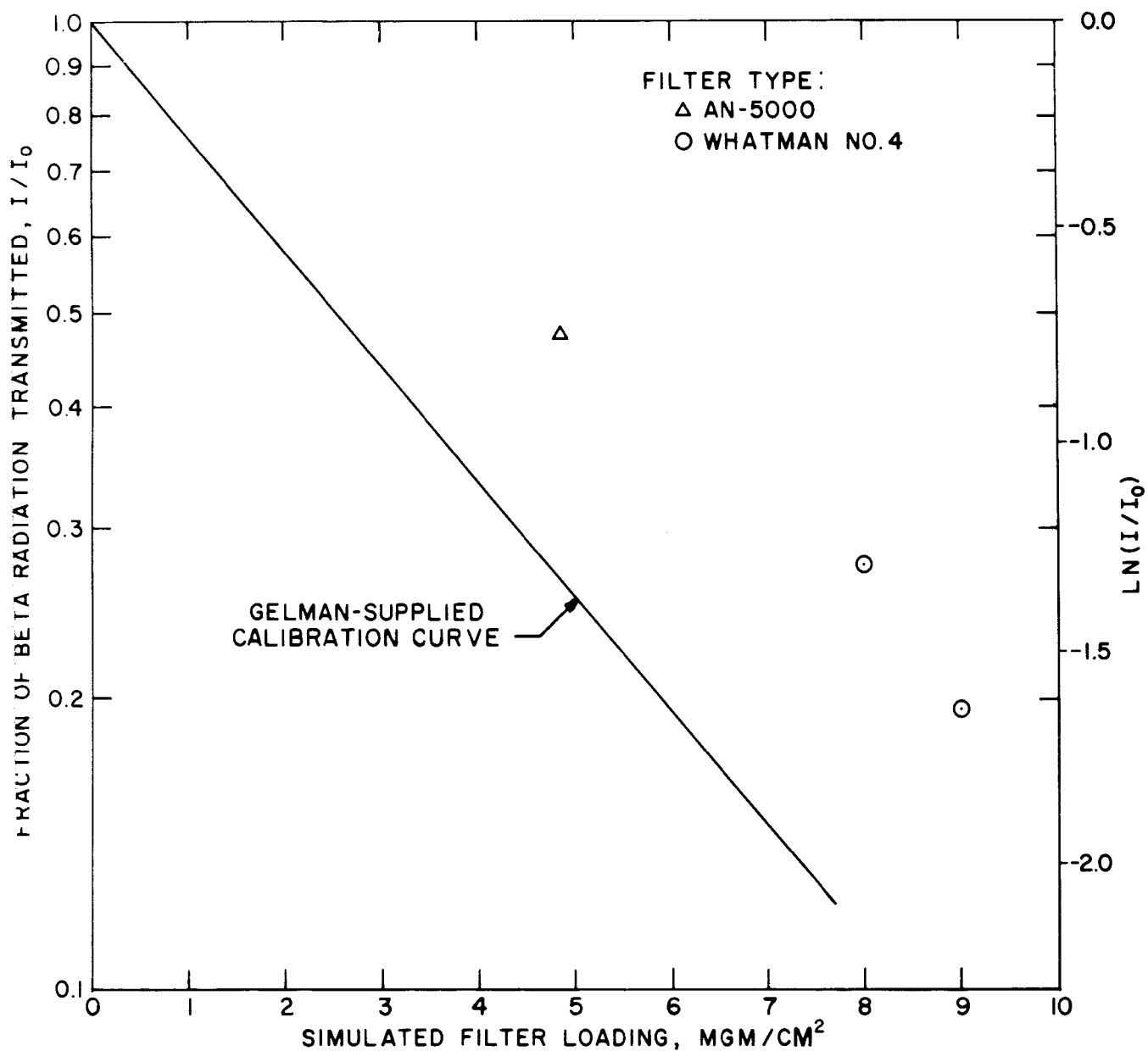


Figure 11. Comparison of Gelman-supplied calibration curve with actual data obtained using Whatman #4 filter paper and Gelman AN-5000 membrane filters to simulate deposit loadings.

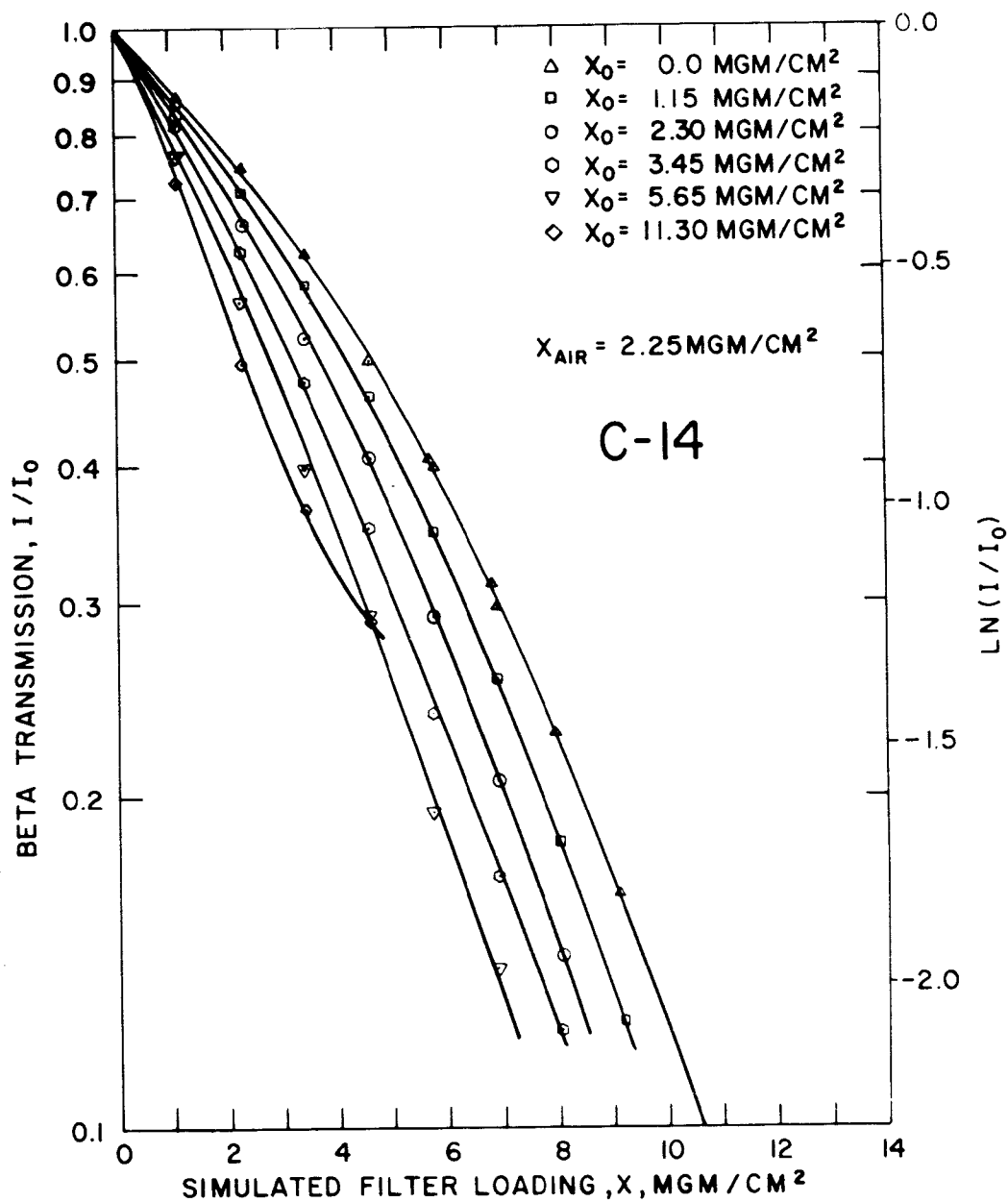


Figure 12. Results of tests using the standard Gelman sensor configuration, C-14, and with six different initial clean filter thicknesses. The filter loading was simulated by other filters (Millipore Type HA and Nuclepore 5 μm pore size). Note that variations in initial clean filter thickness significantly affects the calibration curve.

The filters used in this experiment were Millipore* cellulose membrane filters (Type HA, 0.45 μm pore size, thickness = 5.65 mg/cm^2) and Nuclepore filters** (5 μm pore size, thickness = 1.15 mg/cm^2). It should be noted that the value of X_o does not represent all the mass between the radiation source and detector during the I_o count. An air gap of 1.6 cm ($X_{\text{air}} \approx 2.25 \text{ mg}/\text{cm}^2$) was present, along with the window of the GM counter tube (approx. thickness of 1.5 - 2.0 mg/cm^2).

These curves illustrate that the variation in thickness of filter material has a significant effect on the calibration of an instrument such as the Gelman instrument. Their non-linearity (on a semi-logarithmic scale) also suggests that the calibration curve cannot be assumed to be a true exponential function of the form shown in Equation 4. As the value of X_o increases, the curves seem to become more linear.

The next step was to move the radiation source and detector closer together and thus reduce the thickness of the air gap between them to 0.2 cm ($X_{\text{air}} \approx 0.36 \text{ mg}/\text{cm}^2$). We hoped to separate out any effects of the geometry of the apparatus in this way. These results are shown in Figure 13. Notice that the same general trends in the data are present as in Figure 12. From the results of these two experiments, we suggest the possibility that, independent of the geometrical configuration, there is a very significant error in assuming the calibration curve of a beta instrument to be of the form shown in Equation 4.

To point out the magnitude of this error, Figure 14 presents some of the data from Figure 13 in a different way. Figure 14 shows the effect of the filter thickness (X_o) on the determination of the unknown (X) for a constant output (output = I/I_o). For example, it was stated earlier that Whatman #4 filter paper varies between 8 and 9 mg/cm^2 . Looking at Figure 14, we see that if our output (I/I_o) was measured to be 0.6, and if we did not know the filter paper thickness ($8 < X_o < 9$), then the particle loading on the filter could be anywhere between 3.9 and 4.3 mg/cm^2 - a 10% span. All this would be assuming the nonlinear curves in Figure 13. If linear approximations, such as Equation 4, were used, the error could be larger.

It should be kept in mind that all the above data were obtained with a C-14 radiation source.

*Sold by Millipore Corporation, Bedford, Mass.

**Sold by General Electric Company, Pleasanton, Calif.

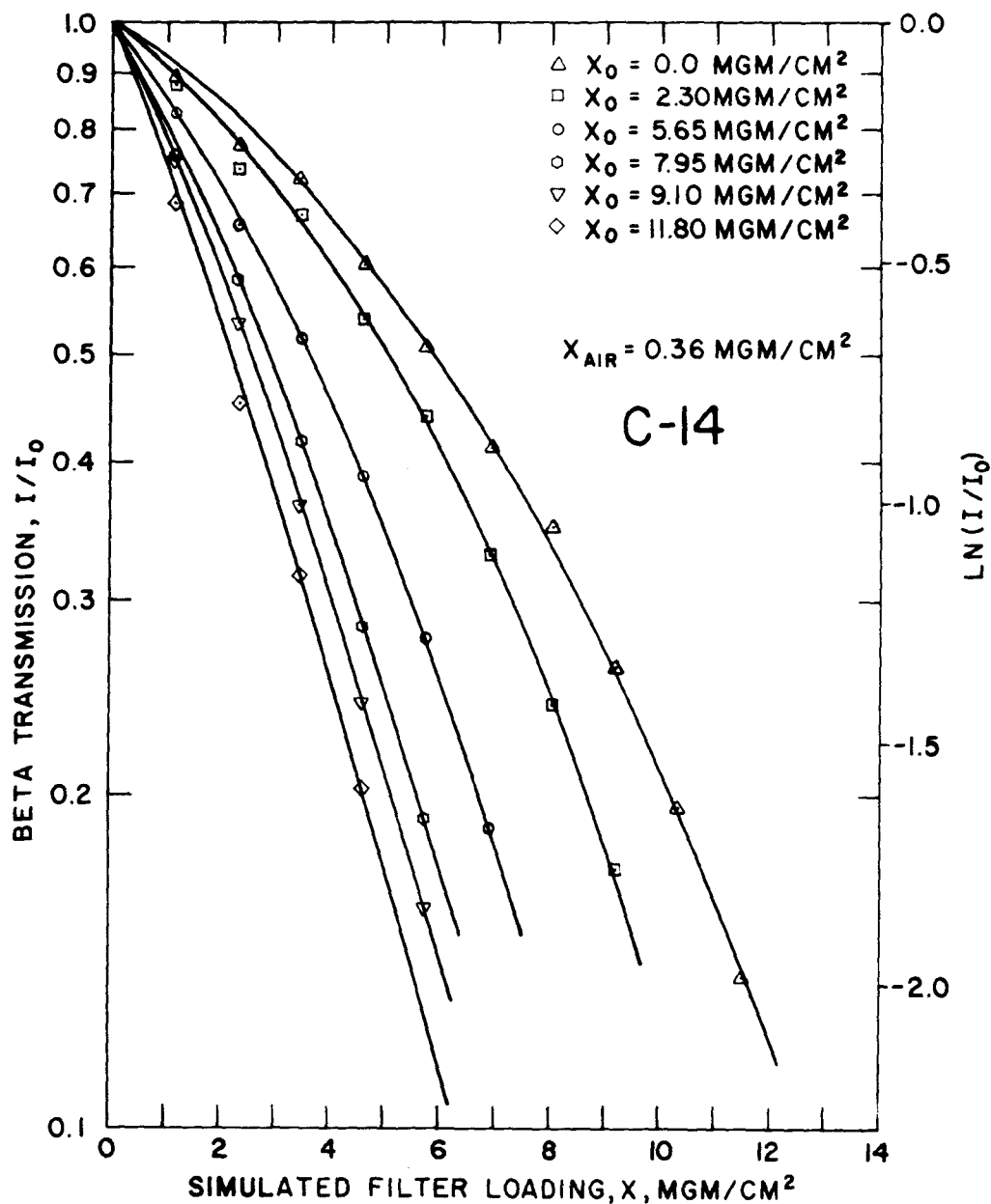


Figure 13. Results of C-14 tests run identically to those in Figure 12 except with a smaller air gap between beta source and detector. The results are similar.

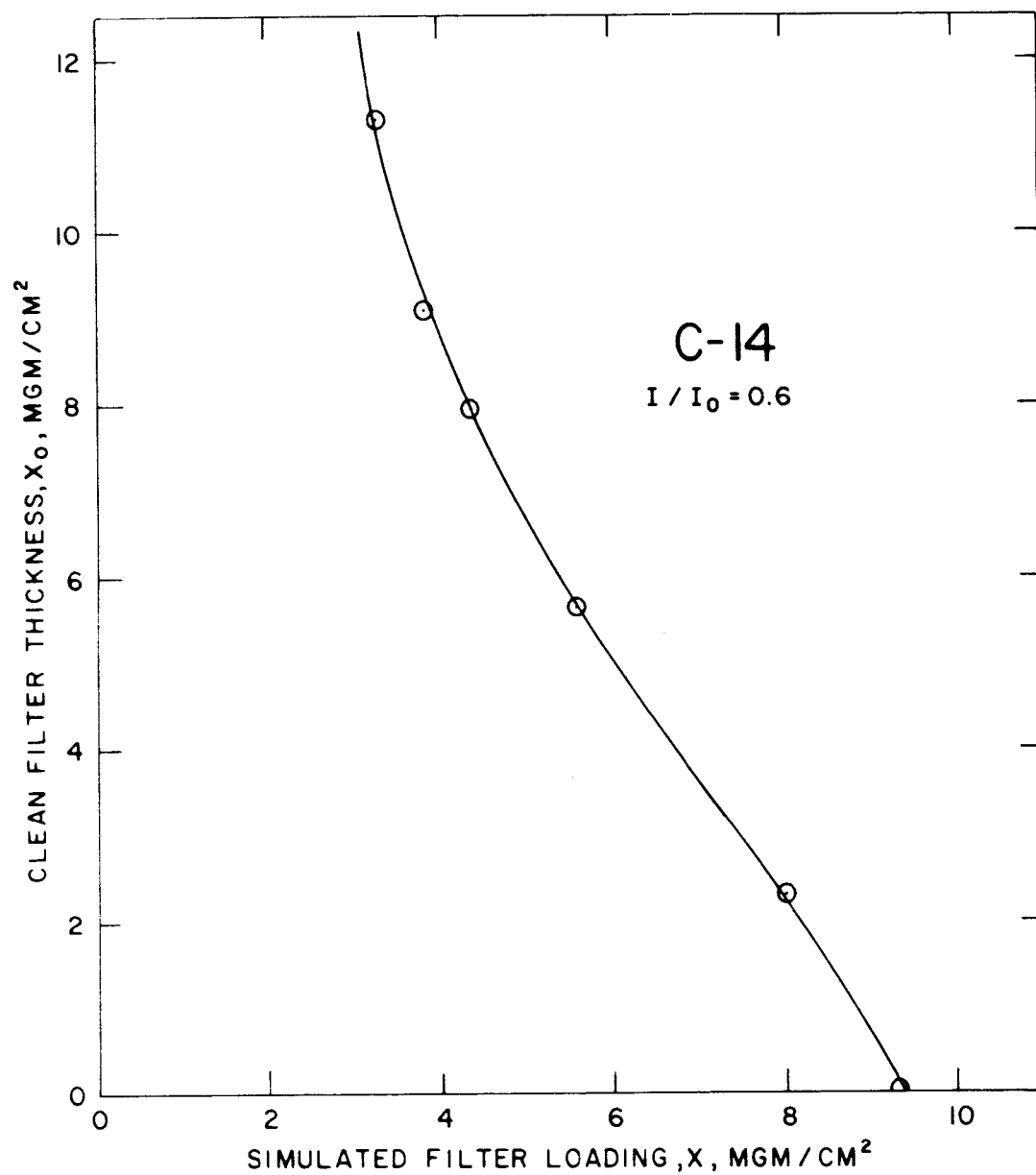


Figure 14. C-14 data of Figure 13 plotted to show that, for a constant beta instrument output ($I/I_0 = 0.6$), the measured filter loading depends significantly on the initial clean filter thickness.

2.3 EXPERIMENTS WITH PROMETHIUM-147

In order to establish criteria with which to evaluate radiation sources for use in beta instruments, a small amount of Pm-147 was purchased. Pm-147 has a short half-life (2.26 years as opposed to 5568 years for C-14) and the radiation is more energetic ($E_{\text{max}} = 0.229$ mev as opposed to 0.155 mev for C-14)*. The maximum amount that can be used without an AEC license is 10 microcuries, as opposed to 50 microcuries for C-14. Our experiments therefore were done with only 10 μc of Pm-147.

The data was taken in the same manner as that of Figure 12 and is presented in Figure 15. These curves cover the same range of filter thicknesses as those for C-14. Two characteristic differences should be emphasized. The first is the nonlinearity of the curves. The curves for Pm-147 are more nearly linear than those for C-14, and therefore more closely approximate Equation 4. Second, as the value of X_0 changes, the curves are not so greatly shifted. As will be explained later, these two differences result from a single fundamental difference in the radiation energy spectra.

The shift in the curves as the value of X_0 changes is portrayed in Figure 16, which is analogous to Figure 14. These two curves can provide a rough comparison of the errors one might expect if the filter weight varied from 8 to 9 mg/cm^2 (e.g., Whatman #4 filter paper). From Figure 16, if the instrument output (I/I_0) was 0.6, and if $8 < X_0 < 9$, the particle loading on the filter could be anywhere from 4.35 to 4.55 mg/cm^2 - a span of 4.6%. The corresponding span for C-14 was 10% over this filter loading range. Thus, the errors due to variations in filter thickness will be about 1/2 as large with Pm-147 as with C-14. In either case, the error will be greater in practice if the linear approximation of Equation 4 is used as is normal practice.

No other radiation source materials were tested under this program.

2.4 RADIATION SOURCE CHARACTERISTICS

In order to gain more information about the radiation characteristics, and hopefully to gain the ability to predict a calibration curve given a radiation source, a study was made of the energy spectra of C-14 and Pm-147. A well-known fact about emitters of beta radiation is that the energy levels of the beta rays (or particles) are not all the same.** That is to say, for a given source or emitter, an escaping beta particle may have an energy level anywhere between nearly zero to a characteristic maximum value for that isotope (E_{max}). Of course, this energy gets depleted little by little as the particle "collides" with atoms or molecules.

*See Volume II, p. 79.

**See Volume II, p. 76.

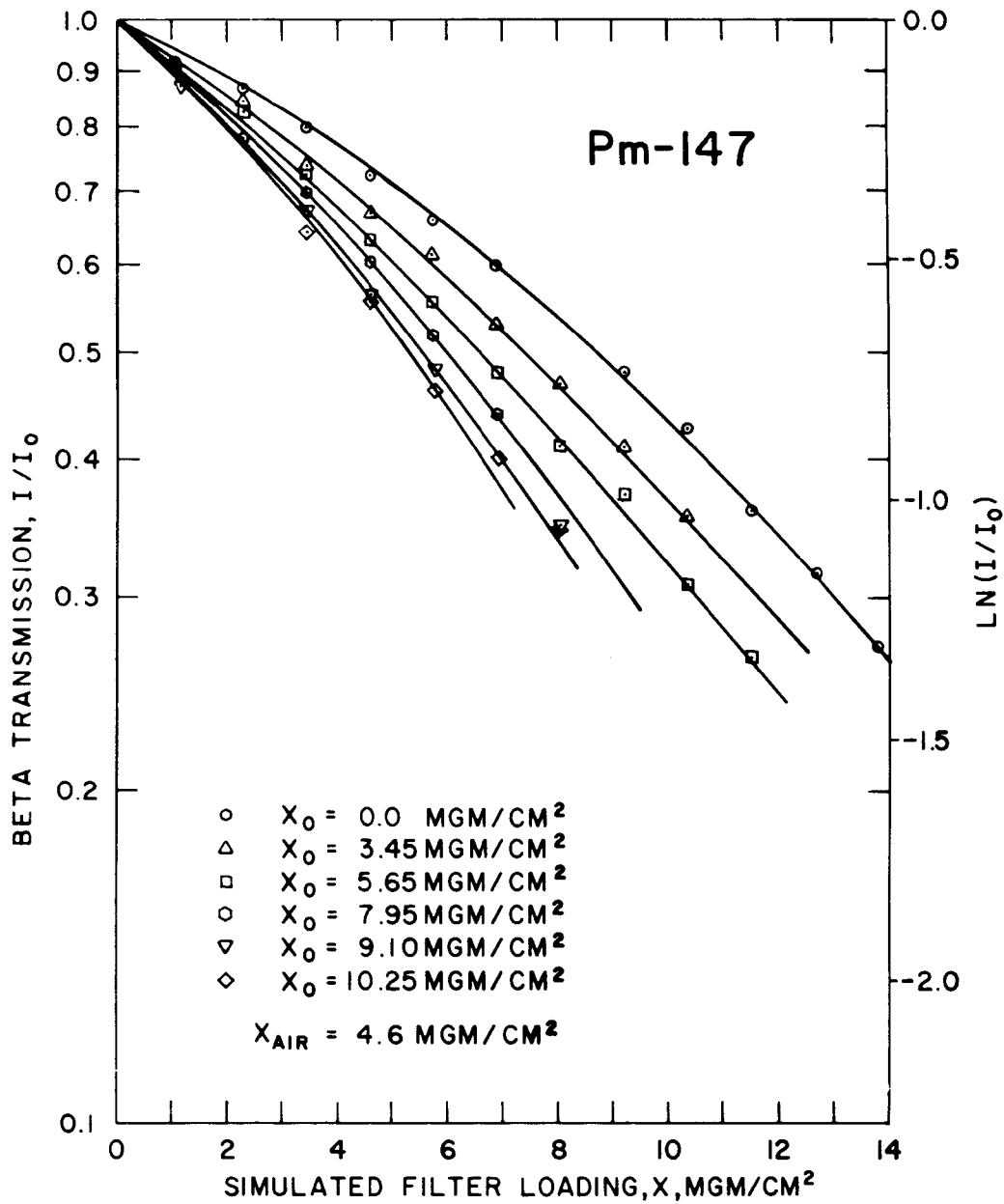


Figure 15. Results of simulated filter loading tests using Pm-147 and six initial clean filter thicknesses, analogous to Figure 12.

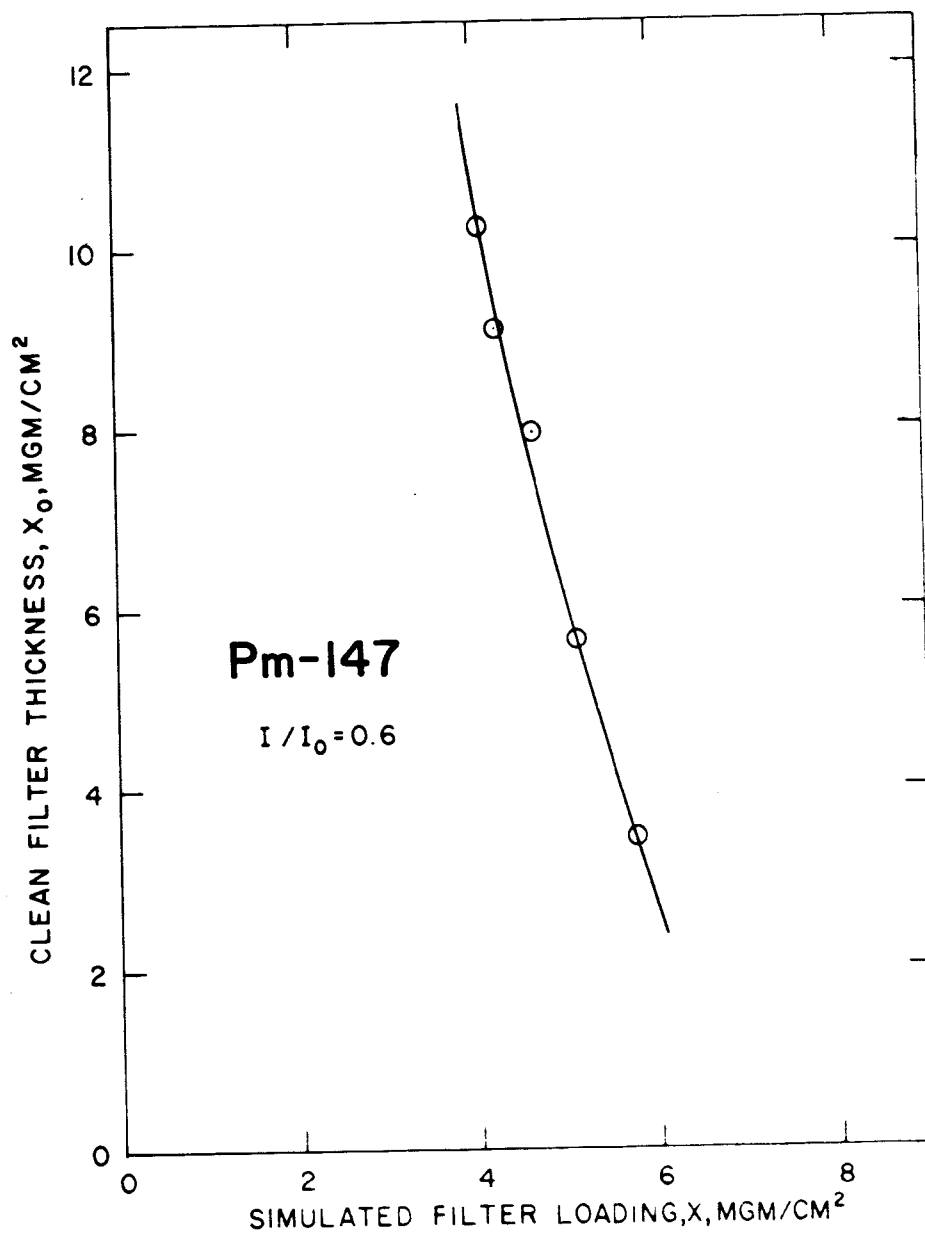


Figure 16. Pm-147 data of Figure 15 plotted to show that, for a constant beta instrument output ($I/I_0 = 0.6$), the measured filter loading depends less strongly on the initial clean filter thickness than does C-14 shown in Figure 14.

A calibration curve, such as those in Figure 13, is really a measure of the amount of radiation that is absorbed (or "stopped") by the deposit on a filter. A prediction of such a curve could easily be made if we knew how much radiation would be absorbed by the filter itself, the air gap between beta source and detector, and the detector window, and also knew how much more would be absorbed if a certain mass of particles was added on the filter. Two more pieces of information are needed to predict the calibration curve. First, we must know the relationship of range versus energy for beta radiation (i.e., how many mg/cm² will a beta particle of known energy penetrate on the average). Second, we must know the cumulative distribution of beta particles versus their energy. This will indicate the fraction of particles emitted with energy greater than a specified energy level.

The relationship of range versus energy has been determined by Friedlander, et al.,* and is shown in Figure 17. Notice that at typical energy levels, the relation is not linear.** The energy distribution curve for a number of beta radiation sources have been theoretically calculated by Hogan, et al.,*** including the spectra for C-14 and Pm-147. These are shown in Figures 18 and 19.

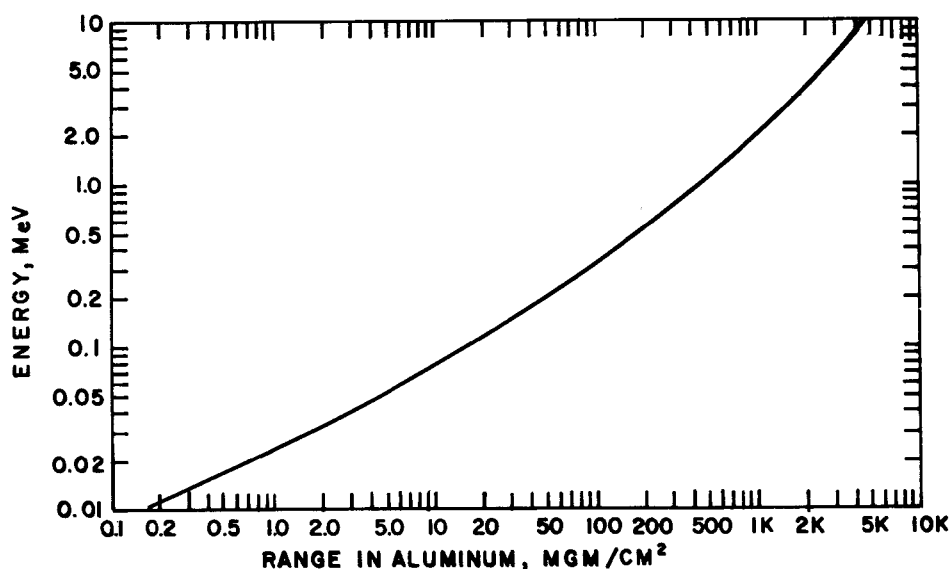


Figure 17. Relationship of the energy required for the beta particle to penetrate a given thickness of aluminum.

*Friedlander, G., Kennedy, J.W., and Miller, J.M., Nuclear and Radiochemistry, 2nd Ed. Wiley, N.Y., N.Y. (1964).

**See Volume II, p. 72.

***Hogan, O.H., Zigman, P.E., Mackin, J.L., "Beta Spectra: II. Spectra of Individual Negatron Emitters", U.S. Naval Radiological Defense Laboratory, Report USNRDL-TR-802, 1964.

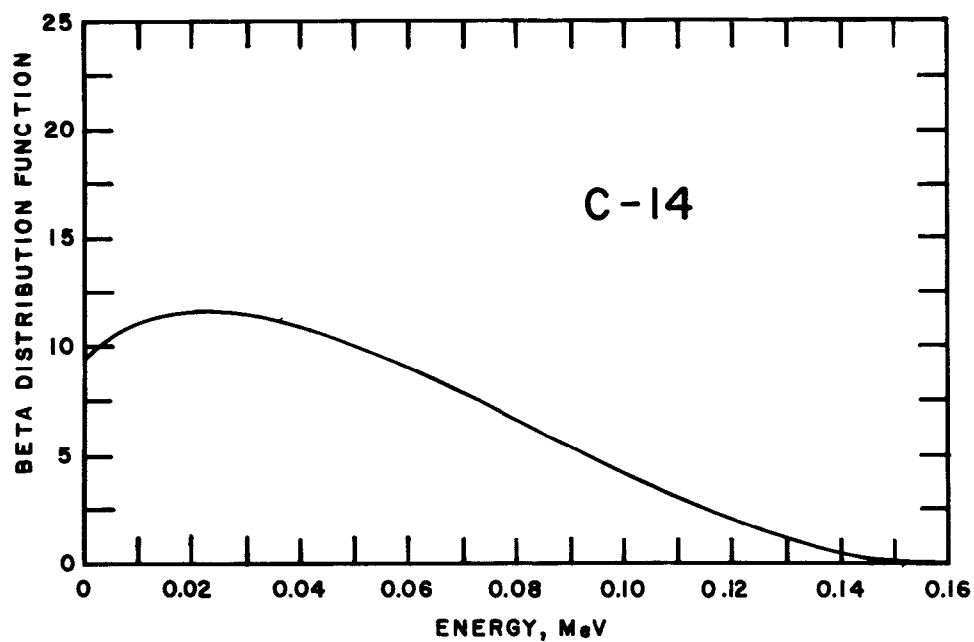


Figure 18. Energy distribution spectrum for a C-14 beta source.

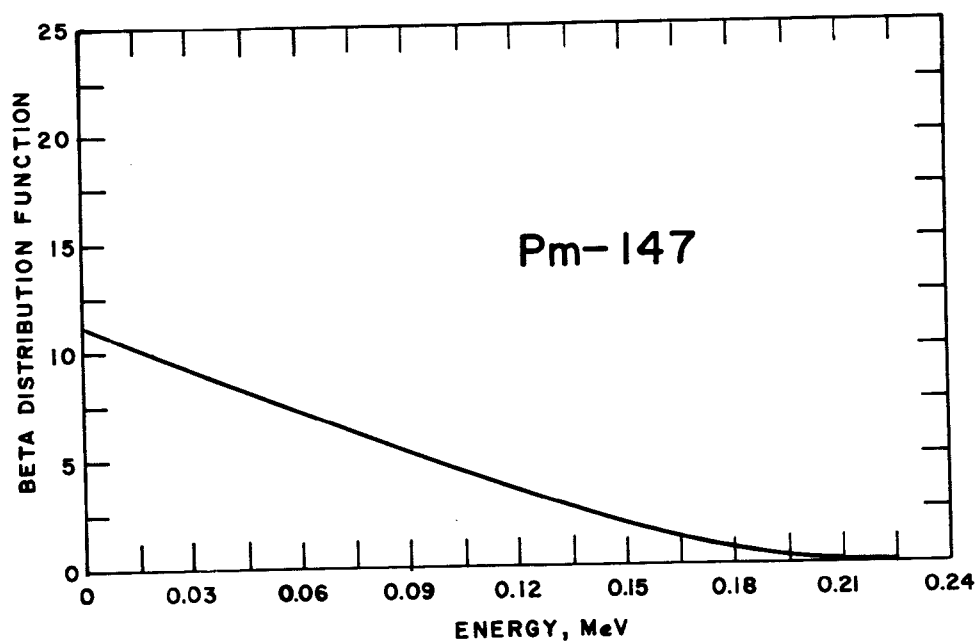


Figure 19. Energy distribution spectrum for a Pm-147 beta source.

These energy spectra must be plotted as the cumulative energy distribution (i.e., fraction of particles with energy greater than E versus E) in order to be meaningful. Figure 20 shows this cumulative energy distribution for C-14. The two curves, Figure 17 and Figure 20, provide the last two pieces of information needed to predict a calibration curve for C-14.

The information in these curves is more useful if the cumulative range distribution is plotted (Figure 21). This is because it is the range of the beta particles (i.e., how much mass in mg/cm^2 is required to stop the particles), not the energy of the particles, which is of interest.

Figure 21 is a form of calibration curve for a C-14 source, though it is somewhat cumbersome to use. First, one would have to measure the thickness in mg/cm^2 of the air gap, the detector window, and the unloaded filter by some other means. This would then tell us the range required of particles to make the zero count. For instance, suppose this combination was $15 \text{ mg}/\text{cm}^2$ thick, including a reasonable value for Whatman #4 filter paper. Referring to Figure 21, this corresponds for C-14 to an intensity ratio of 0.0645, which means that 6.45% of the beta radiation emitted from the source and headed in the direction of the detector will actually reach the detector and be counted. The other 93.55% will be absorbed by the air gap, the filter, and the detector window.

The next step is to make an " I_0 " count; e.g., count beta particles for 10 seconds and note the total. A sample of particulate matter can then be collected on the filter and an "I" count can be made in the same manner as the " I_0 " count was made. The value of $\ln(I/I_0) = (\ln I - \ln I_0)$ is then calculated. We assumed the value of $\ln I_0 = \ln 0.0645 = -2.741$. We also know the difference, $\ln I - \ln I_0$. So in our hypothetical case the value of $\ln I = (\ln I - \ln I_0) + \ln I_0 = \ln (I/I_0) - 2.741$. Suppose we measured $I/I_0 = 0.5$. (This ratio will, of course, always be less than unity.) Then $\ln (I/I_0) = \ln 0.5 = -0.693$ and $\ln I = -0.693 - 2.721 = -3.434$. Referring to Figure 21, this corresponds to a range of $18.1 \text{ mg}/\text{cm}^2$. So we can say that only beta particles with ranges greater than $18.1 \text{ mg}/\text{cm}^2$ are getting through the air gap, the filter, the detector window, and the particulate matter deposited on the filter. This is about 3.2% of the radiation. More importantly, we can say that the thickness of the deposit of particulate matter on the filter is $18.1 - 15.0 = 3.1 \text{ mg}/\text{cm}^2$. This number multiplied by the filter area would yield the total mass on the filter, assuming a uniform deposit.

The nonlinearity of the curve in Figure 21 explains the nonlinearity of the previous calibration curves (Figures 12 and 13). Notice too that at the high end of the curve (i.e., range $>12 \text{ mg}/\text{cm}^2$) the nonlinearity becomes greater. In other words, it is important to know where one is operating on the curve. It is important to know the value of the filter thickness, the air gap, and the detector window.

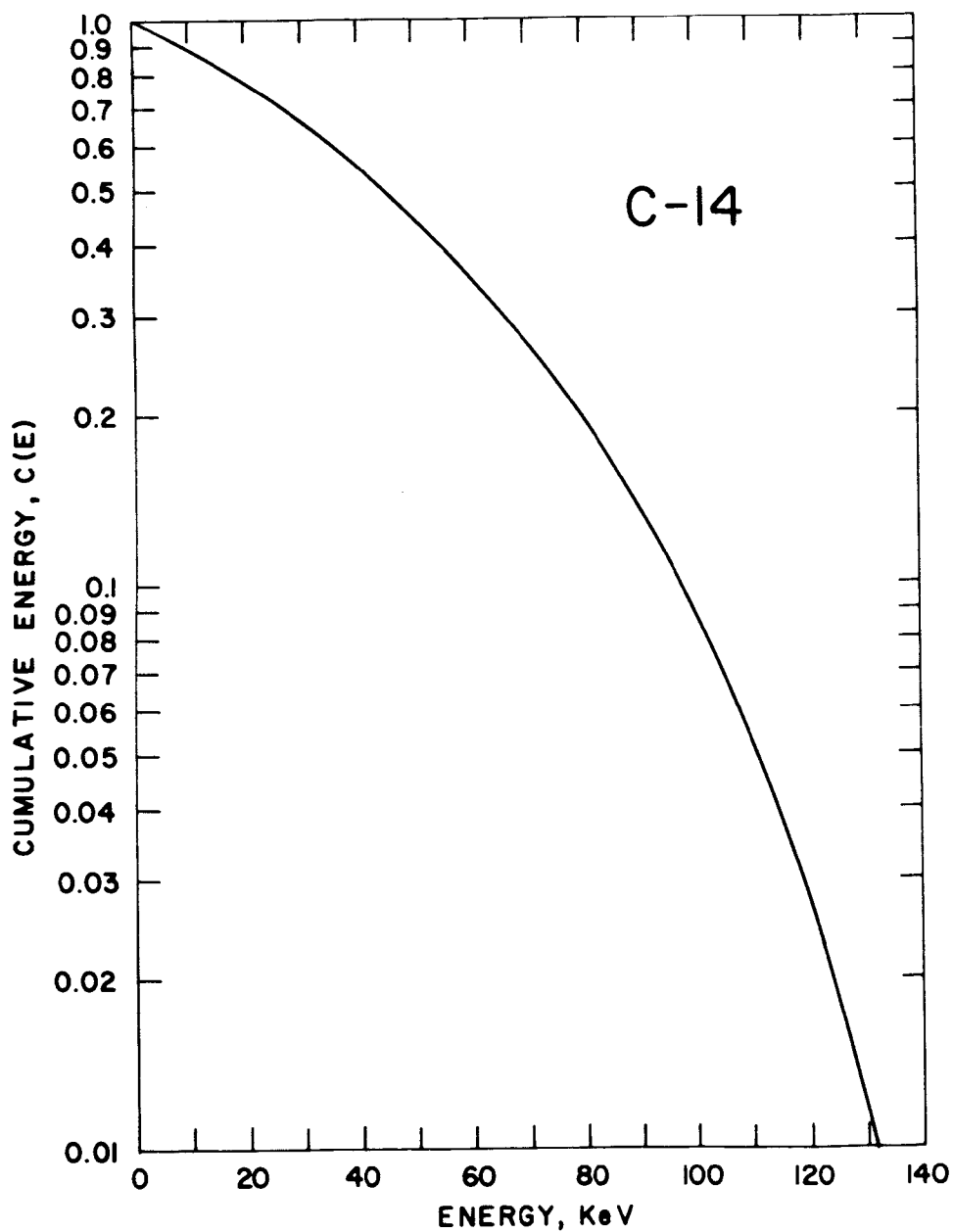


Figure 20. Cumulative energy distribution for a C-14 beta source.

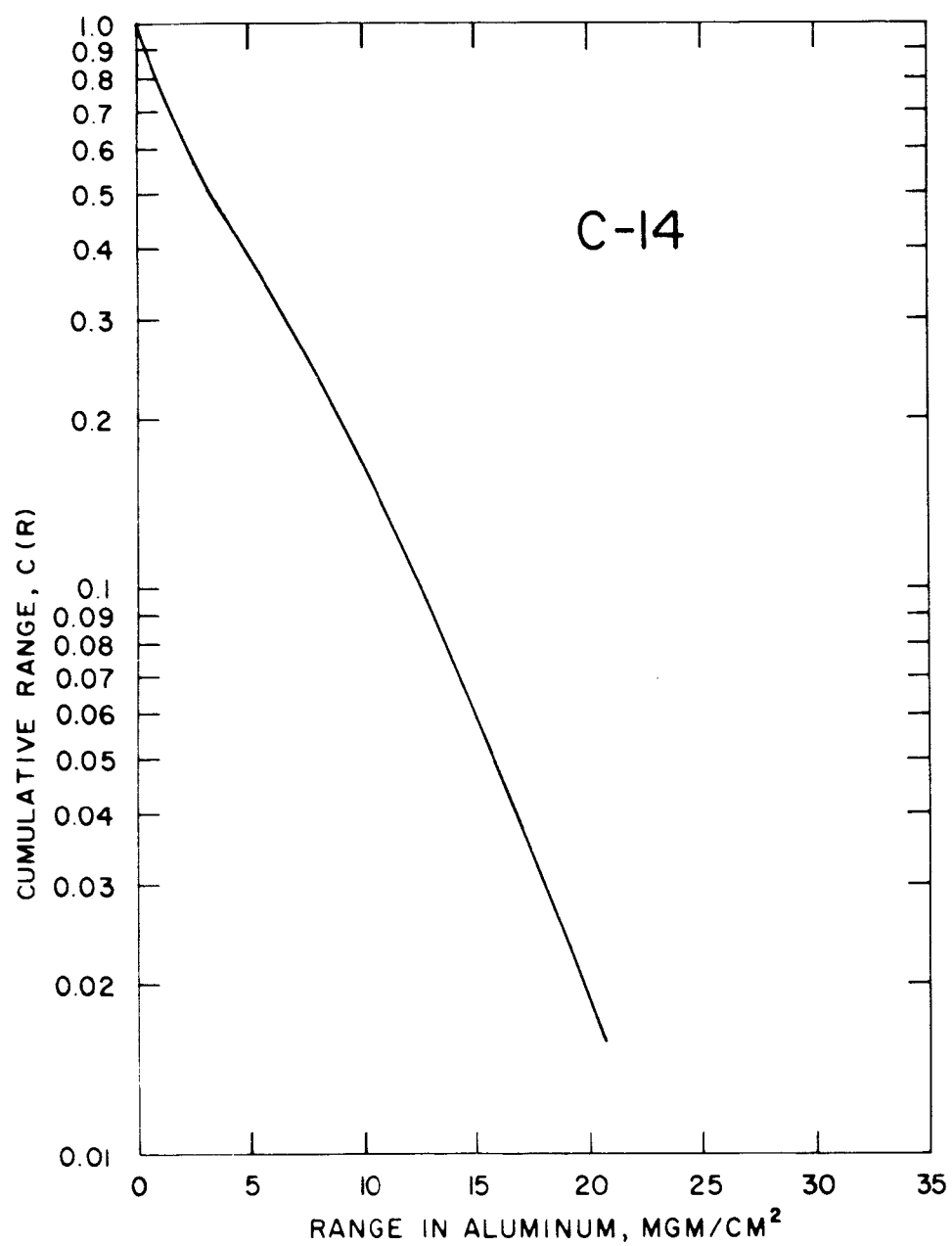


Figure 21. Cumulative range distribution for a C-14 beta source.

To illustrate this even more clearly, recall from the above example that for an intensity ratio of $I/I_0 = 0.5$, we calculated the thickness of the particulate matter to be 3.1 mg/cm^2 . If the thickness of the filter plus air gap plus detector window would have been 16 mg/cm^2 instead of 15 mg/cm^2 , and if we had measured the intensity ratio I/I_0 to be 0.5 as above, we would have found from Figure 21 that the total thickness of air gap plus filter plus detector window plus particulate matter deposited on the filter was 18.85 mg/cm^2 . This results in a deposit of particulate matter of 2.85 mg/cm^2 . An instrument that did not take into account the nonlinearity of Figure 21 would possess an error of about 8%, assuming that the unknown changes would be limited to 1 mg/cm^2 .

Using Figure 19, the cumulative energy distribution of Pm-147 radiation has also been plotted (Figure 22). From Figure 17 and 22 we get the cumulative range distribution of Pm-147 radiation (Figure 23).

Referring back to the examples shown, if we again had a case where the air gap plus filter plus detector window amounted to 15 mg/cm^2 and measured I/I_0 to be 0.5 with Pm-147, the thickness of particulate deposit would be 6.8 mg/cm^2 . If the air gap plus filter plus detector window amounted to 16 mg/cm^2 and I/I_0 was measured to be 0.5, the thickness of the particulate deposit would be 6.7 mg/cm^2 . So an instrument that did not take into account the nonlinearity of Figure 23 would possess an error of about 1.5%, assuming that unknown changes would be limited to 1 mg/cm^2 .

The examples used have demonstrated that, given a range of around 15 - 20 mg/cm^2 , Pm-147 radiation more closely follows the exponential law of Equation 4 and therefore provides better accuracy if the Equation 4 relationship is assumed. It is clear from Figures 21 and 23 that neither curve is linear throughout the spectrum. When considering the application of one of these sources, one has to work with the proper portion of the curve. These curves were not calculated for any other radiation source.

2.5 EXPERIMENTS WITH FLY ASH

An attempt was made to operate the Gelman instrument in our facility at the smoke stack. We found, however, that the deposits of particulate matter on the filter paper were very nonuniform due to the design of the sampling head. Furthermore the seal around the filter leaked. We did not find it feasible to redesign the sampling head during this program to correct these problems.

In order to get some data with real fly ash, another approach was followed. We used our parallel filter system to collect identical samples on two filters (identical, that is, to within $\pm 10\%$). We weighed one filter deposit with a microbalance, and the other we "weighed" with the Gelman instrument. The results of some of these runs are displayed in Figure 24. The broken line is a linear approximation from Figure 13 for $X_0 \approx 7 \text{ mg/cm}^2$, which was the thickness of the filters used for these runs.

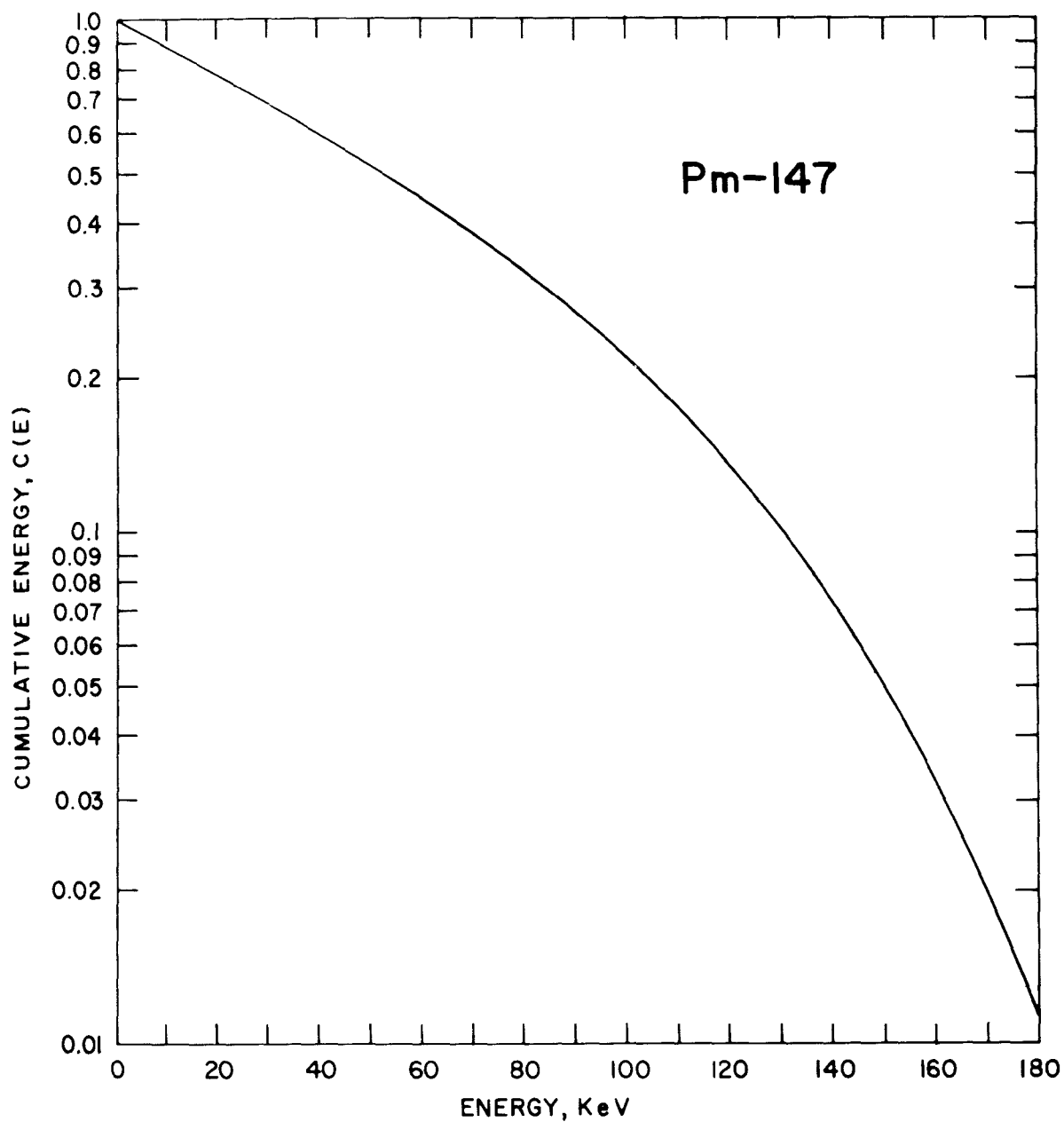


Figure 22. Cumulative energy distribution for a Pm-147 beta source.

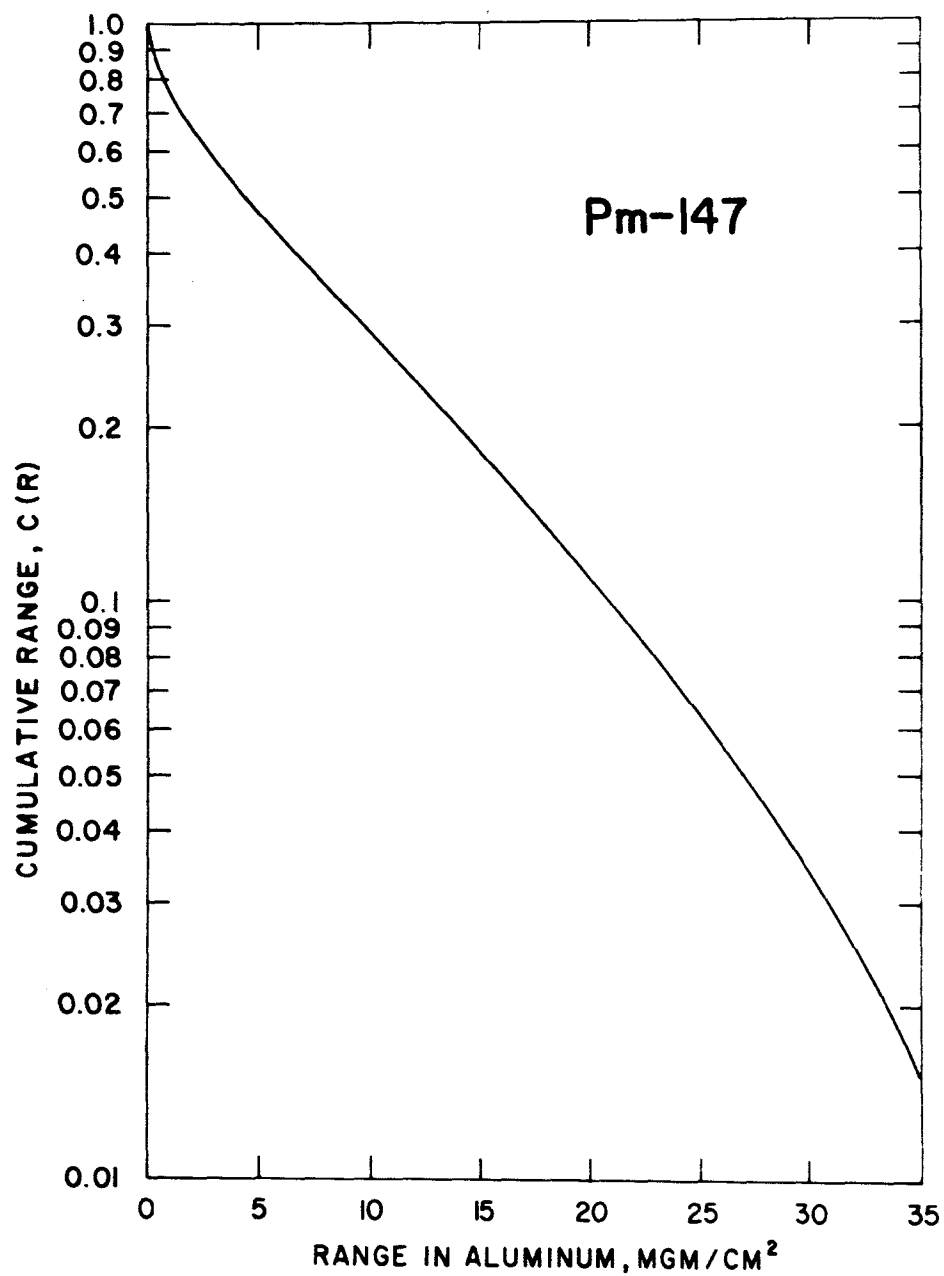


Figure 23. Cumulative range distribution for a Pm-147 beta source.

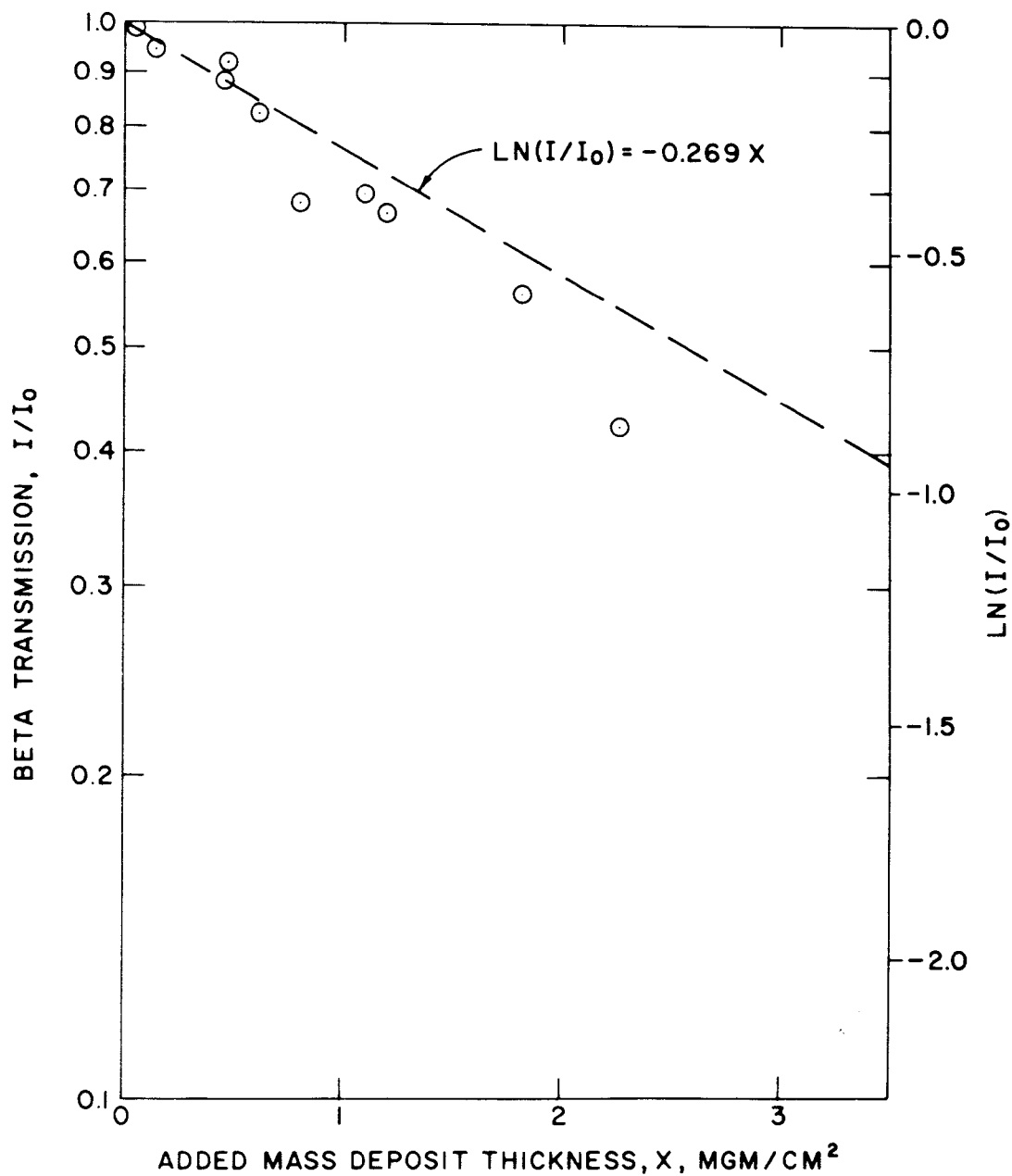


Figure 24. Results of tests with the standard Gelman unit (C-14) using fly ash collected in a separate filter holder as the filter loading.

The data points fall consistently below the broken line. This is explained by the fact that the particulate deposits on the filters were not uniform. There was a somewhat heavier concentration near the center than around the edge. Since the central portion of the filter was "weighed" by the Gelman instrument, one would expect the data to deviate in the direction shown. This data is therefore inconclusive, as it was not possible to measure the variations in deposit thickness on a single filter.

No other experiments were performed with the Gelman instrument on fly ash.

2.6 SUMMARY

The Gelman instrument was first tested in TSI's laboratories to determine the parameters that affect the calibration. It was found that the variations in filter tape thickness and the radiation source characteristics both significantly affect the calibration, even if I_0 is measured on the same section of tape as is I . This should be considered carefully when advanced instrumentation is designed and tested. Some experiments were performed on fly ash aerosol from TSI's stack facility, but the data from these experiments was inconclusive.

SECTION 3. DESIGN OF FIELD EXPERIMENT STATION

3.1 INTRODUCTION

This section describes the field laboratory that was constructed and instrumented by TSI as a part of this contract. Most of the experimental work on the contract was done in this field laboratory, so an understanding of its features and capabilities is important.

The field laboratory is located in the stack of the Northern States Power Company's Allen S. King electrical power generating plant at Bayport, Minnesota. The laboratory is both heated and air conditioned, and therefore can be used at all times of the year. Access to the stack laboratory facility can be gained only through the proper authorities at the King plant.

3.2 NSP POWER PLANT

The King plant, shown in Figure 25, has a rated power output of 550 megawatts. Its location is 25 miles east of TSI on the St. Croix River at the Minnesota-Wisconsin border. The principal fuel is southern Illinois and Eastern Kentucky coal, which has a sulfur content of about 3%. The coal is crushed and burned in 12 cyclone furnaces which are all connected to a single heat exchanger. The plant is equipped with electrostatic precipitators that remove about 99% of the mass of particulate emissions from the flue gas. The stack is 785 feet high. It consists of a central steel chimney which contains the flue gas and an outer concrete supporting shell with an annular space between them. The sampling done under this contract was from the horizontal breeching within the annular space at a point about 10 feet before the effluent reached the vertical steel chimney. The effluent turns an 80° horizontal bend about 25 feet upstream of the sampling point. The internal dimensions of the breeching at the sampling point are 12 feet across and 27 feet high. The vertical steel chimney is 26 feet in diameter. Another identical horizontal breeching empties into the stack directly opposite the sampled breeching.

The choice of the King plant as a test location for instrument development was based on several considerations. It is within convenient driving distance from TSI. It is typical of large, modern, and coal-fired combustion sources. Since it is a base-load plant, operating conditions are relatively constant, allowing one to repeat a test under reasonably constant conditions to locate a problem.

The decision to do experimental work in a smoke stack rather than a simulated stack atmosphere was made because of the difficulty in simulating the inside of a stack. The lack of good measurements of both gas flow and particle flux characteristics in stacks coupled with the lack of an experimental facility for such simulation indicated strongly that instrument testing and development at the time of this work would be profitable only in an actual stack.

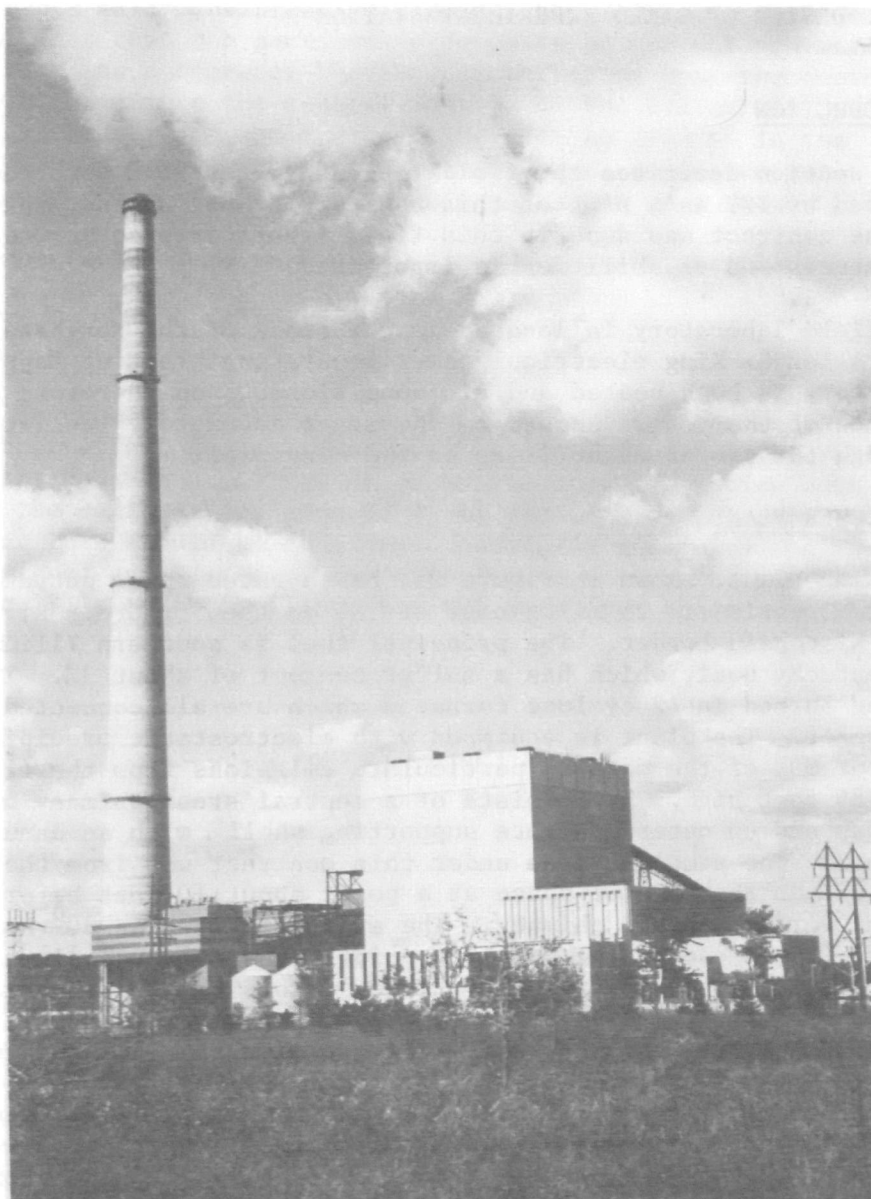


Figure 25. Northern States Power Company's Allen S. King electrical power generating plant, located at Bayport, Minnesota, where the field experiment station was constructed.

3.3 GENERAL LAYOUT

The location of the stack laboratory is about 70 feet above ground level. This is the level at which the flue gas from the electrostatic precipitators enters the vertical stack, as shown in Figure 26. The construction of the stack itself is illustrated in Figure 27, which is a cutaway section of the area where the breeching enters the stack. The laboratory is constructed on a heavy steel floor between the outer concrete shell and the inner steel stack, as shown in Figure 28.

Since it is inside the concrete shell, the stack laboratory is protected from rain and snow. The temperature of the air surrounding the laboratory approximates the outdoor temperature because of the natural ventilating effect in the stack. An air conditioner and a heater have been installed so that the facility can be used in nearly all weather conditions.

As Figures 27 and 28 illustrate, there are seven ports installed in the breeching adjacent to the laboratory. These are 6 inch diameter ports and can be made accessible for sampling from the breeching. Only one of the ports was used on this program.

3.4 INSTRUMENTATION

The purpose of the stack laboratory is to facilitate the evaluation of particle mass sensing instruments using genuine effluent aerosol directly from a smoke stack. The method which we chose to evaluate instruments is to deliver identical samples of stack aerosol to both the instrument and a filter operating in parallel with the instrument. The instrument measurement can then be compared directly to the measurement obtained by weighing the parallel filter. It should be noted that, for the purpose of this work, it is not so important that a truly representative stack aerosol sample reach the instrument and parallel filter. It is much more important that the two samples be identical.

With this in mind, we fabricated the large sampling system shown in Figure 29. It can draw up to 20 CFM of flue gas from the stack and present identical samples to the individual parallel sampling systems as shown in Figure 30. The large sampling system removes a reasonably representative sample of effluent aerosol from the stack with approximately isokinetic conditions. All parts of the large system which are outside of the stack are heated to prevent condensation on the walls. An air ejector pump, operated by an air compressor located at ground level, draws the flue gas through the system. The large sampling tube serves three functions:



Figure 26. A view of the twin electrostatic precipitators and horizontal breeching of the power plant. The field experiment station is located in the right breeching just inside the outer wall of the vertical stack. Effluent passes from bottom to top of the photograph.

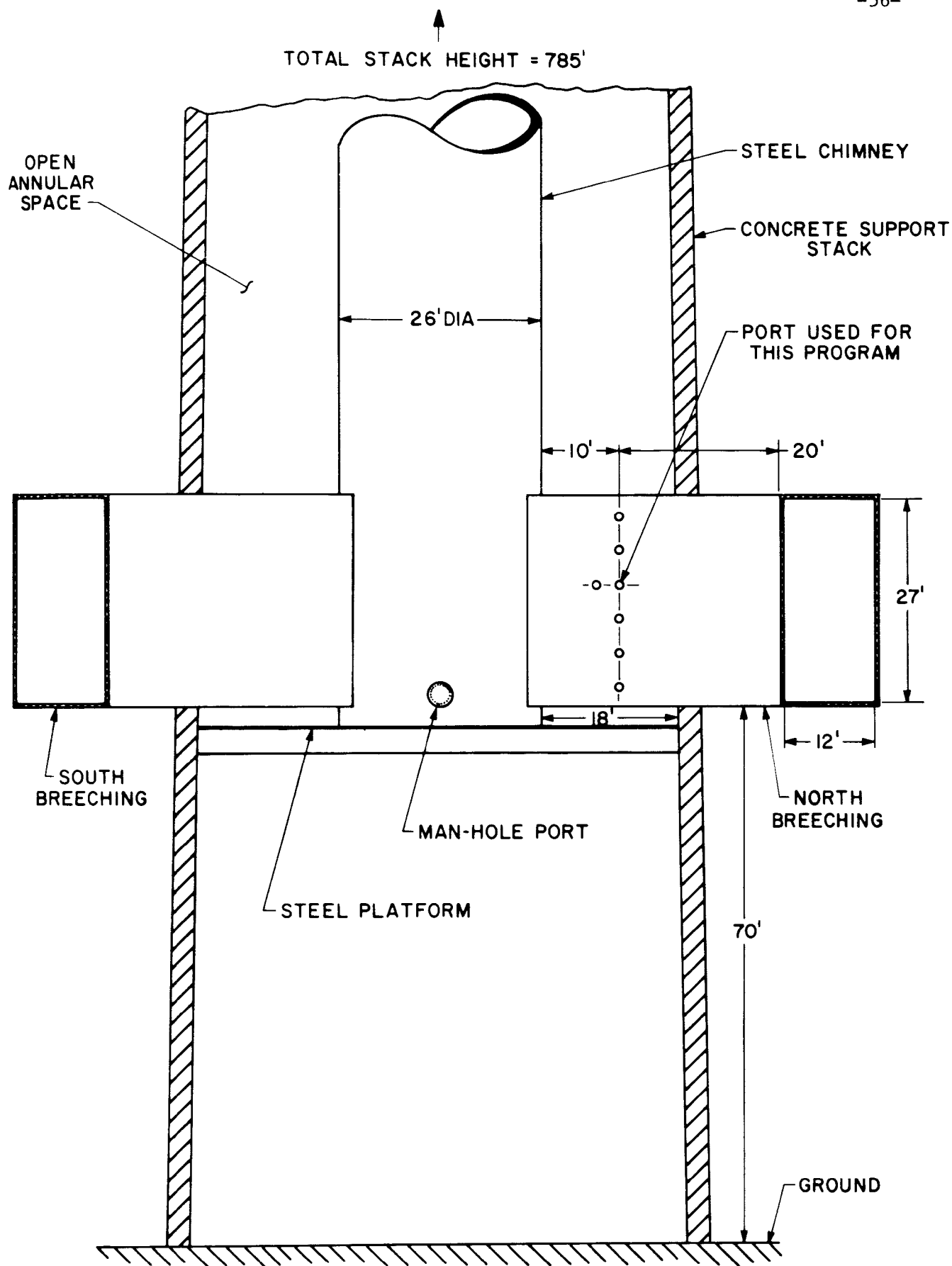


Figure 27. A side view of the horizontal breeching from which samples for the experimental instrument evaluations were drawn.

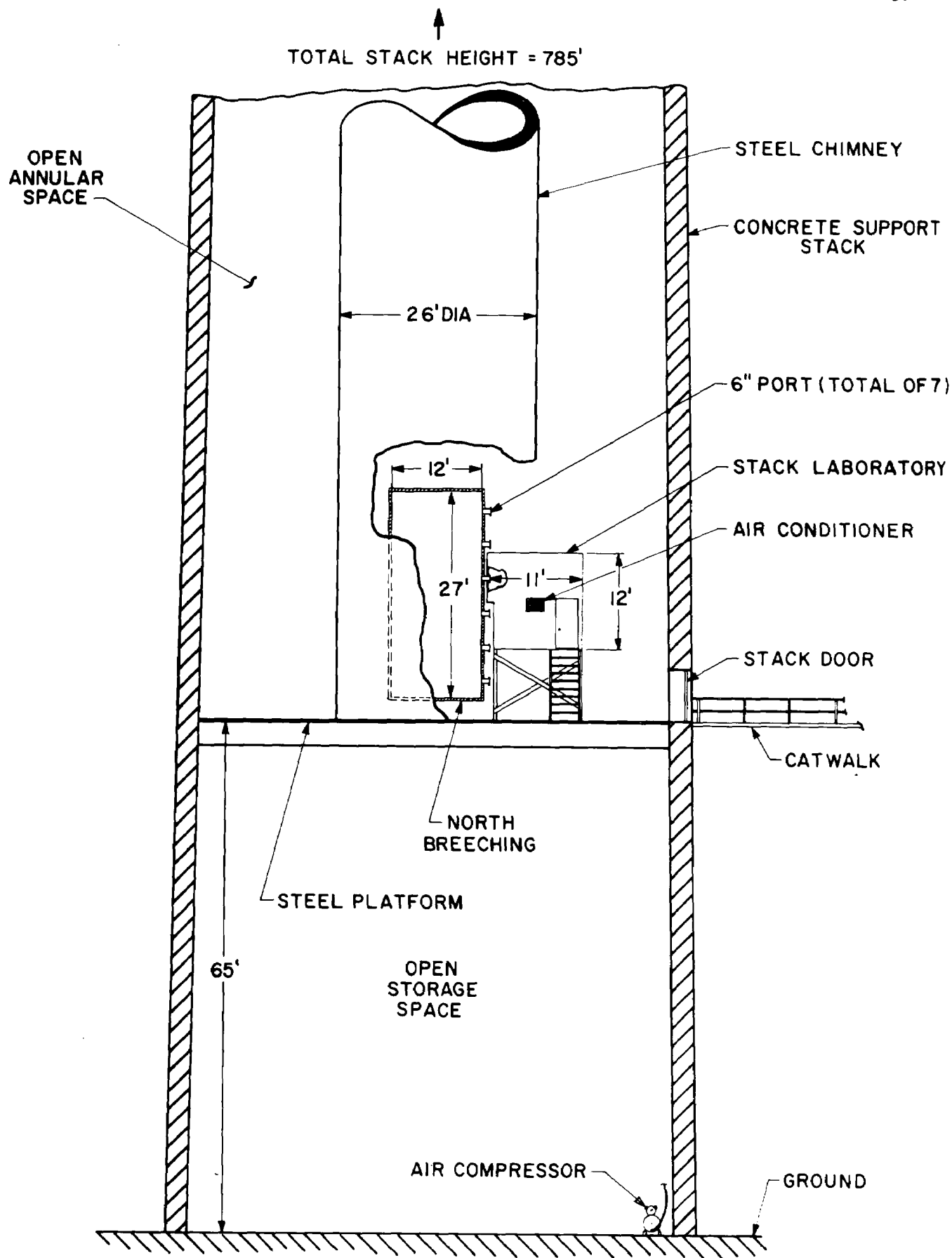


Figure 28. A cross-sectional view of the horizontal breaching showing the location of the laboratory with respect to the breaching and stack.

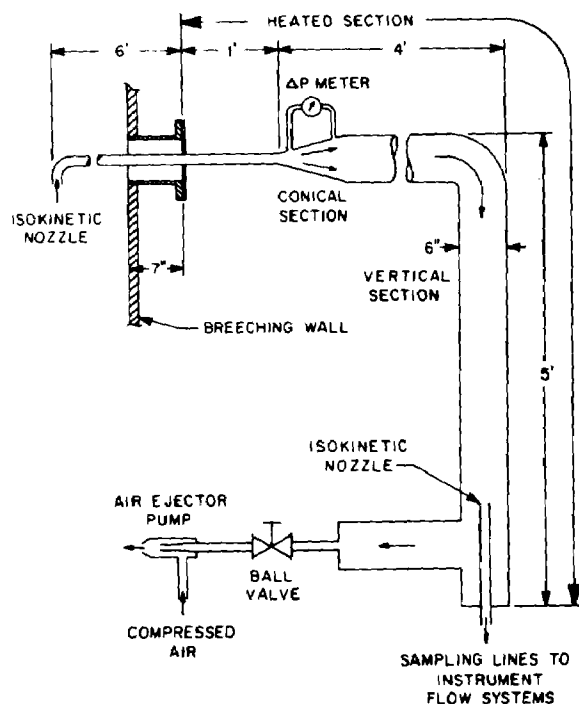


Figure 29. The sampling system which draws a somewhat representative sample of effluent aerosol from the breeching and delivers it to 4 parallel sampling systems serving as many as 4 separate instruments simultaneously.

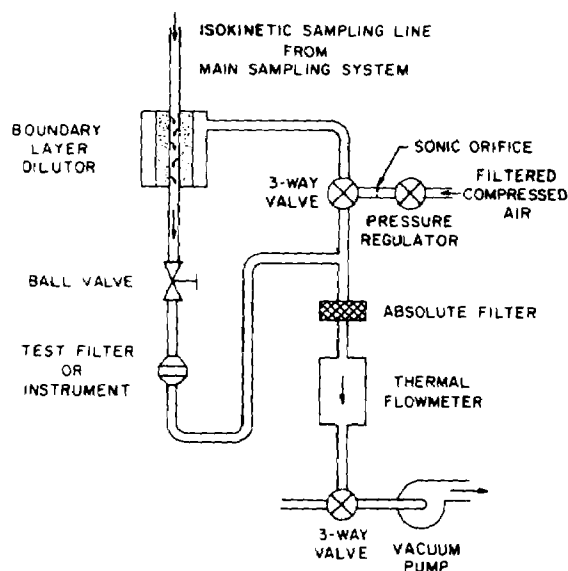


Figure 30. A typical parallel sampling system which removes an aerosol sample from the main sampling system shown in Figure 29, dilutes the sample from 0 - 90%, and delivers the diluted aerosol to the instrument or test filter. Four of these parallel systems can operate simultaneously. Two are designed for 20 - 50 LPM, and two for about 1 LPM, through the instrument or test filter.

1. It is physically large enough so that several identical, but separate, samples can be drawn out vertically downward and routed to several instruments simultaneously. The vertical orientation minimizes the loss of large particles by gravitational effects.
2. It lowers the velocity of the effluent aerosol so that instruments with low sampling rates of a few liters per minute can sample nearly isokinetically without having to use an unreasonably small inlet tube.
3. It is large enough and has enough capacity so that the flow field at the entrance to the individual parallel sampling systems is not distorted when an individual sampling tube is removed or shut off.

The conical expansion section, which connects the 1-inch tube from the stack with the 6-inch downstream tube, is used as a rough, but adequate, flow indicator by measuring the pressure differential from one end to the other.

A pair of parallel sampling systems, as shown in Figure 30, was used for all instrument tests at the stack. The aerosol travels downward with very little change in tube size through the parallel systems. The aerosol first passes through a boundary layer diluter which cools the sample and dilutes it enough to prevent nearly all condensation on the instrument and parallel filter, which are at room temperature. The dilution systems can operate with 0 to 90% clean air. The sampling tubes upstream of the diluters are heated. A ball valve downstream of the diluter is the primary method of beginning and ending a run. The instrument or parallel filter can be installed downstream of the ball valve. Sometimes, as in the beta instrument tests described in Section 5, a right angle bend must be made in the sample line just upstream of the instrument. In all tests on this program, if a bend was required for the beta instrument, an identical bend was installed in the parallel filter line.

The gas is drawn through the parallel systems by vacuum pumps. Dilution air can be regulated and held very constant for operating periods of several hours. Notice that the dilution air and total diluted aerosol flow (mixture of clean air and flue gas) are measured with the same high-precision flow meter. The dilution air is normally measured and adjusted before the start of a run and aerosol flow is measured and adjusted at the beginning of each run. As the filter loads, some adjustment of the total diluted aerosol flow is usually necessary.

The accurate measurement of the dilution (clean) air and total diluted aerosol flow is very important for accurate particle mass concentration measurements and for the comparison of 2 parallel systems. Reasons for the necessity of accurate flow measurements are discussed in Section 4.2.b. We found that Thermo-Systems Inc. thermal mass flowmeters, using a hot-film anemometer sensor in a venturi nozzle, proved satisfactory for this service. The flowmeters, one for each parallel sampling system, are compensated for temperature fluctuations and have a rated accuracy of about $\pm 1\%$ of reading. An "absolute" filter (MSA Model 92706) just upstream of the flowmeter keeps the sensor clean during several months of operation.

A Stauscheibe (S-type) pitot probe was available for making stack velocity measurements.

3.5 SUMMARY

The stack laboratory constructed on a commercial power plant stack is a versatile facility that can be used for many varied types of instrument testing. Several ports are available for sampling from the stack. Pairs of identical parallel sampling systems, using valves, diluters, and precision flowmeters, are available for testing of instruments such as the tests described in Section 5. Modifications can be easily made to accommodate other instruments and sensors.

SECTION 4. CALIBRATION OF STACK FACILITY AT THE FIELD EXPERIMENT STATION

4.1 PROCEDURE

The ability of the sampling facility to deliver identical samples of effluent to each instrument had to be experimentally verified. This was done before, during, and after each instrument test reported elsewhere in this report. Identical 47-mm Gelman Type A glass fiber filters without binder in Gelman stainless steel filter holders were plumbed into the identical legs of the sampling system. One of these filter holders was identified as the parallel filter. The other filter holder, its filter sampler identified as beta filter, substituted for the test instrument during these tests of the sampling system. The test setup during these sampling tests is described in Section 3 of this report.

During all of these tests, the parallel filter was always operated at 50 LPM total diluted aerosol flow rate and 75% dilution, the same condition that was used for most instrument tests. The beta filter was operated at several conditions: 50, 30, and 20 LPM total diluted aerosol flow rate; and 75% and 87.5% dilution. Both filters were always operated for identical sampling times of 2, 3, 5, or 10 minutes.

The procedure began a day or two before the test by weighing enough clean filters to accommodate a single day's sampling on a Mettler micro analytical balance, Model M5/SA. The weighed filters were placed in individual sealed plastic petri dishes, Millipore Cat. No. PD1004700. The operator carried them with him to the stack on the morning of test day.

The facility was always warmed up at least a half hour, and usually nearly one hour before the first run began. Each run was preceded by the cleaning of both filter holders and the careful mounting of filters in both of them. The dilution (clean) air flow was then adjusted. Referring to Figure 30, each run began by opening the upper 3-way valve to allow clean air flow to the diluter, opening the ball valve, and opening the lower 3-way valve to allow the pump to suck a sample through the test filter. The total diluted aerosol flow rate was monitored continuously and adjusted as needed to maintain a constant measured flow rate. Little adjustment was needed during most runs. Each run ended by returning the three valves to their standby position. The dilution air flow rate was checked between each run and any significant changes (very rare) was noted. Each filter was then carefully removed from its holder and placed in its sealed carrier. Preparation for the next run then could begin.

The filters were carried to the balance at the end of the day. Usually, at least one day passed before they could be weighed with each filter stored in its individual, sealed petri dish. The weighing procedure began by opening the petri dish and immediately placing the filter onto the microbalance tray. A static eliminator, 3-M Model 204 with 5 millicuries of Po-210, was waved over the

filter just before actual weighing. Usually, the filters would immediately begin to lose or gain weight in the desiccated microbalance. The earliest possible weighing with the least filter weight change was used for all weights in these tests. We chose the "unchanged" weight because that was most nearly the condition sensed by the beta instruments.

An attempt was made to obtain a rough estimate of particle losses in the vertical straight tube, the 90° elbow, and the horizontal straight tube immediately upstream of the filter holders. The components were carefully cleaned before the three days of runs during August, 1972. After all the runs were completed the three components of each sampling line were removed and carefully washed out with alcohol. The solid sediment was collected and weighed. Although not a precise technique, this method does offer a rough estimate of line losses in a portion of the sampling system.

4.2 RESULTS OF FILTER TESTS

4.2.a. Introduction

The primary set of parallel filter tests for evaluation of the stack sampling facility were conducted on August 25, 30, and 31, 1972. Ideally, these tests would have been completed immediately preceeding the evaluation tests of the beta instruments which were performed on May 15 - 18 and May 22 - 24, 1972. However, scheduling difficulties made such a program impossible. Instead, we performed enough parallel filter tests before and during the beta instrument evaluation tests to assure acceptable operating conditions and reserved the more thorough parallel filter tests for a later date.

The complete data for the August tests are found in Appendix A. Table 3 summarizes the measured stack concentrations (uncorrected for sampling line losses) for each operating condition and for each run. The two filters are designated beta filter for the one which takes the place of the beta test instrument and parallel filter for the one which normally serves as a reference for the beta test instrument. Since 75% dilution and 50 LPM total diluted aerosol flow rate was the condition used most often in the May beta instruments tests, 5 repetitions were run as this condition for each sampling time. Three repetitions were made for every other condition. The sampling systems leading to both filters are intended to be identical.

Note that the operating conditions for the parallel filter on all test runs was 75% dilution, 50 LPM total flow rate, and the same sample time as the beta filter. The beta filter operating conditions were adjusted as indicated in Table 3. It is important to remember that this is not the situation during actual instrument evaluation tests. During nearly all May test runs, both the beta instrument and the parallel filter were operated at identical conditions. Thus, except for the 75% dilution, 50 LPM total flow rate runs, the August runs are not indicative of the expected ratio between test instrument and parallel filter, but rather, are an indication of some of the characteristics and capabilities of the test setup.

Table 3. Measured stack concentration, mgm/m^3 , for both the beta filter and the parallel filter during all August runs. The data is uncorrected for line losses.

Dilution:		75%									87.5%								
Diluted Aerosol Flow Rate, LPM		50			30			20			50			30			20		
Sample Time, Min.		5	10	2	5	10	2	5	10	2	5	10	2	5	10	2	5	10	2
Beta Filter Repetitions	1	85.9	155.5	94.0	115.0	121.7	74.0	89.0	83.9	28.7	59.4	74.2	31.7	54.6	69.4	30.7	40.3	48.6	25.2
	2	119.3	142.8	65.1*	87.7	106.9	69.4	66.1	62.5	17.2	62.3	65.5	22.2	52.1	72.7	19.5	34.3	52.1	22.2
	3	136.9	137.1	66.6	66.6	114.2	68.1	94.6**	62.8	21.4	60.6	68.5	28.8	51.8	70.4	24.9	38.5	54.2	122.0
	4	138.3	141.8	64.7															
	5	146.1	144.8	58.4															
Parallel Filter Repetitions	1	95.8	158.2	93.2	125.3	130.8	77.2	111.9	97.5	27.4	67.7	81.8	35.7	61.8	76.7	33.3	55.4	77.5	32.0
	2	130.5	145.4	79.8*	108.8	123.3	79.9	103.2	71.7	27.2	70.9	77.0	33.4	58.6	82.8	29.3	55.6	84.5	23.5
	3	138.8	135.2	57.7	111.9	130.8	75.8	116.0**	70.9	26.0	67.9	82.4	33.7	55.9	84.6	30.0	55.1	87.2	24.8
	4	141.4	144.4	60.0															
	5	144.8	144.7	60.6															

Note: All 75%, 50 LPM, 5 Min. repetitions were run first; all 75%, 50 LPM, 10 Min. repetitions were run next, etc., in the order shown above.

*Runs before this point run Aug. 25, 1972; runs after this point run Aug. 30, 1972.

**Runs before this point run Aug. 30, 1972; runs after this point run Aug. 31, 1972.

Table 4. Ratio R_F for all August runs. R_F = (beta filter measured concentration/parallel filter measured concentration). The data is uncorrected for line losses. The average R_F and the standard deviation of R_F for each operating condition are also shown.

Dilution:		75%									87.5%								
Diluted Aerosol Flow Rate, LPM		50 ¹			30 ²			20 ²			50 ²			30 ²			20 ²		
Sample Time, Min.		<u>5</u>	<u>10</u>	<u>2</u>	<u>5</u>	<u>10</u>	<u>2</u>	<u>5</u>	<u>10</u>	<u>2</u>	<u>5</u>	<u>10</u>	<u>2</u>	<u>5</u>	<u>10</u>	<u>2</u>	<u>5</u>	<u>10</u>	<u>2</u>
1		.897	.983	1.009	.918	.930	.959	.795	.861	1.047	.877	.909	.888	.883	.905	.922	.727	.627	.788
2		.914	.982	.816*	.806	.867	.869	.641	.872	.632	.879	.851	.665	.889	.878	.666	.617	.617	.945
3		.986	1.014	1.155	.595	.873	.898	.816**	.886	.823	.892	.831	.855	.927	.832	.830	.699	.622	4.919
4		.978	.982	1.077	-	-	-	-	-	-	-	-	-	-	-	-	-	-	-
5		<u>1.009</u>	<u>1.001</u>	<u>.964</u>	-	-	-	-	-	-	-	-	-	-	-	-	-	-	-
Average:		.9568	.9924	1.0042	.7730	.8900	.9087	.7507	.8730	.8340	.8827	.8637	.8027	.8997	.8717	.8060	.6810	.6220	2.2173 (.8665)
Sigma,s:		.0485	.0146	.1279	.1645	.0348	.0459	.0956	.0125	.2075	.0082	.0396	.1204	.0238	.0369	.1292	.0572	.0050	2.37 (.078)

Note: All 75%, 50 LPM, 5 Min. repetitions were run first; all 75%, 50 LPM, 10 Min. repetitions were run next, etc., in the order shown above.

¹ Both filters at same operating conditions

² Beta filter at condition indicated, PF at 50 LPM, 75% dilution, and time indicated

*Before this, run on Aug. 25, 1972; after this run on Aug. 30.

**Before this, run on Aug. 30, 1972; after this run on Aug. 31.

The primary criteria for evaluating the test results was that the ratio of beta filter concentration to parallel filter concentration R_F be nearly 1.0 and, more importantly, be constant. Table 4 shows the ratio R_F for all August runs. Also shown are the average and standard deviation for each operating condition. Figure 31 shows the data points for all runs. Figure 32 shows the standard deviations at various operating conditions. For many types of tests, a reasonable criteria for judging identical parallel filter tests may be that a standard deviation of greater than 0.05 indicates that the technique and system yielded unacceptably inconsistent data.

Several conclusions can be made immediately. Two minute sampling times yield inconsistent data under this mode of operation. Ten minute sampling times are acceptably consistent under any operating conditions. The higher dilution ratio (87.5%) was generally more consistent than 75% dilution, particularly with 5 minute sample time and 20 LPM total diluted aerosol flow rate. Higher flow rates (50 LPM) generally give better consistency than lower flow rates (30 or 20 LPM).

Table 5 identifies the operating conditions which were judged to yield acceptably consistent results in this series of tests. The average ratio R_F for 75% dilution, 50 LPM total diluted aerosol flow rate are between 0.95 and 1.00. The standard deviations are generally lower than for other conditions. The 15 runs at these operating conditions are the ones most indicative of the probable errors encountered during the May instrument tests.

Table 5. Operating conditions which yielded acceptably consistent results during August runs. Also shown are the average ratio R_F (top number in each box) and the standard deviations (bottom number in each box) of the ratio R_F for each operating condition.

Dilution:		75%			87.5%		
Diluted LPM :		50	30	20	50	30	20
Sampling Time	<u>MIN</u>	.9924	.8900	.8730	.8637	.8717	.6220
	10	YES	YES	YES	YES	YES	OK
		.0146	.0348	.0125	.0396	.0369	.0050
	5	.9568	.7730	.7507	.8827	.8997	.6810
		YES	NO	NO	YES	YES	NO
		.0485	.1645	.0956	.0082	.0238	.0572
	2	1.0042	.9087	.8340	.8027	.8060	.8665
		NO	NO	NO	NO	NO	NO
		.1279	.0459	.2075	.1204	.1292	.078

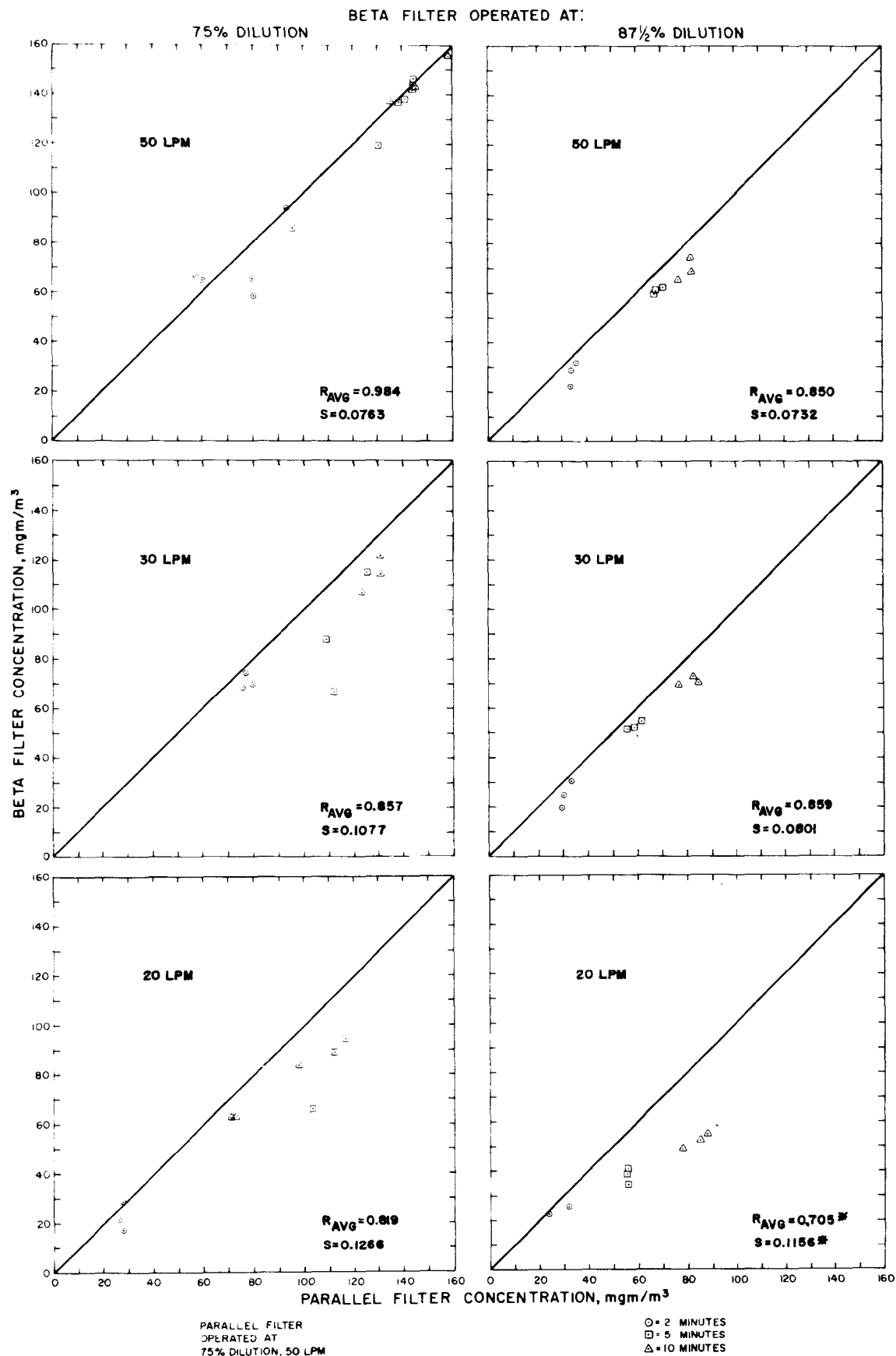


Figure 31. Stack concentration as measured by the beta filter plotted against stack concentration as measured by the parallel filter for all August runs. The diagonal line on each graph represents a perfect (1:1) correlation. Note that the parallel filter was always operated at 50 LPM diluted aerosol flow rate and 75% dilution while the beta filter was operated at the conditions shown.

*One data point was rejected before calculating R_{AVG} and S for this condition.

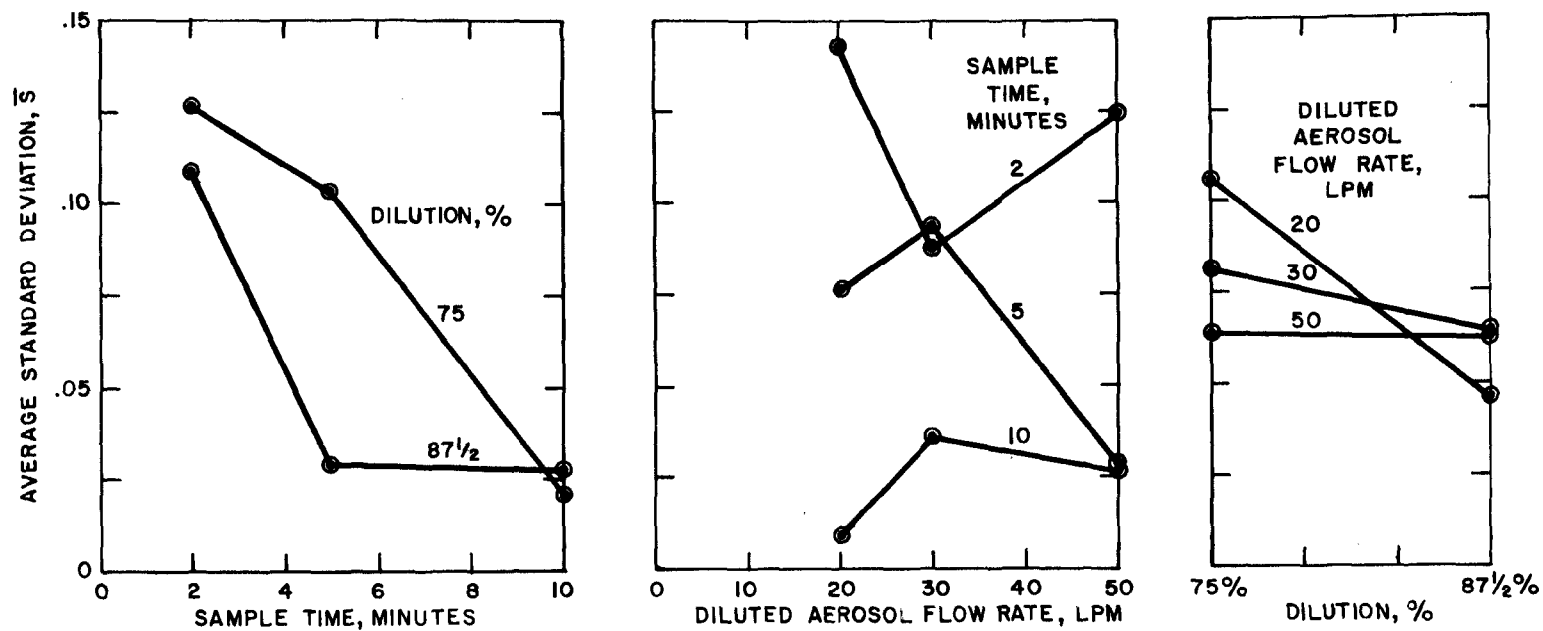


Figure 32. Average standard deviation \bar{S} of the ratio R_F as a function of sample time, diluted aerosol flow rate, and dilution ratio for all August runs. A low standard deviation denotes high reproducibility of the ratio from run to run, but does not denote perfect ($R_F = 1.0$) correlation.

The average measured concentration ratio R_F for nearly all other acceptable conditions ranges from 0.86 to 0.90. Thus, the reference parallel filter usually measured higher stack concentrations. The primary reason for this lack of perfect correlation is probably the inaccuracies of the flow measurements. This argument is strengthened by the fact that the ratios R_F tend to be even lower as total flow decreases and dilution ratio increases. We had considerable trouble earlier in the test program because we were measuring dilution (clean) air flow rate and total diluted aerosol flow rate with 2 separate flowmeters using 2 different measurement principles. We eliminated most of the problem by using a single, highly-accurate, gaseous mass flowmeter to measure both dilution air flow rate and total diluted aerosol flow rate. However, the inaccuracies cannot be entirely eliminated.

All 2-minute samples are rejected because of inconsistent results. The relatively good results shown in Table 5 for 75% dilution, 30 LPM total diluted aerosol flow, and 2 minute sample time is not considered significant.

4.2.b. Gas Flow Measurement

Since gas flow measurements play such an important role in these tests, further discussion is justified. The measurement of stack particle concentration requires the measurement of the weight of particles within a known or measured volume of air. If no dilution of the sample takes place, any errors in the measurement of the air volume will result in a similar error in measured concentration; i.e., a 5% error in air volume measurement results approximately in a 5% error in measured concentration. However, dilution of the sample upstream of the particle collecting device complicates the problem. The measured particle concentration at the collecting device C_{CD} must be multiplied by the dilution ratio R_D ($R_D = \text{total diluted aerosol flow rate } Q_{DA} / \text{undiluted aerosol flow rate } Q_{UA}$) to obtain the stack particle concentration. We concluded during the system design phase that we could not tolerate any available flowmeter in the sample stream upstream of the particle collecting device because of the resulting loss of particles leading to a plugged flowmeter and a changed calibration. Thus, we had to measure dilution (clean) air flow rate Q_{CA} and total diluted aerosol flow rate Q_{DA} to obtain the undiluted aerosol flow rate Q_{UA} :

$$Q_{UA} = Q_{DA} - Q_{CA} \quad (2)$$

The stack concentration C_S (uncorrected for particle sampling line losses) then becomes:

$$C_S = R_D C_{CD} = \frac{Q_{DA}}{Q_{UA}} C_{CD} = \frac{Q_{DA}}{Q_{DA} - Q_{CA}} C_{CD} \quad (3)$$

For example, let us assume that we are using highly accurate flowmeters which have an error of only $\pm 1\%$ of reading for the measurement of Q_{DA} and Q_{CA} .

Also assume that the dilution ratio which we attempt to obtain is $R_D = 8$ (87.5% dilution). Now assume that Q_{DA} is measuring 1% lower than the desired 50 LPM and Q_{CA} is measuring 1% higher than the desired 43.75 LPM. Plugging these values into Eq. (3);

$$C_{S, \text{ Error}} = C_{CD} \frac{Q_{DA}}{Q_{DA} - Q_{CA}} = C_D \frac{49.5 \text{ LPM}}{(49.5 - 44.1875) \text{ LPM}} = (9.3176) C_{CD}$$

We were trying to adjust the flow measurements to obtain:

$$C_{S, \text{ Actual}} = C_{CD} \frac{50}{50 - 43.75} = 8 C_{CD}$$

Thus, the maximum error in measured stack concentration caused by the low $\pm 1\%$ error in the flow measurement is:

$$\% \text{ Error}_{\text{Max}} = \frac{(9.3176 - 8)}{8} 100 = +16.47\%$$

This amount of error could also have been negative. Thus, if one of the parallel systems was positive and the other negative, the difference between the actual particle concentrations entering the two parallel filters could be as much as about 30%.

We chose to measure both clean air flow and total diluted aerosol flow with a single flowmeter using a proper valving system to direct each flow in turn through the flowmeter. This eliminated differences between 2 flowmeters and 2 calibrations as an error. Also, the use of a single flowmeter partially compensates for the need for increasingly accurate flow measurements with increasing dilution because both measurements (Q_{CA} and Q_{DA}) are made on a short segment of the flowmeter calibration curve making the measurements more accurate with respect to each other. Using a single flowmeter does not allow the operator to monitor both flow rates during a run. He must adjust the dilution (clean) air flow before a run, monitor and adjust the total diluted aerosol flow during the run, and recheck the dilution air flow after the run. We found very little change in dilution air during any run. It was necessary to monitor and adjust the total diluted aerosol flow as the filter loaded during most runs.

The flowmeters we used in both sample lines were Thermo-Systems' thermal mass flowmeters (Model 1352-3) utilizing a hot-film anemometer sensor in a venturi nozzle. Both flowmeters were calibrated in clean air at 70°F and the sensors are temperature compensated. Although we feel this flowmeter was the best choice available, the user should understand several facts before using it in an effluent stream. The gas composition (more precisely, the heat transfer characteristics of the gas) was not accurately known and probably did not remain

completely constant. The clean dilution air and the contaminated total diluted air streams could be expected to have somewhat different heat transfer characteristics, although both streams are made up primarily of N_2 . Fluctuating temperature or a temperature different from the calibration temperature could cause measurement inaccuracies, particularly while the total diluted aerosol stream is heating up the sampling line and filter holder at the beginning of a run. We calibrated the flowmeters just before the May tests and again before the August runs. We recommend recalibration against a highly stable reference every 2 - 3 weeks of tests such as these.

Summarizing our thoughts regarding flow measurement errors and their effects on dilution ratio determination, we recommend avoiding dilutions greater than 87.5%. We also recommend operating both of the parallel sampling lines at the same operating conditions. Flowmeters used in the sampling system must be highly accurate and recalibrated often. Direct measurement of undiluted aerosol flow rate probably results in excessive particle line losses. A single flowmeter should measure both dilution air flow and total diluted aerosol flow. Even so, any errors in flow measurement became magnified several-fold because direct measurement of the undiluted aerosol cannot be tolerated.

Most of the lack of correlation between the parallel sampling lines in the August data can be attributed to errors in flow measurements. During all August runs except the 75% dilution, 50 LPM runs, the two parallel sampling lines operated at different flow and dilution conditions. Measurements at all sampling conditions except 75% dilution, 50 LPM resulted in a ratio R_D of less than 0.91. However, the average ratio R_D for the 75% dilution, 50 LPM runs at all sampling times was 0.984. We suspect that the better correlation at that condition and the correspondingly poorest correlation at 87.5% dilution, 20 LPM, was primarily due to one or both of the following reasons:

1. Both sampling lines were operating at identical conditions for the 75% dilution, 50 LPM runs, while operating conditions were not identical on all other runs.
2. 75% dilution, 50 LPM is a preferred compromise operating condition where dilution is sufficient to prevent excessive condensation while not extreme with the resulting flow measurement problems.

Three more topics will be discussed before going on to the beta instrument tests. First, the interesting major effect of sampling time on measured stack concentration. Second, an experimental estimate of sampling line losses in a portion of the line. Third, an experimental correlation between the August runs and several May runs.

4.2.c. Effect of Sampling Time

Table 6 shows the average measured stack concentration for the runs of August 31. Note the striking effect of sampling time on the measured concentration. With 87.5% dilution, the average stack concentration for all 2 minute samples is 30.7 mgm/m³, for all 5 minute samples is 61.0 mgm/m³, and for all 10 minute samples is 81.6 mgm/m³. The 5 minute samples average about twice the concentration measured in 2 minute samples and the 10 minute samples average nearly triple the concentration measured in 2 minute samples.

Table 6. Average stack concentration (uncorrected for line losses) measured by the parallel filter with 87.5% dilution on August 31. Note the strong influence of sampling time.

Diluted Aerosol Flow Rate, LPM		Sampling Time, Min.		
		2	5	10
	50	34.3	68.8	80.3
	30	30.9	58.8	81.4
	20	26.8	55.4	83.1

The same trends appear in the 75% dilution runs, but that data was collected on three different days with three different concentration levels, complicating the analysis. Figure 33 shows the measured concentration for each 87.5% dilution run as a function of time. Any increase or decrease in measured stack concentration as the day progressed is certainly secondary to the differences between 2, 5, and 10 minute sampling times.

We have not yet analyzed this phenomena experimentally to isolate the cause. Although no definite conclusions can be drawn at this time, the August 31 data offers some clues. Several possible explanations include:

1. Sampling flow rate and/or dilution ratio may change with time or with filter loading. Although we adjusted the total diluted aerosol flow rate during every run to maintain constant measured flow rate, little adjustment was necessary for any of the August runs. Dilution (clean) air flow rate was checked before and after most runs and rarely changed. Although this explanation could account for a small part of the effect, it is very doubtful that it can account for the entire effect.

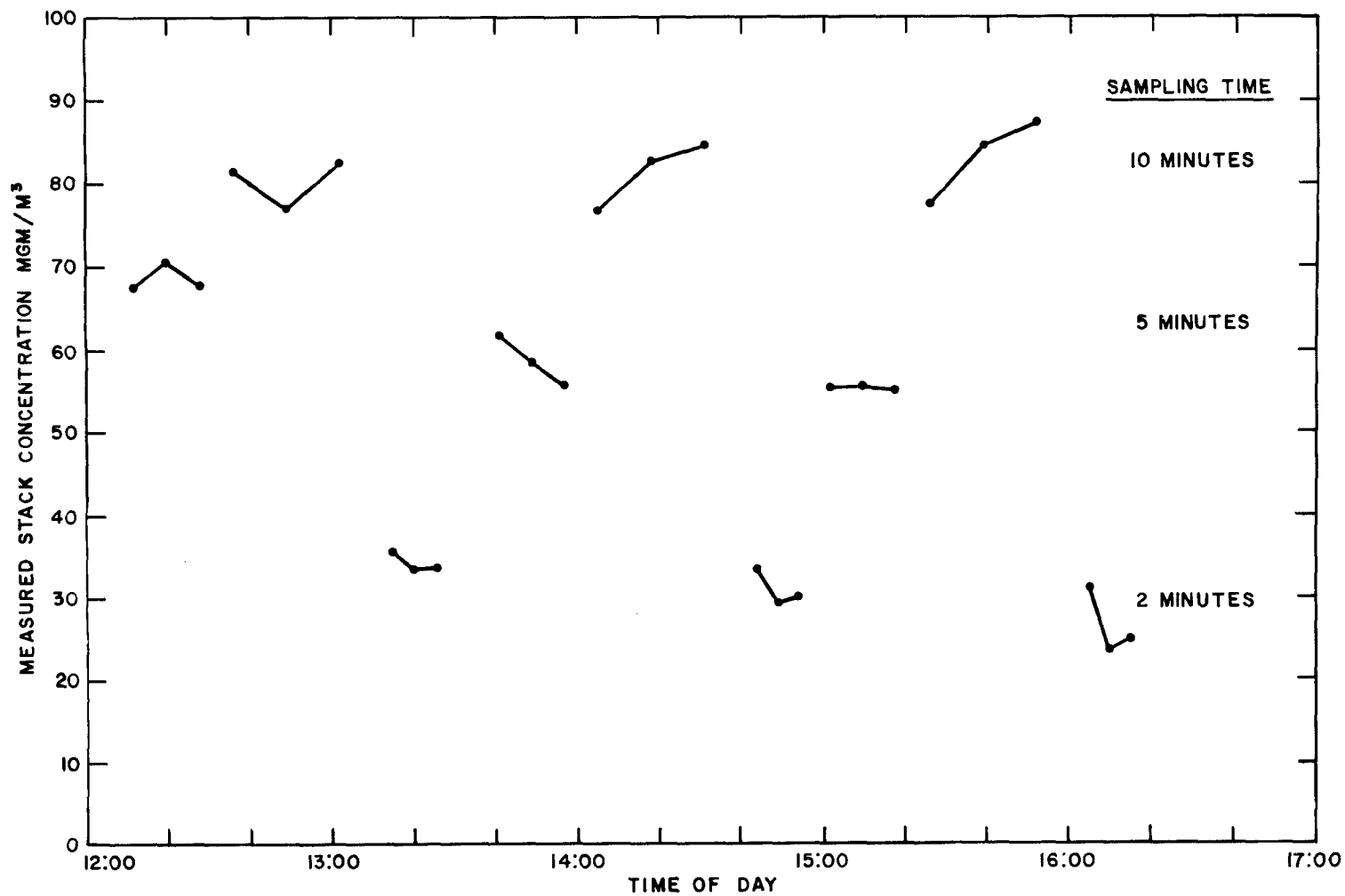


Figure 33. Measured stack concentration (uncorrected for line losses) measured by the parallel filter with 87.5% dilution on August 31. Note the strong influence of sampling time.

2. Particles can build up in the sampling tube upstream of the valve between runs, resulting in a sudden slug of particles at the start of a run. Assuming that the time between runs remains approximately constant, this would result in proportionally extra particles for the 2 minute runs, an effect directly opposite from our data.
3. Changes could be taking place on the filter media which depend upon particle loading and/or time. Weight could be added to the filter by adsorption or absorption of vapors or by chemical reactions at the media-gas phase or particle-gas phase boundary resulting in the precipitation of a previously gaseous material. Weight could be subtracted from the filter by the reverse of those processes. For example, we have observed major decreases in loaded filter weight when it was placed in a low humidity environment for a few minutes. We have also noticed major increases in loaded filter weight when it was placed in a moderate-high humidity environment for a few minutes. These changes were definitely greater than the equivalent change of a clean filter. These observations are mentioned only to indicate that vapors can cause major changes in measured filter loadings outside the stack environment. We suspect even greater effects within the effluent stream, including not only water phase changes, but also other chemical changes.
4. Condensation could occur on the cool sampling tubes between the diluter and the filter holder at the beginning of each run. When the tubes are warm later in the run, little or no condensation may occur. The dilution system was included in the sampling system specifically to reduce or eliminate condensation in the effluent stream as the sample cools to room temperature. Yet, the sampling line loss experiment reported later in this discussion indicates very significant amounts of solid particles deposited on the inside of the tubes between the diluter and the filter holder. It is difficult to explain such large line losses without condensation. Thus, condensation remains one of the most likely explanations for the lower concentration measurements with 2 minute samples.
5. Isokinetic sampling conditions may not be maintained at the point where the two parallel samples remove their respective samples from the main stream of effluent removed from the stack. However, isokinetic sampling conditions do not vary with changes in sampling time, but instead with changes in undiluted aerosol flow rate (i.e., diluted aerosol flow rate and dilution ratio). Since undiluted aerosol flow rate of the parallel filter line did not change at all during the August tests, nonisokinetic sampling would not have any significant effect on the results.

The most probable cause of the lower stack concentrations measured with the short sampling time is No. 4 and/or No. 3 above with No. 1 having a possible secondary effect. No further conclusions can be drawn without further experiments.

It is important to note that, although sampling time had such a large influence on measured concentration, even when both parallel lines were operated with identical conditions, both filters consistently collected nearly the same weight of material. Thus, although the phenomena should certainly be investigated further, the results of the May instrument evaluation program are almost certainly not significantly affected.

4.2.d. Particle Line Losses

We attempted experimentally to obtain an estimate of particle loss in the sampling lines. On each of the parallel lines, we washed the two straight tubes and the elbow which connects the diluter with the filter holder before the August tests. After the entire set of tests were completed, we again washed the components with alcohol, carefully collecting the wash and filtering out the particles onto a weighed glass fiber filter. After the filter dried, we reweighed it, determining the weight of collected particles. The sampling line components were identified as shown in Figure 34. The result-

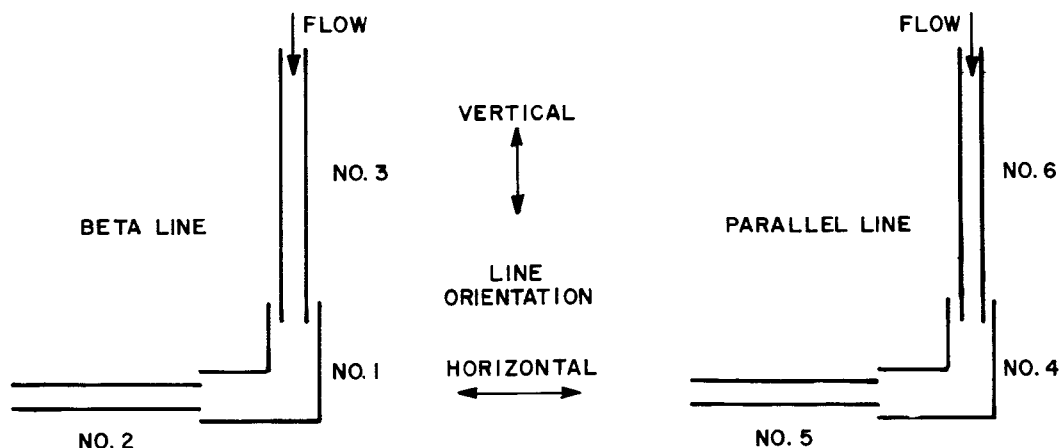


Figure 34. Identification of sampling system components for line loss tests. These 3 components connected the valve just downstream of the diluter with the beta filter or parallel filter.

ing weights are shown in Table 7. Also shown in Table 7 are the approximate total particle weights collected on all filter samples during the entire August test series.

Table 7. Measured weight of particulate material collected for line loss measurement from sampling system components identified in Figure 34.

<u>Part No.</u>	<u>Deposit Collected, mgm</u>
1	4.652
2	35.657
3	<u>32.869</u>
Total on Parts	73.178
Total on Beta Filters	227.000
4	49.648
5	118.304
6	<u>39.655</u>
Total on Parts	207.607
Total on Parallel Filters	404.000

The sampling line loss in the beta filter line amounted to about 24% of the total filter weights plus sampling line loss. The parallel filter line loss was 34% of the total particle weight collected in that sampling line. Although the technique may not be precise and most of the line loss may have occurred during a small number of runs, the weighed amounts should be correct to within better than a factor of 2. The line losses in both sampling lines were greater than expected and may lend greater credibility to condensation as a possible explanation for lower measured concentration with short sampling time (Item 4 in earlier discussion). The parallel filter line was always operated at 75% dilution and 50 LPM diluted aerosol flow rate while the beta filter line was operated half of the time at 87.5% dilution. Thus, the beta filter line carried about half as much particulate mass as the parallel filter line during half of the runs. Although this may explain the greater measured line loss in the parallel filter line, the line loss measurement technique is probably not precise enough to make the difference significant.

The amount of line loss found in each of the 3 system components may offer clues to the collection mechanism. In both sampling lines, the horizontal tube collected the greatest amount, probably largely by gravity settling. The 2 vertical tubes collected similar amounts of material, possibly by condensation and turbulent impaction. We cannot explain the much larger line loss in the elbow of the parallel line, greater than 10 times the line loss in the elbow of the beta filter line.

We need more experimental data before we can draw meaningful conclusions about particle line losses.

4.2.e. Parallel Filter Tests in May

Among the data covering the May beta instrument tests, which will be presented in the next section, the reader will find a number of runs with 2 parallel filters in the sampling lines, just as in the 75% dilution, 50 LPM portion of the August runs. It must be understood that the first of these runs were not meant to evaluate the system, but rather to train the operating personnel and to work out any possible system problems which had developed during the long period of non-use. Most of the other parallel filter runs dispersed throughout the instrument tests were intended only to verify that nothing in the system had gone grossly wrong. However, one set of parallel filter runs was made for the purpose of evaluating the system on May 24, the last day of beta instrument testing. The good correlation between the stack particle concentrations measured by the two filters can be seen in Figure 35. Notice that the sampling time for these runs was only 3 minutes. The scatter in the data compares very well with the scatter found in the August tests at 75% dilution and 50 LPM total diluted aerosol flow rate. The average ratio of filter weights R_F is just over 1.0, similar to the August runs. This data provides experimental evidence that the May and August operating conditions were comparable and that there was no major equipment problem which developed between the 2 sets of tests. The May 24 data also provides additional evidence that the 2 parallel systems correlate very well when operated with identical dilution ratios, flow rates, and sampling times, conditions which did not exist during most of the August runs.

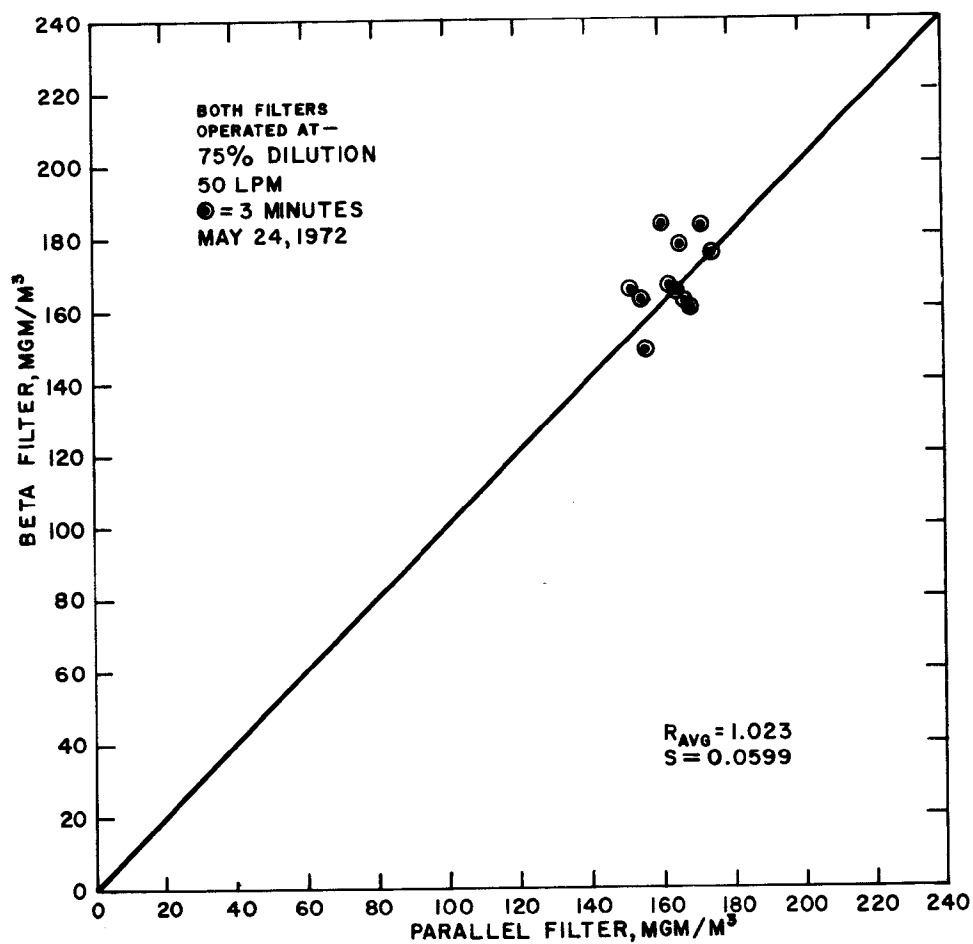


Figure 35. Stack concentration as measured by the beta filter plotted against stack concentration as measured by the parallel filter for May 24 runs. The diagonal line represents perfect (1:1) correlation. Both filters were operated at the same conditions.

SECTION 5. FIELD EVALUATION OF TWO PROTOTYPE BETA INSTRUMENTS

5.1 PROCEDURE

The Environmental Protection Agency furnished two prototype beta instruments, developed under contract by GCA Corporation and Industrial Nucleonics Corp. for field evaluation in the experimental stack facility.

The test set-up for the evaluation of the two beta instruments was identical to the set-up for the parallel filter tests described in Section 4 with the test instrument replacing the beta filter. In most runs, the TSI flowmeter plumbed into the system downstream of the test instrument was used to measure and control total diluted aerosol flow rate during a run. When the swirlmeter supplied with the beta instruments was used to measure and control total diluted aerosol flow rate, the data reported here will note that fact.

The two beta instruments were operated in the manual mode. Before every run, the instrument made its zero beta count. The instrument was then prepared for the sampling step and the run was begun. The total diluted aerosol flow rate was monitored and maintained at a constant value throughout the run. Considerably more adjustment was necessary to maintain constant flow through the beta instruments than through the parallel filter, presumably because of the smaller filter face area and subsequent faster loading in the beta instrument. After the valves were closed ending the run, the instrument made its final beta count and printed out its measured values of total particle loading (weight) and measured particle mass concentration (diluted). Preparations for the next run could then begin.

The operating procedure for the parallel filter was identical with the procedure used in the August sampling facility tests reported in Section 4.

5.2 RESULTS AND DISCUSSION

Tests were conducted with the Industrial Nucleonics (IN) beta instrument¹ on May 15 - 18 and May 23 - 24. Tests were conducted with the GCA Corporation (GCA) beta instrument² on May 22 - 23. The instruments were available only for the 2-week period, limiting the tests and evaluation which could be performed. However, we were able to fulfill the original objective of the experimental portion of this contract: choose the most promising technique for particle mass concentration measurement in the stack of large coal-fired combustion sources (See Vol. I and II of this report) and experimentally prove that the technique is feasible.

1. Duke, Charles R., and Cho, Boong Y., "Development of a Nucleonic Particulate Emission Gauge", Final Report prepared for Environmental Protection Agency under Contract No. 68-02-0210, Industrial Nucleonics Corp., 650 Ackerman Rd., Columbus, Ohio 43202, Feb. 1972.
2. Lilienfeld, P., and Dulchinos, J., "Vehicle Particulate Exhaust Mass Monitor", Final Report prepared for Environmental Protection Agency under Contract No. 68-02-0209, GCA Corp., GCA Technology Div., Bedford, Mass. 01730, Mar. 1972.

Complete data for all runs conducted during May 10 - 24 are shown in Appendix B. As mentioned in an earlier discussion, many parallel filter runs were made to train operators, to make sure the facility was still reliable after many months of idleness and modification, and to make sure nothing had gone grossly wrong with the facility during these tests. However, this discussion will be limited to presenting the beta instrument data and analyzing those results.

Figure 36 shows the comparison between stack concentration measured by the GCA instrument and the stack concentration measured by the parallel filter. We rejected the data from Runs 76 - 77 and 84 - 87 because, even though the GCA instrument data appears acceptable, the concentration measured by the parallel filter appeared significantly higher or lower than data obtained before or after those runs. During Run 95, an operator error lead to the destruction of the Geiger-Muller tube, disabling the instrument for the remainder of the tests.

The 13 valid data points shown in Figure 36 display excellent correlation between the GCA instrument and the parallel filter. The average ratio R_{GCA} ($R_{GCA} = \text{stack particle concentration measured by GCA instrument} \div \text{stack particle concentration measured by parallel filter}$) was 0.982 and the standard deviation of R_{GCA} was 0.0437. The correlation between 2 parallel filters in the August tests were not significantly better than this.

Our only recommendations for improvement after 1 1/2 days of tests are minor: 1) protect the G.M. tube from blowout by the mishandling of the vacuum pump and 2) use an accurate flowmeter downstream of the particle collector.

One must guard against becoming too optimistic about an instrument which displays such good correlation in only 1 1/2 days of tests at a rather constant particle concentration level on a single stack. Somewhat poorer results in earlier tests with artificially-generated uranine aerosol were reported to the authors.³ Much more testing is necessary in a wide variety of stacks operated at a variety of conditions before one could conclude that any instrument is ready for duty as a continuous monitor of particle mass concentration in a stack. However, the results of this test highly recommend the GCA beta instrument for such further testing.

Figure 37 shows the comparison between the stack concentration measured by the IN instrument and the stack concentration measured by the parallel filter. A number of data points were rejected because the parallel filter concentration was significantly higher or lower than runs just before or after the run, because

3. Herling, R. J., Environmental Protection Agency, private communication to the authors, May 1972.

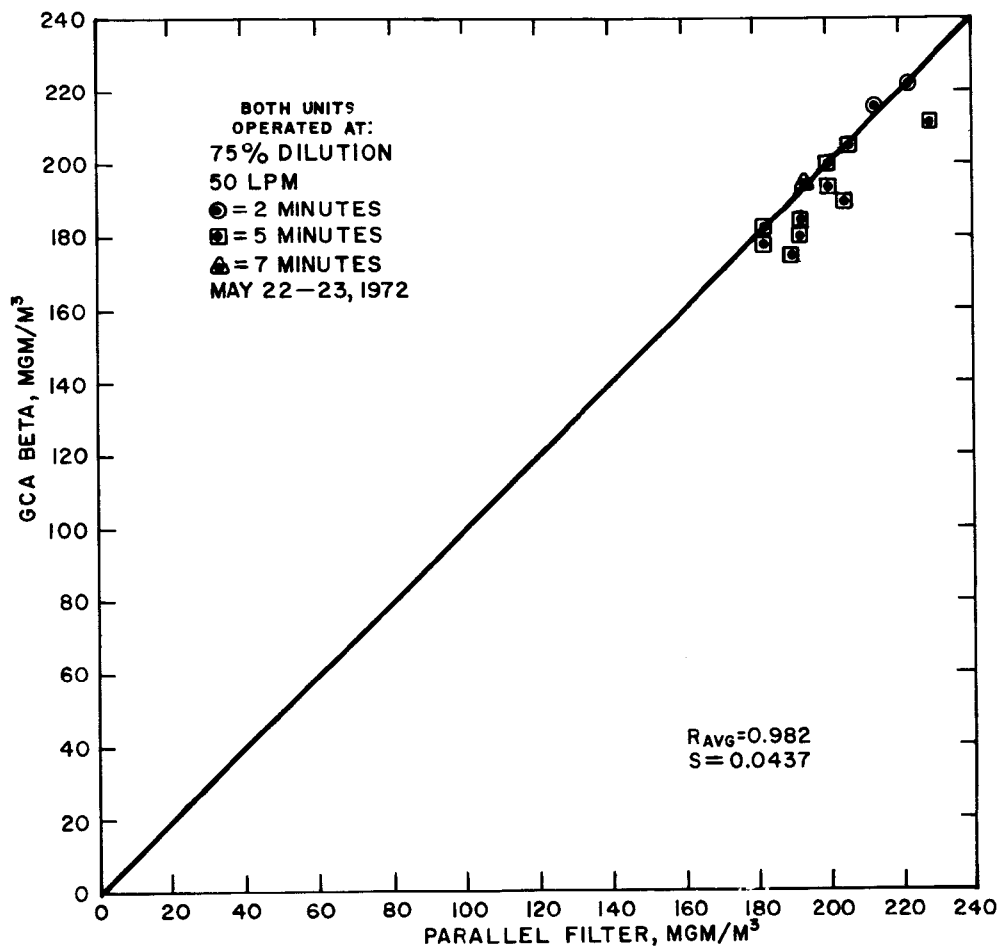


Figure 36. Stack concentration measured by the GCA beta instrument compared with stack concentration measured by the parallel filter. The diagonal line represents perfect (1:1) correlation.

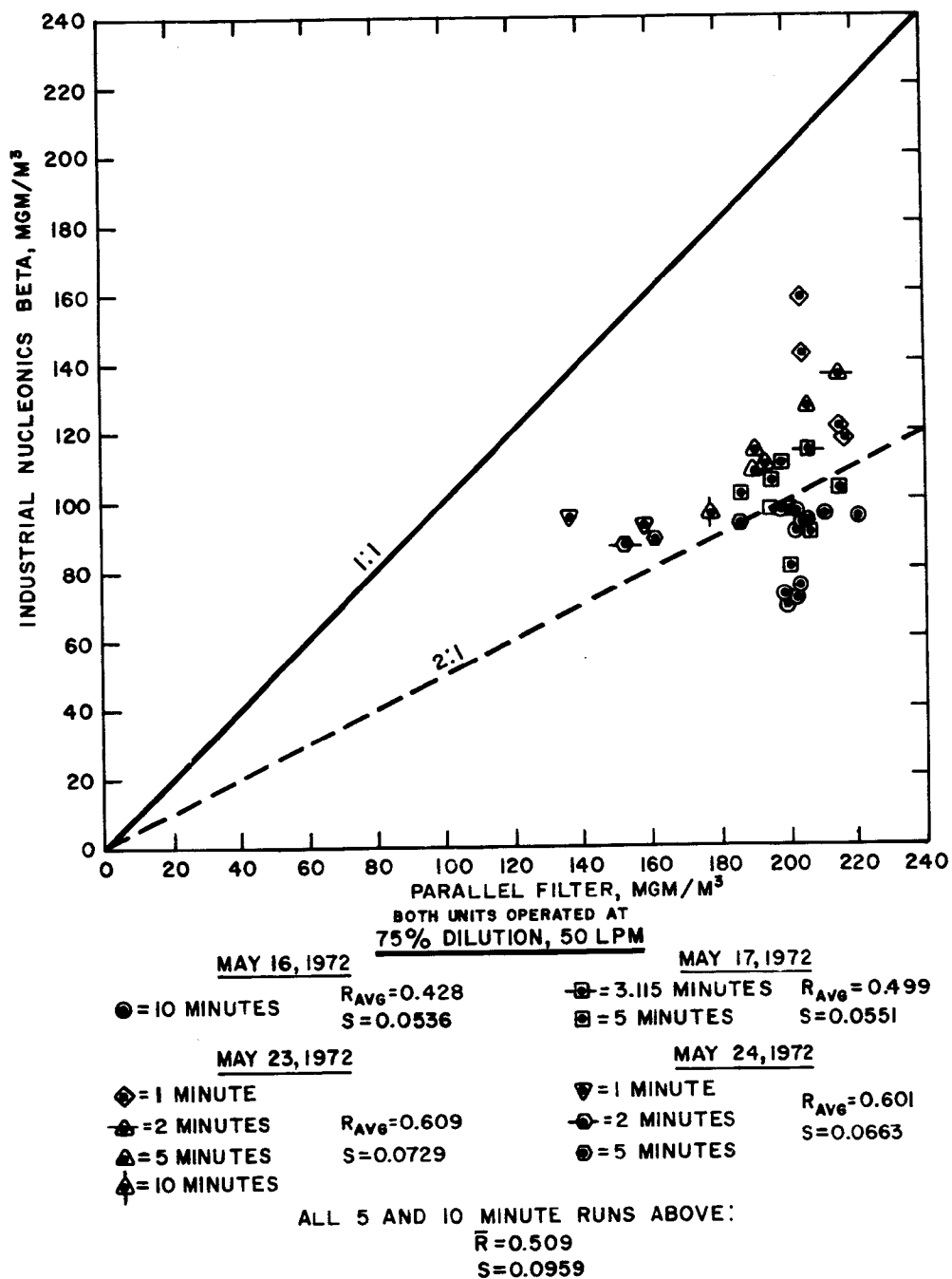


Figure 37. Stack concentration measured by the IN beta instrument compared with stack concentration measured by the parallel filter. The solid diagonal line represents a perfect (1:1) correlation and the dashed diagonal line represents a parallel filter measurement of twice as high as the beta instrument measurement.

it was the first run of the day, or because the IN instrument did not display or print any data at the end of the run. The data points shown in Figure 37 are only from validated runs. Note that some of the higher data points are from 1 or 2 minute runs. These could have been rejected but may offer some clue as to why the correlation was not better.

The IN beta instrument measured stack concentrations about half as high as the parallel filter. The average ratio \bar{R}_{IN} for any single day of tests ranged from 0.428 to 0.609. The standard deviation of R_{IN} for any single day of tests ranged from 0.0536 to 0.0729, all acceptable values. However, the standard deviation for all 5 and 10 minute samples shown in Figure 37 is 0.0959 with $\bar{R}_{IN} = 0.507$.

We have no explanation for the factor-of-2 low measurements by the IN beta instruments. Nearly perfect correlation in earlier tests with artificially-generated uranine aerosol was reported to the authors.³ Since the GCA instrument correlated well with the parallel filter as did an identical parallel filter, it would appear that the problem is within the IN instrument and is not a sampling problem. Both the GCA and IN instrument used the same filter media and both use a swirlmeter upstream of the filter for total diluted aerosol flow rate measurement. However, a TSI mass flow meter was used to monitor and control the flow rate with both instruments. The plumbing for the aerosol sample inside the two instruments was similar, but not identical. We suspect that the somewhat greater scatter of data points with this instrument may be improved when the other low measurement problem is corrected.

The IN instrument, as well as the GCA instrument, was not designed specifically for stack measurements, but rather for auto exhaust measurements. It was intended as a versatile laboratory tool, not as a rugged field instrument. In the case of the IN instrument, we found that the electronics malfunctioned often when the temperature around the instrument exceeded about 80°F. The malfunction was frustrating since the operator was not aware of a malfunction until no data appeared at the end of a run. Such malfunctions are not mentioned as a criticism of the beta radiation sensing technique, but as a deficiency of this specific instrument, limiting its usefulness for stack measurements.

In summary, we strongly recommend extensive stack testing with the GCA instrument under a variety of conditions. We recommend further laboratory work on the IN instrument to find the reason for the lack of correlation in these tests. The discovery of the reason for this problem may result in better, more trouble-free instruments in the future.

SECTION 6. EVALUATION OF TRANSMISSOMETER TECHNOLOGY

6.1 INTRODUCTION

The transmissometer is the only instrument which has been used to any significant extent for monitoring the particle loading in effluents from coal-combustion facilities. There is disagreement regarding what constitutes a good instrument. There is even more disagreement regarding what transmissometers measure.

Transmissometers measure the optical density of the light path of the instrument. The recommended list of features below should result in the best instrument for measuring optical density of flue gases containing particles. The recommendations include nothing which cannot easily be done with commercial technology available in January 1971. Correlation with any other particulate parameter (such as particle surface area or mass concentration) requires interpretation of the specific situation.

It is much more difficult to specify a transmissometer which correlates well with average particulate mass concentration within the light path. The authors feel that, without considerable experimental testing and development, the preferred approach is to design an instrument which does a good job of measuring the parameter which transmissometers are intended to measure: the optical density of the light path.

6.2 RECOMMENDED DESIGN FEATURES

1. Use a stabilized light source.
 - a. Choose a wavelength which avoids interference by infrared sources within the duct.
2. Use a detector that yields an electrical output signal which is linear with incident light intensity.
3. The combination of light source and detector should operate over a well-defined wavelength spectrum which is constant with time.
4. Use pinhole apertures (or small acceptance angles) to avoid collecting scattered and extraneous light and to make the measurement of optical density independent of path length.
5. Compensate automatically for dirty windows, light source aging, line voltage fluctuations and electronic drift.
 - a. When the system is out of tolerance because of dirty windows, etc., a warning should tell the operator to correct the situation.

- b. Keep the source, detector, and all surfaces within the light path clean; provide easy cleaning access to such surfaces when they become dirty; do not install the instrument so that particles can settle onto surfaces within the light path.
 - c. Provide an automatic zero and span check periodically during operation.
 - d. Consider heating all surfaces in contact with flue gas to prevent vapor condensation.
 - e. Consider heating any purge air to prevent condensation of vapors on window and corrosive surfaces.
6. Design the source and detector to align with each other at all time, even during plant shutdown and start up when severe duct distortion may occur.
7. Make the instrument compatible with its environment:
- a. All exterior housings must be weatherproof.
 - b. All seals between flue gas and sensitive apparatus must be gas tight.
 - c. Entire assembly must withstand duct vibrations.
 - d. All components in contact with flue gas must be noncorrosive.

6.3 MINIMUM RECOMMENDATIONS GOVERNING INSTRUMENT INSTALLATION AND OPERATION

1. Install the light beam in a representative axis of the duct:
- a. Consider particulate stratification in horizontal ducts.
 - b. Consider flue gas and particulate concentration profiles.
 - c. Consider bends, expansions, contractions, and obstructions in the duct.
2. Check the instrument thoroughly after installation and:
- a. Check zero and span every time the recorded measurement is checked.
 - b. Check for dirty windows and other such malfunctions weekly.
 - c. Check all parts in contact with flue gas for corrosion every six months.

3. If mass concentration or mass emissions rate correlation is necessary, complete mass calibration is necessary:

- a. After installation.
- b. Whenever certain plant operating conditions change significantly.
- c. Yearly.

6.4 PRESENT COMMERCIAL INSTRUMENTS

There are no commercial transmissometers available which use all the design features recommended above. However, three West German companies make instruments which appear to meet most requirements:

Irwin Sick (Model RM-3g)*
Optik Elektronik
Neuried, West Germany
(Licensed to: Intertech Corporation
262 Alexander Street
Princeton, N.J. 08540)*

Durag Apparatebau GmbH (Model D-R 110)
2 Hamburg 61
Killanstrasse 105, West Germany

AEG (Model R 72)
(address unavailable)

The best of these three is probably the Sick instrument. Figure 38 shows the principle of operation of the instrument.

Several comparative evaluations of these instruments in German power stations burning lignite fuel show that the Sick instrument yields the most reproducible measurements and is the most reliable for long-term operation. 1189, 225, 1188, 1254
The Sick instrument when operating perfectly, correlates reasonably well with particulate mass concentration measured by manually-collected filter samples. However, notice that, in the concentration range where modern, controlled stacks must operate (below 150 milligrams per cubic meter), the accuracy quickly deteriorates until estimated errors are larger than the measurement itself. 1189, 1254

The authors suggest that an "everclear" window^{13,487} at the point where the light beam enters and leaves the flue gas on both ends of the stack may help to prevent contamination of mirror and window surfaces. However, Duwel¹²⁵⁴ indicates that this may not be a significant problem if a purge air system is used. Other

*As this report goes to press, a newer model, RM-4, has become available and is now marketed by Lear Siegler, Inc., 32 Denver Technological Center, Englewood, Colorado 80110.

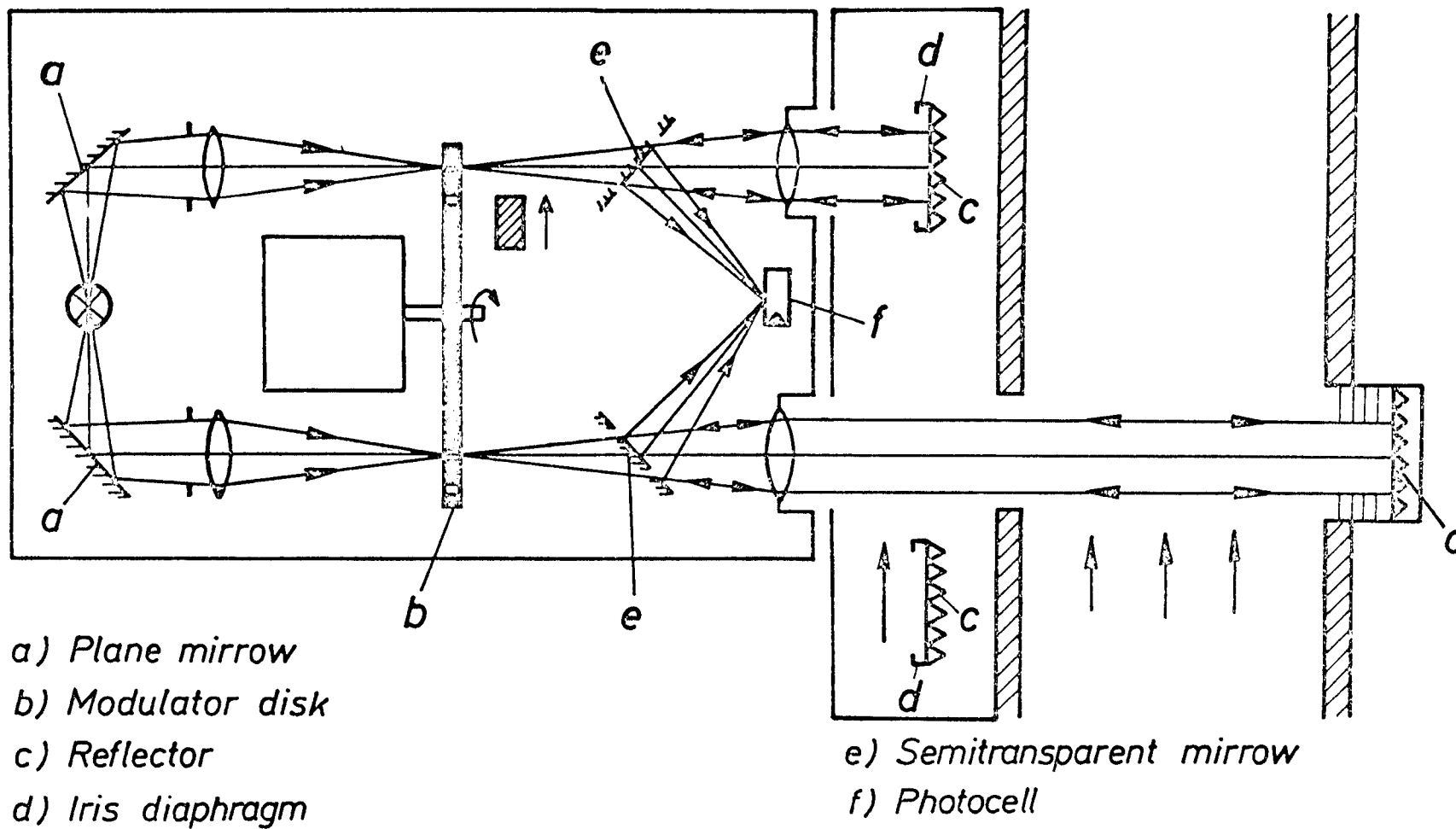


Figure 38. Schematic of optical system on Sick Model RM 3g transmissometer.¹²⁵⁴

possible improvements are the light source and detector. (Sick uses red light and a photodiode detector.) There is no assurance that other choices would be better. Duwel indicated to the authors that Sick has overcome the source and reflector alignment problem in recent models. Improvements in the mechanical or electrical assembly may be possible, but the authors can offer no suggestions without testing the instrument. Duwel indicates that the Sick instrument is now quite reliable once it is installed.

All other known commercial instruments, including all American models, place the light source on one side of the flue gas duct and the detector on the opposite side. Thus, no correction is possible for dirty windows and no automatic zero and span checks are possible. The result is a poorly defined measurement which does not correlate with opacity, optical density, Ringelmann number or particulate mass concentration. No comparative tests of American models have been carried out, but such tests would probably show poor reproducibility and even poorer accuracy.

Thus, the Sick Model RM 3g appears to be the best transmissometer available in January 1971. However, all supporting data is from German lignite-fired sources. Further comparative tests on coal-fired sources is strongly needed.

6.5 MEANING OF THE MEASUREMENT

The instrument specified in Section 6.2 senses the optical density of the light path. The optical density (or opacity) is closely related to the total cross-sectional area of the particles in the light beam if all the particles have diameters greater than 1 or 2 microns (geometrical scattering regime). However, submicron particles present in coal-combustion effluents affect the optical density of the light beam more than an equal total cross-section area of large particles. Therefore, fluctuations in the relatively small amount of submicron particulate material present in any stack will introduce significant and unavoidable error into the total cross-sectional area measurement and make the correlation of measured optical density with any other parameter of the particulate cloud very difficult. Since oil-combustion emissions contain a much higher proportion of submicron particles, the difficulty in correlating optical density with other particulate properties when oil is used as fuel is even greater than with coal.

The optical density measured by a transmissometer has no relationship with the familiar Ringelmann number for several reasons:

1. Ringelmann number is based on dark-colored plumes while the transmissometer measures optical density regardless of the color.
2. A transmissometer senses particles as they exist within the stack (high temperature, non-atmospheric gaseous composition, etc.) while Ringelmann number characterizes plumes in the atmosphere and is affected by extraneous factors such as steam formation, condensation of various vapors, agglomeration of particles, the color of the sky behind the plume, and the direction from which the plume is illuminated.

Many transmissometer manufacturers claim correlation with Ringelmann number and place Ringelmann markings on the readout meters. This is not a valid practice. Nearly all emissions sources experience conditions when Ringelmann number and optical density have entirely opposite trends. For example, the plume from a coal-fired source operating in the winter with ambient air at + 10°F appears white because steam overwhelms the fly ash in the plume. The Ringelmann number may be 0 or 1 indicating "clean" emissions while the optical density within the stack may be very high indicating very "dirty" emissions. Cement plant emissions are the classic example of this phenomena.

A transmissometer must be located in a representative portion of the stack or duct. Because a transmissometer measures an average optical density within the light beam, it has a potential advantage over instruments which sample or measure concentration at a point. However, this advantage is cancelled in many installations because of poor placement of the transmissometer. The flue gas velocity and particulate concentration profiles are just as important for locating a transmissometer as for locating point sampling instruments.

A transmissometer has one very clear advantage over most other instruments. It does not require a sample of flue gas to be removed from the duct. It can measure the optical density of the particles as they exist in the duct without disturbing them in any way.

6.6 CORRELATION OF THE MEASUREMENT WITH MASS

The optical density as measured with the instrument described in Part 2 of this section will correlate moderately with the mass of particles within the light beam under certain conditions. The problem is that the operator cannot easily distinguish the periods of good correlation from those with bad correlation within any given stack. Thus, he is never sure of the accuracy of the mass correlation.

Best mass correlation occurs when all particles have diameters greater than 2 μm , when the volume-surface diameter remains constant, and when the specific gravity of the particles is known and remains constant. As stated earlier, the small mass of submicron particles present in coal-combustion effluents affect the optical density of the light beam more than an equal mass of large particles, making the transmissometer too sensitive to fluctuations in submicron particle concentration. If the mean volume-surface diameter decreases by a factor of two with all other parameters constant, the indicated optical density increases by a factor of two. The particle size distribution (and, thus, the mean volume-surface diameter) of particles in a flue gas stream does not remain constant during normal power plant operating conditions. Factors which can cause significant changes in particle size distribution are:

1. The fraction of rated capacity at which the plant is operating,

2. Coal-burning efficiency,
3. Type and composition of coal used,
4. Sootblowing,
5. Type and efficiency of emissions control equipment, and
6. Operating conditions of control equipment including whether rapping is occurring and whether all banks of an electrostatic precipitator are operating at optimum conditions.

Minor, unnoticed changes in several of these factors can cause major changes in the particle size distribution which can, in turn, render any mass calibration of a transmissometer invalid. These same factors can affect the specific gravity of the particles. The particles in coal-combustion emissions reportedly vary from hollow spheres (specific gravity under 0.5) to very dense solids (specific gravity of about 10.0). The average specific gravity can change drastically with minor unnoticed changes in fuel composition or combustion efficiency, making a mass calibration useless. Perhaps the worst feature of all these problems is that the operator usually does not know if the mass calibration is valid at a specific time.

Every installation requires an extensive calibration for even rough correlation with particulate mass concentration. Calibrations must be repeated periodically, probably at least once every year. Because of the many effects discussed above which result in degradation of the mass correlation, each plant operating condition requires a different calibration. A calibration consists of a complete mass concentration and gas velocity characterization of the stack. The minimum procedure for one calibration consists of a traverse of the stack at the transmissometer installation with a velocity probe and a manual filter-sampling probe. An experienced crew of 3 people can normally calibrate one installation in about 1 - 2 weeks. Any shortcut to a complete calibration such as this results in severe degradation of the accuracy of the mass correlation.

6.7 CONCLUSIONS

A well-designed transmissometer measures the optical density of the light path. Transmissometers cannot measure particulate mass concentration without extensive, periodic calibration. When significant changes occur in the physical properties of the particles, a new calibration must be performed for correlation with particulate mass concentration.

6.8 ACKNOWLEDGMENT

The authors wish to thank Professor B.Y.H. Liu of the Mechanical Engineering Dept., University of Minnesota, for many helpful suggestions and for valuable critical review of an early manuscript of this section.

6.9 REFERENCES

- 487 Crosse, P. A., Lucas, D.H., and Snowsill, W. L., "Design of an "Everclean Window" for the Observation of the Optical Density of Flue Gas", Journal Inst. of Fuel, V. 34, no. 250, p. 503-505 (1961).
- 225 Duwel, L., "Latest State of Development of Control Instruments for the Continuous Monitoring of Dust Emissions", Staub-Reinhalt der Luft (Engl. Trans.), V. 28, no. 2, p. 42-53 (Mar 1968).
- 1254 Duwel, L., "Comparative Investigations of Different Measuring Principles for Continuous Monitoring of Dust Emissions of Lignite Fired Steam-Boiler", Paper presented at Second International Clean Air Congress, Washington, D. C., Dec. 6 - 11, 1970.
- 13 Lucas, D.H., "I. Air Pollution Measurements", Phil. Trans. Royal Society of London, V. A257, p. 143-151 (1969).
- 1189 Schnitzler, H., "Messtand fur die Prufung und Kalibrierung von Registrierenden Staub - und Gasmessgeraten in einem Steinkohle-gefeuerten Kraftwerk", SchrReihe Ver. Wass. - Boden Lufthyg. Berlin-Dahlem, V. 33, Stuttgart (1970).
- 1188 Schnitzler, H., "Untersuchungen uber die Eignung Registrierender Gerate zur Messungdes Staubgehaltes in Abhasen", Gesundheit-Ingenieur, V. 10, p. 307-309 (Jan 1970).
- Sem, G. J., Borgos, J. A., Olin, J. G., Pilney, J.P., Liu, B. Y. H., Barsic, N., Whitby, K. T., and Dorman, F. D., "State of the Art: 1971 Instrumentation for Measurement of Particulate Emissions from Combustion Sources, Volume II: Particulate Mass - Detail Report", Thermo-Systems Inc., St. Paul, Minn., report to EPA under Contract CPA 70-23 (1971).
- Anon, "Operational Handbook, Smoke Density Measuring System RM 3 g", Intertech Corp., Princeton, N.J. (U.S. Licensee for Erwin Sick transmissometers).

SECTION 7. APPENDICES

APPENDIX A

**COMPLETE DATA FOR THE AUGUST TESTS
OF THE SAMPLING SYSTEM**

Table A. Complete data for the August tests of the sampling system.

Runs 1 - 60 plumbed in with same configuration as beta instruments in May tests (see text).

Run No.	Filter No.	Operator	Filter, Beta or Parallel	August Date	Time of Day	Min, Elapsed Time	LPM, Diluted Aerosol	% Dilution Air	Liters, Diluted Aerosol	Micrograms, Particle Weight	Micrograms Per M ³ , Stack Concentration	Ratio: B. Filter Conc. P. Filter Conc.
1	185	B	BF	25	1119	5	50	75	250	5371	85.9	.897
	186	B	PF	25	1119	5	50	75	250	5989	95.8	
2	187	B	BF	25	1149	5	50	75	250	7459	119.3	.914
	188	B	PF	25	1149	5	50	75	250	8155	130.5	
3	189	B	BF	25	1159	5	50	75	250	8555	136.9	.986
	190	B	PF	25	1159	5	50	75	250	8678	138.8	
4	191	B	BF	25	1209	5	50	75	250	8641	138.3	.978
	192	B	PF	25	1209	5	50	75	250	8839	141.4	
5	193	B	BF	25	1222	5	50	75	250	9134	146.1	1.009
	194	B	PF	25	1222	5	50	75	250	9051	144.8	
6	195	B	BF	25	1233	10	50	75	500	19433	155.5	.983
	196	B	PF	25	1233	10	50	75	500	19780	158.2	
7	197	B	BF	25	1247	10	50	75	500	17855	142.8	.982
	198	B	PF	25	1247	10	50	75	500	18180	145.4	
8	199	B	BF	25	1301	10	50	75	500	17133	137.1	1.014
	200	B	PF	25	1301	10	50	75	500	16895	135.2	
9	201	B	BF	25	1316	10	50	75	500	17730	141.8	.982
	202	B	PF	25	1316	10	50	75	500	18055	144.4	
10	203	B	BF	25	1330	10	50	75	500	18097	144.8	1.001
	204	B	PF	25	1330	10	50	75	500	18087	144.7	
11	205	B	BF	25	1344	2	50	75	100	2351	94.0	1.009
	206	B	PF	25	1344	2	50	75	100	2331	93.2	

(continued)

Table A. Complete data for the August tests of the sampling system.

Runs 1 - 60 plumbed in with same configuration as beta instruments in May tests (see text).

Run No.	Filter No.	Operator	Filter, Beta or Parallel	August Date	Time of Day	Min, Elapsed Time	LPM, Diluted Aerosol	% Dilution Air	Liters, Diluted Aerosol	Micrograms, Particle Weight	Micrograms Per M ³ , Stack Concentration	Ratio: B. Filter Conc. P. Filter Conc.
12	207	B	BF	30	1017	2	50	75	100	1627	65.1	.816
	208	B	PF	30	1017	2	50	75	100	1995	79.8	
13	209	B	BF	30	1024	2	50	75	100	1666	66.6	1.155
	210	B	PF	30	1024	2	50	75	100	1443	57.7	
14	211	B	BF	30	1030	2	50	75	100	1617	64.7	1.077
	212	B	PF	30	1030	2	50	75	100	1501	60.0	
15	213	B	BF	30	1036	2	50	75	100	1460	58.4	.964
	214	B	PF	30	1036	2	50	75	100	1515	60.6	
16	215	B	BF	30	1054	5	30	75	150	4312	115.0	.918
	216	B	PF	30	1054	5	50	75	250	7832	125.3	
17	217	B	BF	30	1103	5	30	75	150	3290	87.7	.806
	218	B	PF	30	1103	5	50	75	250	6798	108.8	
18	219	B	BF	30	1112	5	30	75	150	2497	66.6	.595
	220	B	PF	30	1112	5	50	75	250	6991	111.9	
19	221	B	BF	30	1137	10	30	75	300	9129	121.7	.930
	222	B	PF	30	1137	10	50	75	500	16347	130.8	
20	223	B	BF	30	1151	10	30	75	300	8018	106.9	.867
	224	B	PF	30	1151	10	50	75	500	15417	123.3	
21	225	B	BF	30	1205	10	30	75	300	8564	114.2	.873
	226	B	PF	30	1205	10	50	75	500	16350	130.8	
22	227	B	BF	30	1219	2	30	75	60	1110	74.0	.959
	228	B	PF	30	1219	2	50	75	100	1929	77.2	

(continued)

Table A. Complete data for the August tests of the sampling system.

Runs 1 - 60 plumbed in with same configuration as beta instruments in May tests (see text).

Run No.	Filter No.	Operator	Filter, Beta or Parallel	August Date	Time of Day	Min, Elapsed Time	LPM, Diluted Aerosol	% Dilution Air	Liters, Diluted Aerosol	Micrograms, Particle Weight	Micrograms Per M ³ , Stack Concentration	Ratio: B. Filter Conc. P. Filter Conc.
23	229	B	BF	30	1225	2	30	75	60	1041	69.4	.869
	230	B	PF	30	1225	2	50	75	100	1998	79.9	
24	231	B	BF	30	1231	2	30	75	60	1021	68.1	.898
	232	B	PF	30	1231	2	50	75	100	1894	75.8	
25	233	B	BF	30	1244	5	20	75	100	2224	89.0	.795
	234	B	PF	30	1244	5	50	75	250	6996	111.9	
26	235	B	BF	30	1255	5	20	75	100	1652	66.1	.641
	236	B	PF	30	1255	5	50	75	250	6450	103.2	
27	237	B	BF	31	1100	5	20	75	100	2366	94.6	.816
	238	B	PF	31	1100	5	50	75	250	7251	116.0	
28	239	B	BF	31	1109	10	20	75	200	4194	83.9	.861
	240	B	PF	31	1109	10	50	75	500	12189	97.5	
29	241	B	BF	31	1122	10	20	75	200	3124	62.5	.872
	242	B	PF	31	1122	10	50	75	500	8966	71.7	
30	243	B	BF	31	1135	10	20	75	200	3141	62.8	.886
	244	B	PF	31	1135	10	50	75	500	8863	70.9	
31	245	B	BF	31	1148	2	20	75	40	287	28.7	1.047
	246	B	PF	31	1148	2	50	75	100	684	27.4	
32	247	B	BF	31	1153	2	20	75	40	172	17.2	.632
	248	B	PF	31	1153	2	50	75	100	681	27.2	
33	249	B	BF	31	1158	2	20	75	40	214	21.4	.823
	250	B	PF	31	1158	2	50	75	100	649	26.0	

(continued)

Table A. Complete data for the August tests of the sampling system.

Runs 1 - 60 plumbed in with same configuration as beta instruments in May tests (see text).

Run No.	Filter No.	Operator	Filter, Beta or Parallel	August Date	Time of Day	Min, Elapsed Time	LPM, Diluted Aerosol	% Dilution Air	Liters, Diluted Aerosol	Micrograms, Particle Weight	Micrograms Per M ³ , Stack Concentration	Ratio: B. Filter Conc. P. Filter Conc.
34	251	B	BF	31	1212	5	50	87.5	250	1855	59.4	.877
	252	B	PF	31	1212	5	50	75	250	4234	67.7	
35	253	B	BF	31	1220	5	50	87.5	250	1947	62.3	.879
	254	B	PF	31	1220	5	50	75	250	4433	70.9	
36	255	B	BF	31	1228	5	50	87.5	250	1893	60.6	.892
	256	B	PF	31	1228	5	50	75	250	4244	67.9	
37	257	B	BF	31	1236	10	50	87.5	500	4637	74.2	.909
	258	B	PF	31	1236	10	50	75	500	10199	81.6	
38	259	B	BF	31	1249	10	50	87.5	500	4095	65.5	.851
	260	B	PF	31	1249	10	50	75	500	9619	77.0	
39	261	B	BF	31	1302	10	50	87.5	500	4284	68.5	.831
	262	B	PF	31	1302	10	50	75	500	10300	82.4	
40	263	B	BF	31	1315	2	50	87.5	100	396	31.7	.888
	264	B	PF	31	1315	2	50	75	100	889	35.7	
41	265	B	BF	31	1320	2	50	87.5	100	278	22.2	.665
	266	B	PF	31	1320	2	50	75	100	835	33.4	
42	267	B	BF	31	1326	2	50	87.5	100	360	28.8	.855
	268	B	PF	31	1326	2	50	75	100	843	33.7	
43	269	B	BF	31	1341	5	30	87.5	150	1024	54.6	.883
	270	B	PF	31	1341	5	50	75	250	3865	61.8	
44	271	B	BF	31	1349	5	30	87.5	150	977	52.1	.889
	272	B	PF	31	1349	5	50	75	250	3662	58.6	

(continued)

Table A. Complete data for the August tests of the sampling system.

Runs 1 - 60 plumbed in with same configuration as beta instruments in May tests (see text).

Run No.	Filter No.	Operator	Filter, Beta or Parallel	August Date	Time of Day	Min, Elapsed Time	LPM, Diluted Aerosol	% Dilution Air	Liters, Diluted Aerosol	Micrograms, Particle Weight	Micrograms Per M ³ , Stack Concentration	Ratio: B. Filter Conc. P. Filter Conc.
45	273	B	BF	31	1357	5	30	87.5	150	971	51.8	.927
	274	B	PF	31	1357	5	50	75	250	3493	55.9	
46	275	B	BF	31	1405	10	30	87.5	300	2603	69.4	.905
	276	B	PF	31	1405	10	50	75	500	9592	76.7	
47	277	B	BF	31	1418	10	30	87.5	300	2725	72.7	.878
	278	B	PF	31	1418	10	50	75	500	10346	82.8	
48	279	B	BF	31	1431	10	30	87.5	300	2640	70.4	.832
	280	B	PF	31	1431	10	50	75	500	10575	84.6	
49	281	B	BF	31	1444	2	30	87.5	60	230	30.7	.922
	282	B	PF	31	1444	2	50	75	100	832	33.3	
50	283	B	BF	31	1449	2	30	87.5	60	244	19.5	.666
	284	B	PF	31	1449	2	50	75	100	733	29.3	
51	285	B	BF	31	1454	2	30	87.5	60	187	24.9	.830
	286	B	PF	31	1454	2	50	75	100	749	30.0	
52	287	B	BF	31	1502	5	20	87.5	100	504	40.3	.727
	288	B	PF	31	1502	5	50	75	250	3462	55.4	
53	289	B	BF	31	1510	5	20	87.5	100	429	34.3	.617
	290	B	PF	31	1510	5	50	75	250	3478	55.6	
54	291	B	BF	31	1518	5	20	87.5	100	481	38.5	.699
	292	B	PF	31	1518	5	50	75	250	3443	55.1	
55	293	B	BF	31	1526	10	20	87.5	200	1215	48.6	.627
	294	B	PF	31	1526	10	50	75	500	9691	77.5	

(continued)

Table A. Complete data for the August tests of the sampling system.

Runs 1 - 60 plumbed in with same configuration as beta instruments in May tests (see text).

Run No.	Filter No.	Operator	Filter, Beta or Parallel	August Date	Time of Day	Min, Elapsed Time	LPM, Diluted Aerosol	% Dilution Air	Liters, Diluted Aerosol	Micrograms, Particle Weight	Micrograms Per M ³ , Stack Concentration	Ratio: B. Filter Conc. P. Filter Conc.
56	295	B	BF	31	1539	10	20	87.5	200	1302	52.1	.617
	296	B	PF	31	1539	10	50	75	500	10560	84.5	
57	297	B	BF	31	1552	10	20	87.5	200	1354	54.2	.622
	298	B	PF	31	1552	10	50	75	500	10896	87.2	
58	299	B	BF	31	1605	2	20	87.5	40	126	25.2	.788
	300	B	PF	31	1605	2	50	75	100	801	32.0	
59	301	B	BF	31	1610	2	20	87.5	40	111	22.2	.945
	302	B	PF	31	1610	2	50	75	100	587	23.5	
60	303	B	BF	31	1615	2	20	87.5	40	610	122.0	4.919
	304	B	PF	31	1615	2	50	75	100	620	24.8	

APPENDIX B
COMPLETE DATA FOR THE MAY TESTS
OF TWO BETA INSTRUMENTS

Table B. Complete data for the May tests of two beta instruments.

Runs 1 - 23 plumbed in short and vertical downstream of diluter.

Runs 24 - 127 plumbed in with configuration necessary for beta instruments (see text).

Run No.	Filter No.	Operator*	Beta** or Parallel Filter	May Date	Time of Day	Min, Elapsed Time	CFM Diluted Aerosol	% Dilution Air	Liters Diluted Aerosol	Micro-grams, Particle Weight	Micrograms Per M ³ Stack Concentration	Ratio: Beta Weight P.Filter Wt.	Comments
1	1	G	BF	10	1515	15	1.0	50	425	5313	25.0	1.095	
	2	G	PF	10	1530					5038	23.7		
	3	G	BF	10	1535	20	1.0	50	567	7575	26.8	1.016	
	4	G	PF	10	1555					7457	26.4		
	5	B	BF	11		15	1.0	50	425	6041	28.5	1.053	
	6	B	PF	11						5741	27.0		
	7	B	BF	11		15	1.0	50	425	6951	32.7	1.097	
	8	B	PF	11						6338	29.8		
	9	B	BF	11						9226	32.6		
	10	B	PF	11	1155	20	1.0	50	566.4	8611	30.4	1.073	
	11	B	BF	11						9695	34.2		
	12	B	PF	11	1235	20	1.0	50	566.4	8920	31.5	1.090	
	13	B	BF	11						13813	32.5		
	14	B	PF	11	1302	30	1.0	50	850	12780	30.1	1.080	
	15	B	BF	11						7164	33.7		
	16	B	PF	11	1340	15	1.0	50	425	6631	31.2	1.081	
	17	B	BF	11						7634	35.9		
	18	B	PF	11	1407	15	1.0	50	425	6926	32.6	1.102	
	19	B	BF	11						8978	42.2		
	20	B	PF	11	1427	15	1.0	50	425	8114	38.2	1.107	

*G operator = GJS (author)

B operator = JAB (author)

**BF = 47-mm filter substituted for the beta instrument

PF = 47-mm parallel filter

Table B. Complete data for the May tests of two beta instruments.

Runs 1 - 23 plumbed in short and vertical downstream of diluter.

Runs 24 - 127 plumbed in with configuration necessary for beta instruments (see text).

Run No.	Filter No.	Operator	Beta or Parallel Filter	May Date	Time of Day	Min, Elapsed Time	CFM Diluted Aerosol	% Dilution Air	Liters Diluted Aerosol	Micro-grams, Particle Weight	Micrograms Per M ³ Stack Concentration	Ratio: Beta Weight P.Filter Wt.	Comments
11	21	B	BF	11	1449	15	1.0	50	425	10088	41.0	1.109	
	22	B	PF	11						9106	42.9		
12	23	B	BF	11	1513	30	1.0	75	1060	10900	41.2	1.316	First run @4:1
	24	B	PF	11						8285	31.3		
13	25	B	BF	12	1235	30	1.0	75	1060	15596	58.9	1.243	Ran 1 dry run before this
	26	B	PF	12						12543	47.4		
14	27	B	BF	12	1321	20	1.0	75	707	11811	66.8	1.270	
	28	B	PF	12						9297	52.6		
15	29	B	BF	12	1347	20	1.0	75	707	14820	83.9	1.170	
	30	B	PF	12						12659	71.7		
16	31	B	BF	12	1412	20	1.0	75	707	16645	94.2	1.167	
	32	B	PF	12						14273	80.9		
17	33	B	BF		1438	20	1.0	75	707	16332	92.5	1.111	
	34	B	PF	12						14706	83.3		
18	35	B	BF	12	1502	20	1.0	75	707	15790	89.4	1.108	
	36	B	PF	12						14260	80.7		
19	37	B	BF	12	1527	20	1.0	75	707	15049	85.2	1.104	
	38	B	PF	12						13637	77.2		
20	39	B	BF	12	1552	20	1.0	75	707	14333	81.1	1.105	
	40	B	PF	12						12968	73.5		
21	41	B	BF	15	1015	15	1.0	75	530	12735	96.1	(1.137) 0.880	Trial Run. Reversed flowmeters from Run 20.
	42	B	PF	15						14472	109.4		

(continued)

Table B. Complete data for the May tests of two beta instruments.

Runs 1 - 23 plumbed in short and vertical downstream of diluter.

Runs 24 - 127 plumbed in with configuration necessary for beta instruments (see text).

Run No.	Filter No.	Operator	Beta or Parallel Filter	May Date	Time of Day	Min, Elapsed Time	CFM Diluted Aerosol	% Dilution Air	Liters Diluted Aerosol	Micro-grams, Particle Weight	Micrograms Per M ³ Stack Concentration	Ratio: Beta Weight P.Filter Wt.	Comments
22	43	B	BF	15	1040	15	1.0	75	530	11173	84.4	(1.047) 0.956	Same flowmeter config. as 21
	44	B	PF	15						11680	88.3		
23	45	B	BF	15	1058	30	1.0	75	1060	22864	86.4	(1.005) 0.995	May have lost some of 45 filter on o'ring, same flowmeter as 21
	46	B	PF	15						22972	86.8		
24			IN*	15	1505	5	50**	75	197.3	12977	208	0.419	IN plumbed through flowmeter. Filter torn, ran dry run before this.
	47	B	PF						250	30978	496		
25			IN	15	1535	5	50***	75	257	6574	102.3	0.510	Filter torn
	48	B	PF						250	12896	206.4		
26			IN	15	1550	5	50***	75	253.1	6513	102.9	0.512	Good run
	49	B	PF						250	12720	203.6		
27			IN	15	1600	5	50**	75	219.8	1951	31.2	0.151	Good run
	50	B	PF						250	12926	206.8		
28			IN	15	1615	10	50***	75	499.9	10682	85.5	0.423	Good run
	51	B	PF						500	25280	202.4		

*IN = Industrial Nucleonics beta instrument

**denotes flow rate adjusted by TSI flowmeter, LPM

***denotes flow rate adjusted by β swirlmeter, LPM

There was a leak in the β flow system downstream of filter but upstream of TSI flowmeter.

All volumes used in calculations are values indicated by β instrument.

Table B. Complete data for the May tests of two beta instruments.

Runs 1 - 23 plumbed in short and vertical downstream of diluter.

Runs 24 - 127 plumbed in with configuration necessary for beta instruments (see text).

Run No.	Filter No.	Operator	Beta or Parallel Filter	May Date	Time of Day	Min, Elapsed Time	LPM, Diluted Aerosol	% Dilution Air	Liters Diluted Aerosol	Micro-grams, Particle Weight	Micrograms Per M ³ Stack Concentration	Ratio: Beta Weight P.Filter Wt.	Comments
29	52	G	BF	16	1050	5	50	75	250	13663	219	.888	IN plumbed through swirl-meter. Filter tore, stuck to screen.
	53	G	PF	16						15387	246		
30	54	G	BF	16	1110	5	50	75	250	10037	160.6	.628	Same as above
	55	G	PF	16						15982	256		
31	56	G	BF	16	1135	5	50	75	250	11601	185.8	.914	Stuck to screen, soaked
	57	G	PF	16						12690	203		
32	59	G	BF	16	1155	5	50	75	250	11273	180.6	.898	Good run
	58	G	PF	16						12551	201		
33	60	G	BF	16	1210	5	50	75	250	11488	184	.844	Good run
	61	G	PF	16						13612	218		
34	62	G	BF	16	1225	5	50	75	250	10348	165.6	.835	Good run
	63	G	PF	16						12390	198.4		
35		G	IN	16	1245	10	50	75	500	9090	72.7	.364	IN plumbed through swirl-meter.
	64	G	PF	16						24950	199.7		
36		G	IN	16	1300	10	50	75	500	12046	96.5	.488	
	65	G	PF	16						24801	198.4		
37		G	IN	16	1320	10	50	75	500	12065	96.5	.474	
	66	G	PF	16						25438	203.4		
38		G	IN	16	1335	10	50	75	500	8976	71.8	.354	
	67	G	PF	16						25390	203.1		

(continued)

Table B. Complete data for the May tests of two beta instruments.

Runs 1 - 23 plumbed in short and vertical downstream of diluter.

Runs 24 - 127 plumbed in with configuration necessary for beta instruments (see text).

Run No.	Filter No.	Operator	Beta or Parallel Filter	May Date	Time of Day	Min, Elapsed Time	LPM, Diluted Aerosol	% Dilution Air	Liters Diluted Aerosol	Micro-grams, Particle Weight	Micrograms Per M ³ Stack Concentration	Ratio: Beta Weight P.Filter Wt.	Comments
39		G	IN	16						12008	96.1		
	68	G	PF	16	1350	10	50	75	500	26533	212	.453	
40		G	IN	16						11917	95.3		
	69	G	PF	16	1405	10	50	75	500	27605	221	.432	
41		G	IN	16						11733	93.9		
	70	G	PF	16	1425	10	50	75	500	25847	207	.454	
42		G	IN	16						12102	96.9		
	71	G	PF	16	1440	10	50	75	500	24613	197	.492	
43		G	IN	16						11697	93.6		
	72	G	PF	16	1455	10	50	75	500	25757	206	.454	
44		G	IN	16						9375	75		
	73	G	PF	16	1515	10	50	75	500	25499	204	.368	
45		G	IN	16						11437	91.5		
	74	G	PF	16	1530	10	50	75	500	25349	203	.451	
46		G	IN	16						8750	70		
	75	G	PF	16	1545	10	50	75	500	25015	200	.350	
47		G	IN	17						6032	96.5		Plumbed IN to
	76	G	PF	17	1225	5	50	75	250	12300	197	.490	eliminate swirl-meter
48		G	IN	17						6379	102.1		
	77	G	PF	17	1240	5	50	75	250	11679	187.1	.546	
49		G	IN	17						6584	105.3		
	78	G	PF	17	1250	5	50	75	250	12258	196.1	.538	

(continued)

Table B. Complete data for the May tests of two beta instruments.

Runs 1 - 23 plumbed in short and vertical downstream of diluter.

Runs 24 - 127 plumbed in with configuration necessary for beta instruments (see text).

Run No.	Filter No.	Operator	Beta or Parallel Filter	May Date	Time of Day	Min, Elapsed Time	LPM, Diluted Aerosol	% Dilution Air	Liters Diluted Aerosol	Micro-grams, Particle Weight	Micrograms Per M ³ Stack Con- centration	Ratio: Beta Weight P.Filter Wt.	Comments
50		G	IN	17	1300	5	50	75	250	6073	97.2	.481	
	79	G	PF	17						12623	202		
51		G	IN	17	1325	5	50	75	250	6492	103.9	.481	
	80	G	PF	17						13515	216		
52		G	IN	17	1350	5	50	75	250	-	-	-	
	91	G	PF	17						-	-		
53		G	IN	17	1405	5	50	75	250	6908	110.4	.556	
	92	G	PF	17						12411	198.6		
54		G	IN	17	1420	3.115	50	75	155.75	4463	114.5	.556	
	93	G	PF	17						8022	207		
55		G	IN	17	1430	5	50	75	250	5657	90.5	.438	
	94	G	PF	17						12908	207		
56		G	IN	17	1440	5	50	75	250	5052	80.9	.401	
	95	G	PF	17						12561	201		
57		G	IN	17	1450	5	50	75	250	-	-	-	
	96	G	PF	17						12045	192.8		
58		G	IN	17	1505	5	50	75	250	-	-	-	
	97	G	PF	17						12608	202		
59		B	IN	18	1140	5	50	75	250	5703	91.3	.333	3 min. count time. power plant normal
	113	B	PF	18						17100	274		
60		B	IN	18	1150	5	50	75	250	6557	105	.386	3 min. count time, power plant normal
	114	B	PF	18						16979	272		

(continued)

Table B. Complete data for the May tests of two beta instruments.

Runs 1 - 23 plumbed in short and vertical downstream of diluter.

Runs 24 - 127 plumbed in with configuration necessary for beta instruments (see text).

Run No.	Filter No.	Operator	Beta or Parallel Filter	May Date	Time of Day	Min, Elapsed Time	LPM, Diluted Aerosol	% Dilution Air	Liters Diluted Aerosol	Micro-grams, Particle Weight	Micrograms Per M ³ Stack Concentration	Ratio: Beta Weight P.Filter Wt.	Comments
61		B	IN	18						4181	66.9		3 min. count time, power plant normal
	115	B	PF	18	1200	5	50	75	250	12640	202	.331	
62		B	IN	18						2157	34.5		3 min. count time, power plant normal
	116	B	PF	18	1315	5	50	75	250	13801	221	.156	
63		B	IN	18						6280	100.5		3 min. count time, power plant beginning fly ash reinjection shut-off.
	117	B	PF	18	1358	5	50	75	250	13394	214	.470	
64		B	IN	18						3693	59		3 min. count time, fly ash reinject off.
	108	B	PF	18	1415	5	50	75	250	12694	203	.291	
65		B	IN	18						5588	89.5		3 min. count time, fly ash reinject off.
	109	B	PF	18	1426	5	50	75	250	11709	187	.478	
66		B	IN	18						-	-	-	3 min. count time, fly ash reinject off.
	110	B	PF	18	1440	5	50	75	250	11456	183	-	
67		B	IN	18						-	-	-	3 min. count time, fly ash reinject off.
	111	B	PF	18	1455	2 1/2	50	75	125	5693	182	-	
68		B	BF	19			42.5		212.5	7750	146		2.20
	118	B	PF	19	1314	5		75	106	3521	133		
	119	B	BF	19			42.5		106.25	3900	147		2.28
69		B	PF	19	1327	2 1/2		75	53	1713	129		
	121	B	BF	19			42.5		212.5	7269	137		2.42
70		B	PF	19	1337	5		75	106	2997	113.2		
	122	B	PF	19			21.2						

(continued)

Table B. Complete data for the May tests of two beta instruments.

Runs 1 - 23 plumbed in short and vertical downstream of diluter.

Runs 24 - 127 plumbed in with configuration necessary for beta instruments (see text).

Run No.	Filter No.	Operator	Beta or Parallel Filter	May Date	Time of Day	Min, Elapsed Time	LPM, Diluted Aerosol	% Dilution Air	Liters Diluted Aerosol	Micro-grams, Particle Weight	Micrograms Per M ³ Stack Con- centration	Ratio: Beta Weight P.Filter Wt.	Comments
71	98	B	BF	19	1410	5	21.2	75	106	2925	110.5	.770	
	99	B	PF	19			42.5		212.5	7622	143.5		
	100	B	BF	19	1422	2 1/2	21.2	75	53	1276	96.3	.695	
72	101	B	PF	19			42.5		106.25	3680	138.6		
	102	B	BF	19	1430	5	21.2	75	106	3216	121.4	.822	
	103	B	PF	19			42.5		212.5	7853	147.8		
73	81	B	BF	19	1450	5	28.3	75	141.5	4390	124	1.27	
	104	B	PF	19			28.3		141.5	3464	98		
	82	B	BF	19	1500	5	28.3	75	141.5	3822	108	1.50	
74	105	B	PF	19			28.3		141.5	2541	71.9		
		G	GCA*	22	1145	10	50	75	(568)**	25310	203	1.295	
75	123	G	PF	22					500	19560	157		
		G	GCA	22	1200	5	50	75	(294)**	13320	213	0.840	
76	124	G	PF	22					250	15862	254		
		G	GCA	22	1220	5	50	75	(284)**	11900	190	0.930	
77	125	G	PF	22					250	12795	205		
		G	GCA	22	1235	5	50	75	(282)**	11250	180	0.933	
78	126	G	PF	22					250	12060	193		
		G	GCA	22	1410	5	50	75	(287)**	12100	194	0.965	NSP switched off fly ash reinjec- tion @≈ 1300
79	127	G	PF	22					250	12547	201		

*GCA = GCA Corporation beta instrument

**Number shown in GCA indicated flow, flow rate operated with TSI flowmeter
and all calculations based on TSI flowmeter.

(continued)

Table B. Complete data for the May tests of two beta instruments.

Runs 1 - 23 plumbed in short and vertical downstream of diluter.

Runs 24 - 127 plumbed in with configuration necessary for beta instruments (see text).

Run No.	Filter No.	Operator	Beta or Parallel Filter	May Date	Time of Day	Min, Elapsed Time	LPM, Diluted Aerosol	% Dilution Air	Liters Diluted Aerosol	Micro-grams, Particle Weight	Micrograms Per M ³ Stack Con- centration	Ratio: Beta Weight P.Filter Wt.	Comments
81		G	GCA	22					(290)*	11430	183		
	132	G	PF	22	1430	5	50	75	250	11452	183	0.997	
82		G	GCA	22					(287)*	10930	175		
	131	G	PF	22	1445	5	50	75	250	11923	191	0.918	
83		G	GCA	22					(289)*	11100	178		
	130	G	PF	22	1500	5	50	75	250	11458	183	0.969	
84		G	GCA	22					(294)*	11930	191		
	129	G	PF	22	1520	5	50	75	250	8860	142	1.348	
85		G	GCA	22					(288)*	11300	181		
	128	G	PF	22	1535	5	50	75	250	15250	244	0.741	
86		G	GCA	23					(291)*	11800	189		Sampling system still cool
	133	G	PF	23	1015	5	50	75	250	15206	244	0.777	
87		G	GCA	23					(290)*	10490	167		Sampling system nearly warm.
	134	G	PF	23	1030	5	50	75	250	11600	186	0.905	
88		G	GCA	23					(118)*	5400	216		
	135	G	PF	23	1045	2	50	75	100	5344	214	1.010	
89		G	GCA	23					(287)*	11480	184		
	136	G	PF	23	1100	5	50	75	250	12041	193	0.955	
90		G	GCA	23					(407)*	17020	194		
	137	G	PF	23	1120	7	50	75	350	16784	192	1.014	
91		G	GCA	23					(291)*	12520	200		
	138	G	PF	23	1135	5	50	75	250	12576	201	0.995	

*See note for run 76

Table B. Complete data for the May tests of two beta instruments.

Runs 1 - 23 plumbed in short and vertical downstream of diluter.

Runs 24 - 127 plumbed in with configuration necessary for beta instruments (see text).

Run No.	Filter No.	Operator	Beta or Parallel Filter	May Date	Time of Day	Min, Elapsed Time	LPM, Diluted Aerosol	% Dilution Air	Liters Diluted Aerosol	Micro-grams, Particle Weight	Micrograms Per M ³ Stack Concentration	Ratio: Beta Weight P.Filter Wt.	Comments
92		G	GCA	23	1150	2	50	75	(116)*	5540	222	0.995	
	139	G	PF	23					100	5567	223		
		G	GCA	23					(290)*	12820	205		
93		G	GCA	23	1205	5	50	75				0.994	
	140	G	PF	23					250	12888	206		
		G	GCA	23					(289)*	14300	229		
94		G	GCA	23	1310	5	50	75				1.082	NSP reduced rapping intensity on first 2 rows of wires @1230 - 1300
	141	G	PF	23					250	13213	211		
		G	GCA	23					-	-	-	-	GCA-GM tube blew out
95		G	GCA	23	1325	5	50	75				-	
	142	G	PF	23					250	2622	41.96		
		-	-	-					-	-	-	-	
96		G	GCA	23	1335	5	50	75				-	
	143	G	PF	23					250	8866	142		
		G	IN	23					(267)	7150	114		
97		G	IN	23	1410	5	50	75				0.600	IN with swirl-meter in place, TSI flowmeter for calculations
	144	G	PF	23					250	11931	191		
		G	IN	23					(257)	7970	127		
98		G	IN	23	1425	5	50	75				0.617	
	145	G	PF	23					250	12913	207		
		G	IN	23					(117)	3390	136		
99		G	IN	23	1435	2	50	75				0.628	
	146	G	PF	23					100	5400	216		
		G	IN	23					(52)	1980	158		
100		G	IN	23	1440	1	50	75				0.772	
	147	G	PF	23					50	2566	205		
		G	IN	23					(253)	6750	108		
101		G	IN	23	1450	5	50	75				0.567	
	148	G	PF	23					250	11914	191		

*See note for run 76

(continued)

Table B. Complete data for the May tests of two beta instruments.

Runs 1 - 23 plumbed in short and vertical downstream of diluter.

Runs 24 - 127 plumbed in with configuration necessary for beta instruments (see text).

Run No.	Filter No.	Operator	Beta or Parallel Filter	May Date	Time of Day	Min, Elapsed Time	LPM, Diluted Aerosol	% Dilution Air	Liters Diluted Aerosol	Micro-grams, Particle Weight	Micrograms Per M ³ Stack Concentration	Ratio: Beta Weight P.Filter Wt.	Comments
102		G	IN	23	1500	1	50	75	(52)	1770	142	0.690	
	149	G	PF	23					50	2565	205		
103		G	IN	23	1508	1	50	75	(50)	1510	121	0.560	
	150	G	PF	23					50	2696	216		
104		G	IN	23	1520	10	50	75	(538)	11980	96	0.542	
	151	G	PF	23					500	22141	178		
105		G	IN	23	1534	1	50	75	(53)	1480	118	0.547	
	152	G	PF	23					50	2709	217		
106		G	IN	23	1610	5	50	75	(258)	6850	110	0.565	
	153	G	PF	23					250	12113	194		
107		B	IN	24	1035	5	50	75	-	-	-	-	No data from IN
	154	B	PF	24					250	12513	200.4		
108		B	IN	24	1050	5	50	75	(257)	5770	89.64	0.561	
	155	B	PF	24					250	10288	161.8		
109		B	IN	24	1100	1	50	75	(53)	1220	93.16	0.615	
	156	B	PF	24					50	1985	158.8		
110		B	IN	24	1107	2	50	75	(105)	2310	87.80	0.599	
	157	B	PF	24					100	3855	154.4		
111		B	IN	24	1116	?	50	75	?	-	-	-	IN stopped too soon
	158	B	PF	24						4907	-		
112		B	IN	24	1124	5	50	75	(264)	6110	92.68	0.525	
	159	B	PF	24					250	11639	186.4		

(continued)

Table B. Complete data for the May tests of two beta instruments.

Runs 1 - 23 plumbed in short and vertical downstream of diluter.

Runs 24 - 127 plumbed in with configuration necessary for beta instruments (see text).

Run No.	Filter No.	Operator	Beta or Parallel Filter	May Date	Time of Day	Min, Elapsed Time	LPM, Diluted Aerosol	% Dilution Air	Liters Diluted Aerosol	Micro-grams, Particle Weight	Micrograms Per M ³ Stack Concentration	Ratio: Beta Weight P.Filter Wt.	Comments
113	160	B	IN	24	1135	1	50	75	-	-	-	-	No data from IN
		B	PF	24					50	1970	157.6		
		B	IN	24					(52)	1210	92.88		
114					1144	1	50	75				0.705	
	161	B	PF	24					50	1716	137.2		
	163	B	BF	24						17191	275.2		
115					1238	5	50	75	250			1.274	
	162	B	PF	24						13495	216		
	164	B	BF	24						11700	187.2		
116					1306	5	50	75	250			-	
	-		-							-	-		
	166	B	BF	24						6654	177.6		
117					1321	3	50	75	150			1.067	Fly ash rein- jection turned off at 1315
	165	B	PF	24						6230	166.4		
	167	B	BF	24						6856	182.8		
118					1327	3	50	75	150			1.138	
	168	B	PF	24						6022	160.8		
	169	B	BF	24						6197	165.2		
119					1334	3	50	75	150			1.082	
	170	B	PF	24						5728	152.8		
	171	B	BF	24						6018	160.4		
120					1340	3	50	75	150			0.948	
	172	B	PF	24						6348	169.2		
	173	B	BF	24						6837	182.4		
121					1348	3	50	75	150			1.055	
	174	B	PF	24						6480	172.8		
	175	B	BF	24						5570	148.4		
122					1354	3	50	75	150			0.952	
	176	B	PF	24						5855	156.4		
	177	B	BF	24						6078	162.4		
123					1400	3	50	75	150			1.041	Fly ash rein- jection turned on at 1400
	178	B	PF	24						5831	155.6		

(continued)

Table B. Complete data for the May tests of two beta instruments.

Runs 1 - 23 plumbed in short and vertical downstream of diluter.

Runs 24 - 127 plumbed in with configuration necessary for beta instruments (see text).

Run No.	Filter No.	Operator	Beta or Parallel Filter	May Date	Time of Day	Min, Elapsed Time	LPM, Diluted Aerosol	% Dilution Air	Liters Diluted Aerosol	Micro-grams, Particle Weight	Micrograms Per M ³ Stack Concentration	Ratio: Beta Weight P.Filter Wt.	Comments
124	179	B	BF	24	1406	3	50	75	150	6070	161.6	0.962	
	180	B	PF	24						6311	168.4		
125	181	B	BF	24	1412	3	50	75	150	6219	166.0	1.014	
	182	B	PF	24						6130	163.6		
	183	B	BF	24						6172	164.4		
126	184	B	PF	24	1418	3	50	75	150	6207	165.6	0.995	
	106	B	BF	24						6570	175.2		
127					1424	3	50	75	150			1.000	
	107	B	PF	24						6570	175.2		